المدرسة الوطنية المتعددة التقنيات

قسم الآلية

Ecole Nationale Polytechnique

Département d'Automatique

End-of-studies project dissertation

for obtaining the State Engineer's degree in Automation and Control

Study of the Hybrid PV-Wind Installation of the Process Control Laboratory at ENP

Realized by:

Ms. MEZAACHE Taqwa

Publicly presented and defended on the 2nd of July, 2024, in front of the jury composed of:

President	Pr. TADJINE Mohamed	ENP
Examiner	Pr. BOUDANA Djamel	ENP
Promoter	Pr. BERKOUK El Madjid	ENP
Guest	Dr. BENACHOUR Ali	ENP

ENP 2024

المدرسة الوطنية المتعددة التقنيات

قسم الآلية

Ecole Nationale Polytechnique

Département d'Automatique

End-of-studies project dissertation

for obtaining the State Engineer's degree in Automation and Control

Study of the Hybrid PV-Wind Installation of the Process Control Laboratory at ENP

Realized by:

Ms. MEZAACHE Taqwa

Publicly presented and defended on the 2nd of July, 2024, in front of the jury composed of:

President	Pr. TADJINE Mohamed	ENP
Examiner	Pr. BOUDANA Djamel	ENP
Promoter	Pr. BERKOUK El Madjid	ENP
Guest	Dr. BENACHOUR Ali	ENP

ENP 2024

المدرسة الوطنية المتعددة التقنيات

قسم الآلية

Ecole Nationale Polytechnique

Département Automatique

Mémoire de projet de fin d'études

pour l'obtention du diplôme d'Ingénieur d'État en Automatique

Etude de l'installation hybride PV-éolien du laboratoire de commande des processus de l'ENP

Réalisé par :
Mme. MEZAACHE Taqwa

Présenté et soutenu publiquement le 2 Juillet 2024, devant le jury composé de:

Président	Pr. TADJINE Mohamed	ENP
Examinateur	Pr. BOUDANA Djamel	ENP
Promoteur	Pr. BERKOUK El Madjid	ENP
Invité	Dr. BENACHOUR Ali	ENP

ENP 2024

ملخص

في هذا العمل، قمنا بدراسة ومحاكاة نظام هجين يجمع بين الطاقة الشمسية وطاقة الرياح مع تخزين البطارية في الوضع المستقل. كان هدفنا الرئيسي فهم كيفية عمل هذا النظام وتحسين أدائه. تم نمذجة ومحاكاة الجزء الكهروضوئي وجزء الرياح من النظام، بما في ذلك تقنيات تحسين نقطة الطاقة القصوى (MPPT) بالإضافة الى نظام التخزين. كما تم اجراء دراسة تقنية اقتصادية باستخدام برنامج HOMER Pro لتقييم كفاءة الطاقة والجدوى الاقتصادية والتأثير البيئي لنظامنا الهجين. أخيرًا، قمنا بمحاكاة كاملة للنظام باستخدام أداة Simulink/MATLAB حيث دمجنا جميع النماذج واقترحنا نظامًا لإدارة الطاقة وتقييم الأداء في ظل ظروف مختلفة. سمح لنا هذا المشروع بفهم تشغيل النظام بشكل أفضل وتقييم إمكانياته للاستخدام المستقبل.

كلمات مفتاحية : الطاقات المتجددة، الطاقة الشمسية، توربينات الرياح، النظام الهجين، آلة التيار المستمر، تتبع نقطة الإستطاعة القصوى، بطارية تخزين، إدارة الطاقة.

Résumé

Dans ce travail, nous avons réalisé une étude et une simulation d'un système hybride PV-éolien avec stockage de batterie en mode autonome. Notre objectif est de comprendre son fonctionnement, d'améliorer ses performances, et d'évaluer son potentiel d'utilisation en mode autonome. Nous avons examiné les sources d'énergie renouvelable, en particulier l'énergie éolienne et solaire. Ensuite, nous avons modélisé ces systèmes, les avons commandés en utilisant le MPPT, et effectué une analyse technico-économique avec HOMER Pro. Enfin, une simulation intégrée dans Simulink/MATLAB nous a permis d'évaluer la gestion de l'énergie et les performances du système dans diverses conditions.

Mots clés : Energies renouvlables,Photovoltaique, eoliennes, système hybride, hacheur, MPPT, Batterie, gestion d'energie.

Abstract

In this work, we conducted a study and simulation of PV-Wind hybrid system with battery storage system in standalone mode. Our main goal was to understand how this system operates and improve its performance.A modeling and simulation of the photovoltaic and wind systems, including Maximum Power Point Tracking (MPPT) techniques using DC/DC converters . Then a techno-economic study using HOMER Pro software. Finally, we conducted a thorough simulation of the system using Simulink/MATLAB, integrating all components and proposing an energy management system to evaluate performance across varied conditions. This project enhanced our understanding of system operation and assessed its potential.

Keywords : Renewable Energy, Photovoltaic, wind turbines, Hybrid system, DC/DC converter, MPPT, Battery, Energy management.

Dedication

<div dir="rtl">

﴿ وَآخِرُ دَعْوَاهُمْ أَنِ الْحَمْدُ لِلَّهِ رَبِّ الْعَالَمِينَ ﴾

</div>

"

*To the resilient Palestinians in Gaza, who inspire
hope and determination,
To my loving father, who taught me strength and
compassion,
To my nurturing mother, whose wisdom guides me
always,
To my brothers, Abed and Zahed, and my sister,
Yakine,
To my dear friends, Hadil, Sara, Zahra, Wissal and
Asma for their unwavering encouragement ,*

"

- Taqwa

Acknowledgments

All praise is to Allah first and foremost, the Most Gracious, and the Most Merciful, I am grateful to Allah who has given me grace and strength to complete this dissertation. Then, may blessings and peace be upon our Prophet Muhammad and upon all his Family and Companions.

I would like to express my sincere gratitude and appreciation to all those who have contributed to the completion of this work.

I would like to express my gratitude and sincere thanks to my supervisor, Pr. E.M BERKOUK for their guidance, expertise, and unwavering support.

I would also like to extend our heartfelt thanks to the members of the jury for their evaluation and critical review of this thesis. Their expertise and feedback significantly enriches the quality of this research.

I would like to extend my heartfelt gratitude to all the teachers in the Department of Control and Automation, for their dedicated efforts in imparting knowledge to us, contributing significantly to our academic and personal growth.

My deepest appreciation goes to my family and friends for their unconditional love and support, and to all the people who have been by our side throughout this thesis journey.

Contents

List of Tables

List of Figures

List of Acronyms

RES   Renewable Energy Sources

PV   Photovoltaic

STC   Standard Test Conditions

BESS   Battery Energy Storage System

WT   Wind Turbine

ES   Electrochemical Storage

EMS   Energy Management System

MPPT   Maximum Power Point Tracking

SOC   State of Charge

DCM   Direct Current Machine

DCG   Direct Current Generator

WECS   Wind Energy Conversion System

HES   Hybrid Energy System

PES   Power Management System

OM   Operation and Maintenance

NPC   Net Present Cost

Chapter 1

General Introduction

1 Motivation and Challenges

In recent years, there has been a notable shift in the global energy landscape, marked by significant transformations because of the complicated and increasing of electrical energy demand. This is due to economic development, industrial progress, and societal growth. This shift has highlighted the limitations and risks associated with fossil fuels as a primary source of energy, emphasizing their environmental impact, unsustainability, and contribution to climate change[1]. The need for transitioning towards a safer and more sustainable energy model for present and future generations is well articulated[2].
Renewable energies, such as solar and wind offer a promising alternative with significant untapped potential, crucial for transitioning to a sustainable and less carbon-intensive energy system[3].These sources naturally replenish over time, reducing reliance on depleting fossil fuels and combating global warming. The advantages of renewable energies include environmental sustainability, inexhaustibility, versatility, affordability, and the capacity to lower $CO2$ emissions [3]. Additionally, understanding the co-benefits of renewable energy, such as public health benefits, can accelerate the transition to environmentally friendly energies by increasing public awareness.

Algeria, being the largest country in Africa, has experienced a significant increase in energy demand due to substantial growth in residential, commercial, and industrial sectors over the past decade. Despite its heavy dependence on fossil fuels for electricity generation**01**, the country has been actively promoting renewable energy sources to diversify its energy mix and enhance energy security. Algeria has implemented legal and regulatory frameworks to encourage investments in renewable energies. Given Algeria's geographical advantages, solar and wind energy are among the most efficient options for sustainable energy production. However, the variability in wind speeds and solar irradiance, which depend on weather conditions, presents a significant challenge. To mitigate the intermittent nature of these renewable energy sources, hybrid systems that combine solar and wind energy can be employed. These systems can balance the production flow and meet the load demand by compensating for the fluctuations in each energy source[4]. Additionally, for off-grid applications, an effective storage system is crucial. Batteries are commonly used for this purpose, ensuring a stable and reliable energy supply.
The integration of renewable energy sources in standalone systems necessitates control strategies to balance energy generation and demand[5]. Energy storage solutions like batteries play a crucial role in enhancing system reliability and cost-effectiveness during emergencies, contributing to efficient power management and constant voltage and frequency supply to consumers[6].

2 Objectives and Contributions

The primary objective of this research is to design a hybrid renewable energy system that integrates solar photovoltaic panels and wind turbines with a battery storage system, ensuring a stable and reliable power supply for a bloc of research laboratories. To achieve this, we will first develop the control systems for each individual energy source. Then, we will proceed to the final stage, which involves integrating all components of the hybrid system. This will be followed by a load profiling and techno-economic study and the implementation of an energy management strategy to ensure efficient utilization of the produced energy.

3   Organization of the thesis

Our thesis is divided into four chapters, each with a specific objective:

- **Chapter 1:** This chapter presents an overview of renewable energy sources, including statistics on their availability and electricity production in Algeria and globally. It provides a literature review on solar and wind energy conversion, existing energy storage systems, classification of hybrid systems, various hybrid system configurations, and energy management methods for these systems. The chapter concludes by introducing the hybrid system considered in this study.

- **Chapter 2:** This chapter focuses on the modeling of the photovoltaic chain. We will discuss Maximum Power Point Tracking (MPPT) algorithms, particularly the Perturb and Observe (P&O) method. Then, we will integrate a battery storage system to build a control system for charge and discharge management and DC bus voltage stabilization.

- **Chapter 3:** This chapter deals with the wind energy conversion chain. The modeling of the wind chain begins with the turbine model and the mathematical model of the DC machine, the control of the wind energy conversion system involves implementing Maximum Power Point Tracking (MPPT) algorithms to optimize energy output from wind turbines

- **Chapter 4:** This chapter integrates all elements into a unified standalone hybrid system (PV-Wind-Battery). It conducts a techno-economic study using HOMER Pro software to determine the load profile that the system can support, based on real weather conditions. Additionally, an energy management system is developed and implemented using MATLAB/Simulink to optimize the utilization of available renewable resources, enhancing the system's efficiency. The chapter aims to validate the technical and economic feasibility of the hybrid system, estimate the load profile, and develop an energy management system implemented using MATLAB/Simulink.

    Finally, a general conclusion summarizes the main results achieved and the potential research perspectives opened by this work.

Chapter 2

Background & state-of-the-art

1 Introduction

The global demand for electricity has shown a consistent upward trend over the past fifty years, with consumption reaching around 25,500 terawatt-hours in 2022. During the period from 1980 to 2022, electricity usage has more than tripled [7]. Concurrently, pollution stemming from the combustion of fossil fuels has notably escalated in recent decades, resulting in adverse environmental and health consequences. This highlights the imperative need to increasingly rely on renewable energy sources to address these challenges and establish a sustainable energy landscape.

This chapter will explore various renewable energy sources in the context of electricity production, focusing particularly on photovoltaic and wind energies as primary sources for our case study. Additionally, we will delve into the operational principles of hybrid energy systems by introducing the proposed architecture for our study.

2 Renewable Energy

Renewable energy comes from unlimited, naturally replenished resources, such as the sun, tides, and wind. It can be used for electricity generation, space and water heating and cooling, and transportation. Renewable energy has two advantages over the fossil fuels that provide most of our energy today. First, there is a limited amount of fossil fuel resources (like coal, oil and natural gas) in the world. Second, renewable energy produces far less carbon dioxide (CO_2) and other harmful greenhouses gases and pollutants. Most types of renewable energy produce no CO_2 at all once they are running.

2.1 Motivation and applications

Renewable energy sources (RES) have garnered significant attention in recent decades due to their potential in addressing energy crises and environmental concerns[8].Their versatility and sustainability have led to widespread adoption across various sectors, offering a cleaner and more sustainable alternative to traditional fossil fuels.
The utilization of RES such as solar, wind, biomass, geothermal, and hydro-power enables access to energy to meet the demand for electricity, heating, and cooling[9].
Many countries are actively developing various renewable energy technologies to meet energy demands while reducing carbon emissions [10].Research has also highlighted growing public acceptance and enthusiasm for investing in renewable electricity[11].
Studies comparing renewable, nuclear energy, and fossil fuels have assessed their costs, emissions reductions, and energy security implications for power systems [12].
Renewable energy applications span various sectors, including residential, commercial, industrial, and medical facilities, offering sustainable alternatives to conventional energy sources while reducing environmental impact[13].

2.2 Renewable Energy Sources

Renewable energy sources are derived from various natural processes that are continuously replenished. These sources include: geothermal, wind, biomass, hydropower and solar Figure 2.1
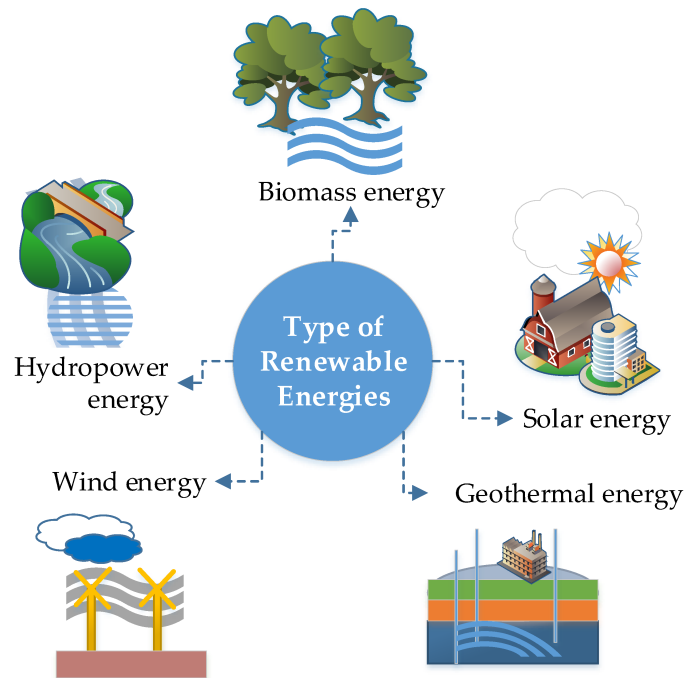
Figure 2.1: The types of renewable energy resources

2.2.1 Solar Energy

Derived from solar radiation through photovoltaic or thermal systems. The transformation process involves the conversion of sunlight into electricity using photovoltaic cells or the heating of a fluid (water or other liquids) through solar thermal collectors. In 2023, the worldwide solar capacity had reached approximately 770 gigawatts (GW), contributing to approximately 3.8% of the total global electricity consumption[14].

2.2.2 Wind Energy

Wind turbines convert the kinetic energy of wind to generate electricity.At the close of 2023, the worldwide wind power capacity stood at approximately 743 gigawatts (GW), constituting approximately 6.5% of global electricity consumption[14].

2.2.3 Hydropower

Hydropower, also known as water power, involves using falling or fast-running water to generate electricity or power machinery by converting water's gravitational potential or kinetic energy.

In 2020, hydropower constituted approximately 16.1% of the world's electricity consumption, with the total global installed capacity surpassing 1,300 gigawatts [14].

2.2.4 Geothermal Energy

Geothermal power is extracted from the Earth's internal heat flow. .Offering the dual potential for electricity generation or direct application in heating and cooling systems. In 2023, geothermal energy contributed to around 0.3% of global electricity consumption[14]

2.2.5 Biomass

Biomass energy, derived from organic sources like wood, crop residues, and animal waste, undergoes conversion into heat, electricity, or bio fuels. This renewable energy source constituted approximately 1.9% of global energy consumption in 2019[14].

2.3 Utilizing Renewable Energy for Electricity Generation

Electricity is an essential energy source that permeates various facets of society, including transportation, household activities, communication, industries, and entertainment. It serves as a fundamental pillar for economic growth across nations globally[15].The economic growth and population growth conduct to more electricity demand.The world's demand for electricity grew by 2.2% in 2023, Global electricity demand is expected to rise at a faster rate over the next three years, growing by an average of 3.4% annually through 2026[16].
This section focuses on the utilization of renewable energy sources for electricity generation. While non-renewable sources have traditionally been relied upon, their unsustainable nature and environmental impacts prompt a transition to sustainable alternatives. Renewable sources are examined as viable options for sustainable electricity production, with the goal of mitigating the risks associated with non-renewable energy while maintaining a reliable power supply[15].

2.4 Renewable Energy Status in the World

Most countries have recognized the importance of RE as a valuable component of their energy portfolio[17]. In response to increasing energy demands, many nations have shown a keen interest in investing in RE sources. This interest has prompted significant investments and the implementation of new policies and programs, particularly in developing countries, aimed at diversifying energy generation and increasing the penetration of renewable sources. According to a report by the International Energy Agency (IEA), there has been a noticeable shift in investment from fossil fuels to clean energy, with projections indicating a nearly doubling of investment in clean energy by 2023 as shown in fig 2.2. This indicates a growing global commitment to transitioning towards cleaner and more sustainable energy sources.
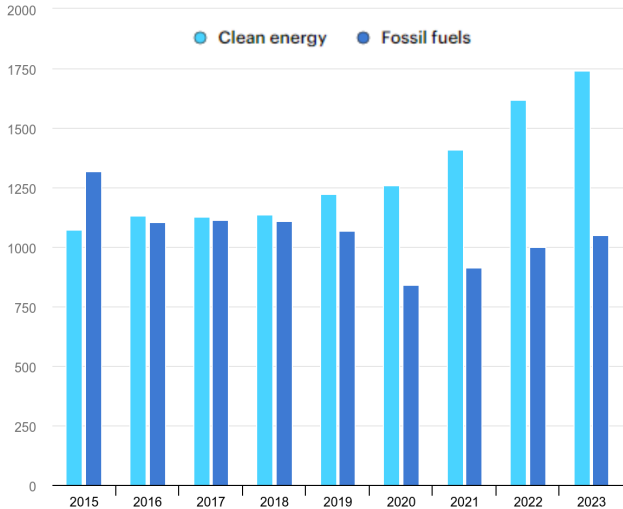
Figure 2.2: Global energy investment in clean energy and in fossil fuels, 2015-2023[18]

2.5 Renewable Energy Status in Algeria

The rapid industrialization and population growth in Algeria have resulted in an unprecedented surge in energy demand, necessitating a critical reassessment of sustainable energy sources to address the depletion of finite fossil fuels and their environmental impact.

Algeria's annual electricity consumption is 49 billion kWh, with an average of 1,217 kWh per person. By 2030, the electricity demand is projected to nearly double due to population growth , rising incomes, greater use of electrical devices, and increased electrically driven industrial processes[19].

In response to these challenges, Algeria has set ambitious targets, aiming to integrate 27% of renewable energy generation into its energy mix by 2030 (Fig 2.3). This commitment underscores Algeria's recognition of the imperative to transition towards cleaner and more sustainable energy sources to meet its growing energy needs while mitigating environmental impacts.
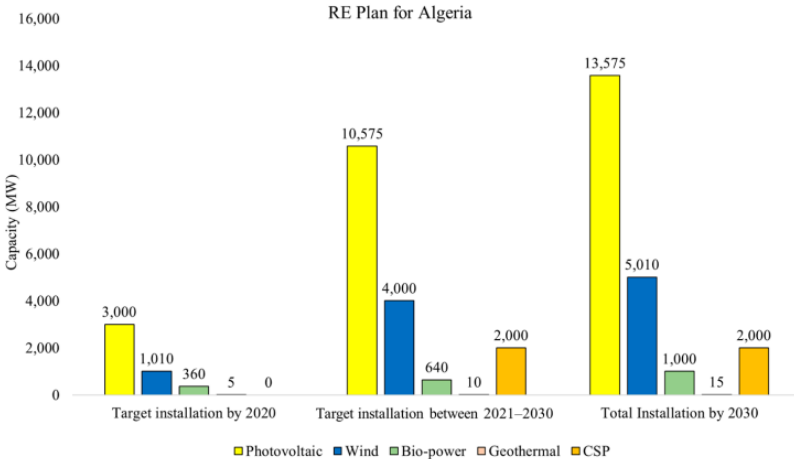
Figure 2.3: Algeria RE current and future generation plan[20]

3 Solar Energy

3.1 Motivation and applications

For thousands of years, solar energy has been a fundamental resource sustaining human endeavors. It can be harnessed directly as light energy to generate electricity through Photovoltaic (PV) Cells or utilized as thermal energy for a multitude of applications, including heating, cooking, drying, and electricity generation in thermal systems. However, in recent decades, the predominant method for solar electricity generation has been the utilization of PV cells due to their efficiency and reliability[21]. Remarkably, within just 60 minutes, the Earth receives sufficient energy from the sun to satisfy its energy requirements for an entire year[22]. This underscores the remarkable potential and efficiency of solar energy as a sustainable power source, demonstrating its significance in meeting global energy demands.

Solar photovoltaic (PV) systems harness sunlight to produce electricity, powering homes, businesses, and even entire communities. Additionally, solar thermal systems utilize solar radiation to generate heat for water heating, space heating, and industrial processes. Beyond electricity and heat generation, solar energy contributes to environmental sustainability by providing clean and renewable power for transportation, such as solar-powered vehicles and electric cars.

3.2 Principles of Photovoltaic Systems

3.2.1 PV Cell

The photovoltaic cell is the basic element of a solar system. It is defined as a device capable of converting light energy into electric current through the physical process known as the photovoltaic effect.

The PV cell consists of the mixture of semiconductor material type P and N. So, it is practically possible to consider a PV cell as a diode[23], Sunlight is composed of photons packets of solar energy.These photons contain different amounts of energy that correspond to the different wavelengths of the solar spectrum. Electricity is produced when photons are absorbed by the PV cell. The absorbed photon transfers its energy to an electron in a semiconductor atom, allowing the electron to leave its normal position and become part of an electrical current in a circuit. The PV cell has unique electrical properties, including a built-in electric field, that generate the voltage needed to drive the current through an external load Fig 2.4 [24].
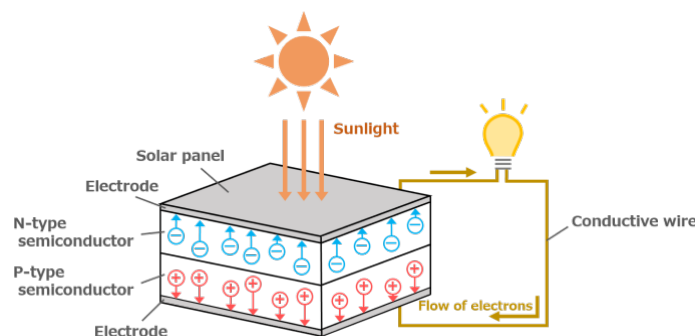
Figure 2.4: PV cell

1. **PV cell model**
   A PV cell model can be represented by a single-diode model or a double-diode model as shown in Fig 2.5

(a) Equivalent circuit of a single diode model   (b) Equivalent circuit of a double diode model
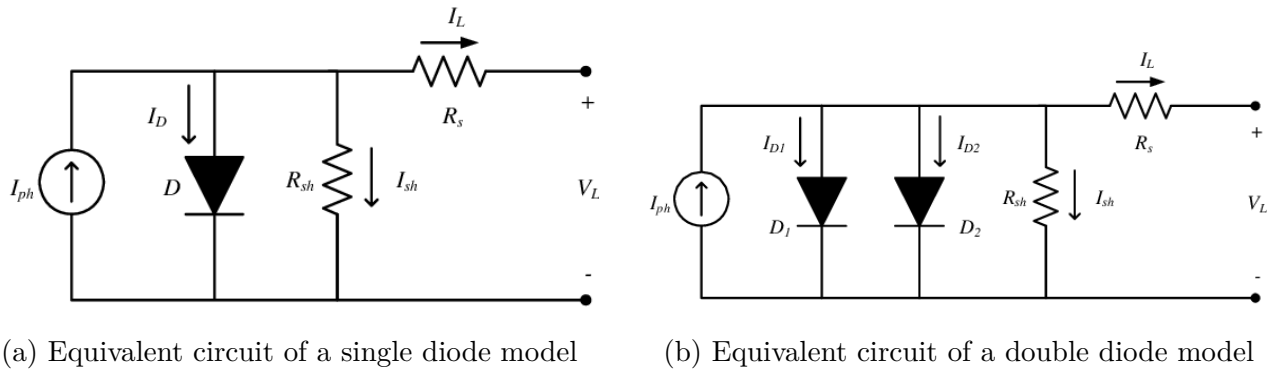
Figure 2.5: Equivalent circuit model

2. **PV cell characteristics**
   The photovoltaic cell present a non-linear I(V) characteristic. Figure2.6illustrates the I(V) and P(V) characteristic of a silicon-based PV cell for a given irradiance and temperature.
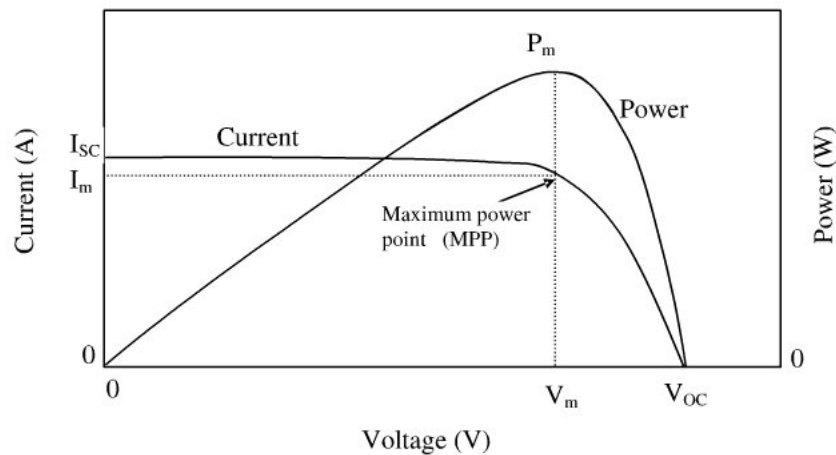
Figure 2.6: I-V and P-V Characteristics of Solar Cell[25]

3.2.2 PV module

Due to output current and output voltage of a PV cell is small, so PV cells are connected in series to increase output voltage and in parallel to raise output current. This set of cells is called a module.

To raise output power, PV modules are assembled and connected together to create a panel, which would also be connected together to create an array.

Photovoltaic (PV) modules or cells can be connected in series and parallel configurations to increase voltage and current output, respectively. In a series configuration, the voltage output of each module or cell is added together to achieve the desired voltage level. In a parallel

23

configuration, the current output of each module or cell is added together to increase the overall current output. The way the modules or cells are connected and their number depend on the application and the needs.

4 Wind Energy

4.1 Motivation and applications

Wind energy is increasingly recognized as a crucial solution for renewable electricity generation. It is distinguished among other renewable sources by its accessibility, environmental sustainability, and year-round availability[26]. These attributes are driving a growing interest in wind power generation within the field of electrical productionWind energy is widely applied in both mechanical and electrical sectors. Mechanically, it powers water-pumping systems through multi-blade windmills, effectively utilizing wind power for this purpose. Additionally, wind energy is extensively employed in electricity generation using wind turbines, which come in various sizes and types commercially, ranging from 400 watts to 5 megawatts[27]. The operation of wind turbines involves converting wind energy into electricity through a straightforward process: as the wind rotates the blades, they turn a shaft connected to a generator, thus producing electricity. This study will specifically focus on wind energy utilization through wind turbines.

4.2 Wind Turbines

A wind turbine is a device that transforms the kinetic energy of the wind into electricity. It accomplishes this by utilizing the force of the wind to drive an electric generator, which produces electricity. This generated electricity is then transmitted from the turbine to an available transformer, where it is converted to the appropriate output voltage.

4.2.1 Classification of WTs

Wind turbines can be classified from various perspectives, with one of the most common being the configuration of the turbine concerning the axis of rotation.

- **Horizontal-Axis Wind Turbines:**
  Horizontal axis wind turbines are the most widely used type of wind turbine, characterized by a rotor shaft positioned in the direction of the wind parallel to the Earth's surface, as depicted in Fig 2.7a. These turbines can feature a single, double, or three-bladed rotor design[28]. The blades of a wind turbine are designed to rotate by the aerodynamic lift force. This occurs due to the pressure difference created between the upper and lower faces of the turbine blades. The airspeed is faster on the front side of the blade, creating a low-pressure area, while the airspeed is slower on the rear side, creating a high-pressure area. The high-pressure air moves the blades upward, generating an aerodynamic lift. This relationship is known as Bernoulli's principle, which states that where the pressure is high, the speed will be low for a fluid. The turbine blades are attached to the rotor of

an electrical generator, which converts the mechanical energy generated by the turbine into electrical energy.

- **Vertical-Axis Wind Turbines:**
  A vertical axis wind turbine (VAWT) is a type of wind turbine where the rotor spins around a vertical axis, which is perpendicular to the direction of the wind.Because the rotor spins perpendicular to the wind, VAWTs don't require specific aerodynamics in their design[29].

(a) Horizontal-axis wind turbine

(b) Vertical-axis wind turbine

Figure 2.7: Types of wind turbines

We chose a horizontal-axis wind turbine for our project due to its superior advantages over the vertical-axis design, specifically its higher efficiency in converting wind energy into electricity and simplified maintenance requirements.

4.2.2 Wind Turbine Working Principle

A wind turbine is a device that transforms a portion of the kinetic energy of wind (a moving fluid) into available mechanical energy on a transmission shaft, and then into electrical energy through a generator[30].
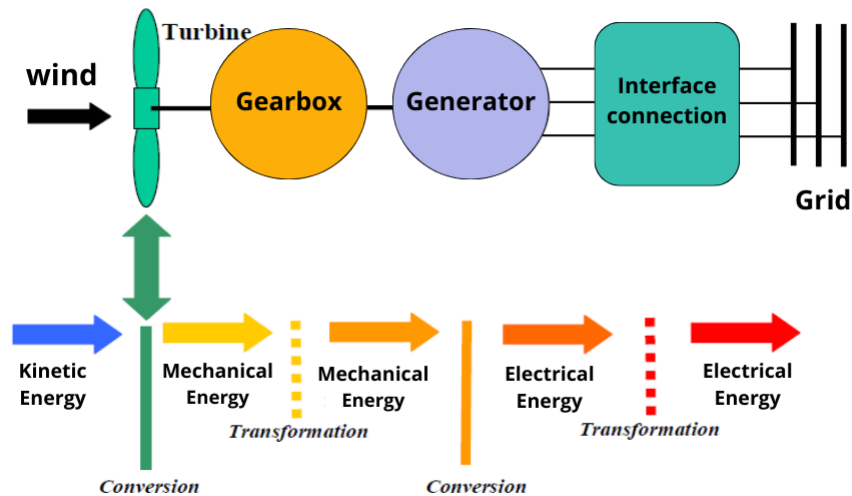
Figure 2.8: Principle of wind energy conversion

4.2.3 Basic Components of Wind Energy Conversion System

Diagram of different parts of wind turbine
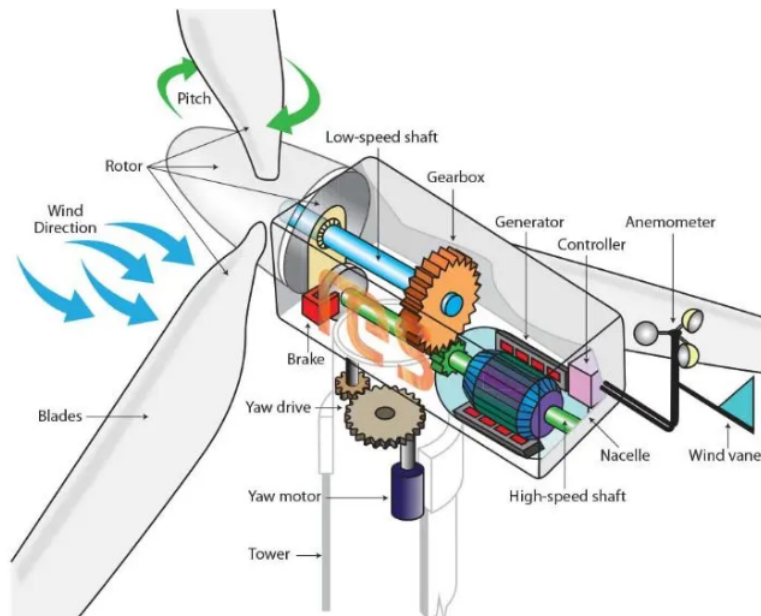
Figure 2.9: Wind Turbine Components [31]

As it is shown on Figure 2.9, there are many components in a wind turbine. Wind turbine components can be categorized into subsystems, which include:

- **Rotor**: Consisting of Blades and Hub

- **Drive Train**: Comprising the Low-Speed Shaft, Bearings, Couplings, Gearbox, High-Speed Shaft, and Brakes

- **Electrical**: Involving the Generator and Power Electronics

- **Control**: Including Pitch motor and gears, Yaw motor, gears and brakes, as well as sensors for wind and direction

- **Support Structures**: Tower, Nacelle

Next, Each subsystem's component will be discussed individually:

- **Blades**: designed to capture the kinetic energy of the wind, rotating as the wind blows, driving the rotor and converting wind energy into mechanical energy.

- **Hub** : serving as the connection point for the blades.

- **GearBox** : It serves to increase the rotational speed of the low-speed shaft coming from the rotor hub. This increased speed is necessary for efficient electricity generation by the generator.

- **Brake** is a safety mechanism used to control the rotation of the rotor blades.

- **Generator** : is responsible for converting mechanical energy into electrical energy. There are several types of generators used in wind turbines, including:AC Synchronous Generators, AC Asynchronous Generators, DC generator.

- **Yaw system**: responsible for orienting the rotor towards the wind. It ensures that the wind turbine captures the maximum amount of wind energy by aligning the rotor disk perpendicular to the wind direction.

- **Anemometer** : is a device used to measure wind speed.

- **Wind vane** : is an instrument used to determine the direction of the wind.

- **Tower** : houses all the key components of a contemporary wind energy conversion system, excluding the rotor. Positioned atop the tower, it serves as a central structure for these components.

- **Nacelle** :A streamlined enclosure that houses the generator, gearbox, control systems, and other essential components.

5 Energy Storage

The increasing use of renewable energy sources and the necessity for transportation methods with lower CO_2 emissions have sparked renewed interest in energy storage, which has become a fundamental aspect of sustainable development. Energy storage plays a central role in renewable energy plants, allowing for the smoothing of power fluctuations, improving system flexibility, and enabling the storage and distribution of electricity generated by variable renewable sources such as wind and solar. Various storage technologies are utilized in electric power systems, including electrochemical, mechanical, electromagnetic methods[32].

5.1 Electrochemical storage

Various types of electrochemical storage (ES) technologies are utilized, including batteries and fuel cells.ES offers several advantages. It meets a multitude of power and energy storage requirements and is both scalable and modular. Moreover, it demonstrates high efficiency, with many electrochemical storage technologies achieving impressive round-trip efficiency rates.

5.1.1 Batteries Energy Storage Systems

The preferred mode of electrical energy storage currently prevalent in our daily lives remains the accumulator, whether in the form of mobile phones or cars, batteries are widely used.The technology is based on the chemical concept of a cell: chemical energy is stored. Fundamentally, the basic element of a battery consists of two electrodes serving as the anode and cathode, along with an electrolyte in contact with these electrodes allowing for the circulation of ions and thus the creation of a current[30].Among the numerous pathways currently being developed[32]:

- Leade-acid batteries: commonly used to power installations that cannot withstand power outages (photovoltaic or hybrid installations in isolated sites)

- Lithium ion (Lieion) batteries and All pathways derived from lithium batteries : commonly used for uninterrupted power in emergency systems, solar storage, electronics, mobility aids, and electric vehicles.

- Nickel-cadmium batteries: widely used in all electric vehicles. The main drawback of this pathway lies in the use of Cadmium, which is a heavy metal.

5.1.2 Fuel cells

A fuel cell uses the chemical energy of hydrogen or other fuels to cleanly and efficiently produce electricity. If hydrogen is the fuel, the only products are electricity, water, and heat. Fuel cells are unique in terms of the variety of their potential applications; they can use a wide range of fuels and feedstocks and can provide power for systems as large as a utility power station and as small as a laptop computer.

5.2 Mechanical storage

Mechanical energy storage systems are used to store excess mechanical or electrical energy as kinetic energy in flywheels, potential energy in water, or compression energy in air, to be used as mechanical or electrical energy during high demand times. The three main mechanical energy storage systems are pumped hydro storage (PHS), compressed air energy storage (CAES), and flywheel energy storage (FESS).

5.3 Electrical storage

Electric energy storage primarily involves the utilization of supercapacitors and magnetic storage techniques[32].

- Super capacitor energy storage : utilizes polarized liquid layers to enhance capacitance, offering higher energy and power density. It's often integrated with batteries in wind energy setups to mitigate rapid power fluctuations[32].

- Superconducting magnetic energy storage:ses a coil of superconducting material cooled cryogenically to store energy in a magnetic field generated by direct current flow. It offers high efficiency but is not ideal for wind energy systems due to temperature sensitivity[32].

6   Hybrid Energy systems

6.1   Motivation and applications

Hybrid systems, which integrate diverse energy sources and storage solutions, are a notable trend in renewable energy technology. Among these, combining wind and solar PV energy, coupled with battery storage units, stands out as the most effective hybrid configuration. This setup caters to various applications while adapting to seasonal variations. For example, wind power compensates for reduced solar energy output during monsoon months, while solar PV systems dominate during the post-winter period when wind energy production diminishes [33]. Despite the individual drawbacks of each technology, hybrid energy systems are utilized to mitigate the intermittency, uncertainty, and limited availability of single renewable energy sources, thereby enhancing overall system reliability [34].
The adoption of such multi-source systems has significantly progressed across diverse industries, including automotive, marine, aviation, electronic devices, and power stations [35].

6.2   Classifications of hybrid systems

HRESs are categorized based on various criteria, with the most commonly used classifications. Figure 2.10 illustrates various potential combinations of Hybrid Energy Systems.
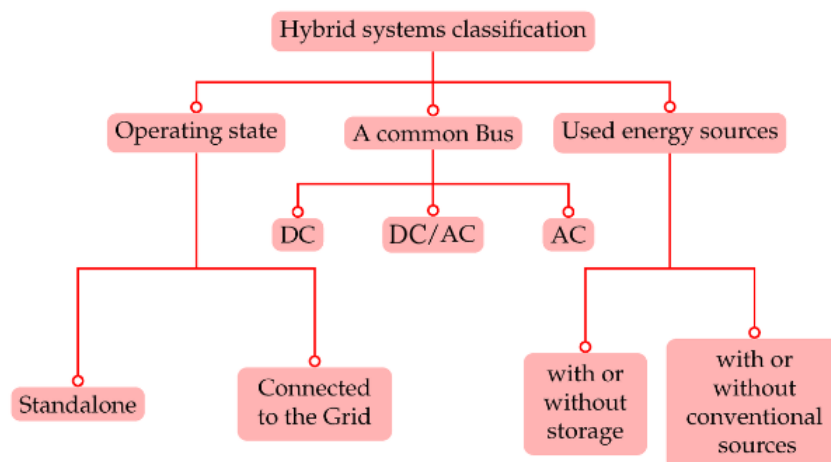
Figure 2.10: Various types of Hybrid Energy Systems [36]

6.2.1   Operating State

There are two main categories of hybrid energy systems [30]:

1. The first group includes systems that operate in parallel with the electrical grid, known as "grid-connected" systems.

2. The second group comprises systems that operate autonomously known as "standalone systems", providing for the needs of consumers located in remote areas without access to the electrical grid.

6.2.2   Bus configuration

Hybrid energy systems can be classified based on their common bus architecture into three main categories: common DC bus, common AC/DC bus, and common AC bus[36]:

- **Common DC bus architecture**: A hybrid system featuring a DC bus. It integrates a wind turbine generator and a photovoltaic generator connected to the DC bus via converters, along with an energy storage system linked through a bi-directional converter. This setup enables the system to power both AC and DC loads, requiring a DC/AC converter for AC load supply[36].

- **Common AC bus architecture**: A hybrid system with a shared AC bus, where the PV and the wind turbine is connected to the AC bus via a DC/AC converters. The storage system is connected to a bi-directional DC/AC converter. This configuration enables the AC/DC converter to supply DC loads, and other renewable resources can be integrated[36].

- **AC and DC bus architecture**: A hybrid system featuring two buses: an AC bus and a DC bus. In this setup, sources with alternative current are linked to the AC bus, while sources with direct current are connected to the DC bus.This configuration is widely favored for its flexibility in combining power resources and loads [36].

6.2.3   Used energy sources

Depending on the content of the hybrid system, two criteria can be considered:

- The presence or absence of a conventional energy source, which could be a diesel generator or a gas turbine, among others.

- The presence or absence of a storage device, which ensures better satisfaction of electrical loads.

6.3   Energy management of Hybrid systems

Energy management is essential for smart grid efficiency, reliability, and cost-effective, environmentally friendly goods and services production. The goal is to optimize profits (minimize

costs) and enhance competitive positions while minimizing environmental impact. This approach is defined as "the wise and efficient use of energy". However, due to the intermittent nature of renewable energy sources and the random demand of the load, different management and supervision strategies have been proposed for hybrid power systems. The challenge is to control the converters associated with each source to achieve specific objectives, such as maximizing generated power or adapting production to demand[36].The literature has proposed various energy management system strategies to tackle challenges in hybrid power systems, utilizing both conventional and artificial intelligence-based methods.
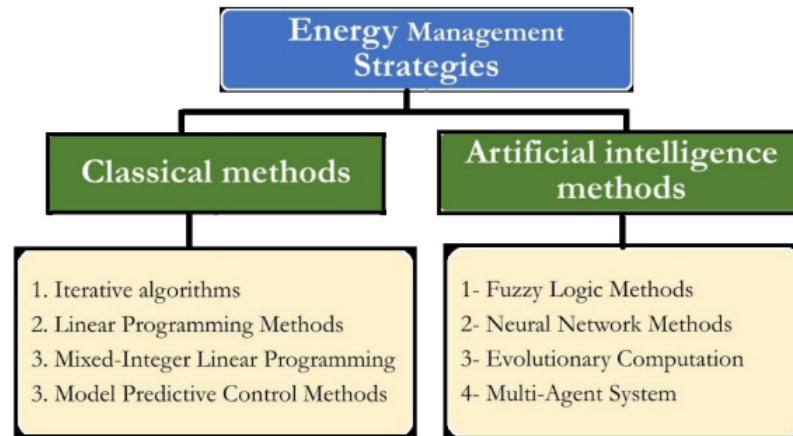
Figure 2.11: Classifications of EMSs[36].

These systems aim to minimize costs, reduce fuel consumption, maximize the use of renewable energy sources, and prolong the lifespan of energy storage units by effectively distributing power based on demand and operational conditions. By utilizing advanced control algorithms and simulation tools like Simulink, researchers have demonstrated significant improvements in energy security, system effectiveness, cost optimization, and overall performance of hybrid energy systems[37].

7 Presentation of Studied Hybrid System

In our research, we concentrate on standalone hybrid system that combines two renewable energy sources: photovoltaic generator connected to the DC bus via DC/DC converters with MPPT control, and wind power system utilizing a DC generator. To integrate the wind turbine with the DC bus, connecting a DC/DC converter is essential to regulate the wind turbine's DC voltage, ensuring compatibility with the DC bus. These renewable energy sources are paired with an electrochemical battery storage system. The hybrid configuration examined in this project feature a DC bus, which makes the system ideal for microgrid applications and powering continuous loads, offering enhanced reliability due to the combined renewable sources and battery storage, efficient energy management through optimization of both energy sources, and scalability for adapting to various power demands.
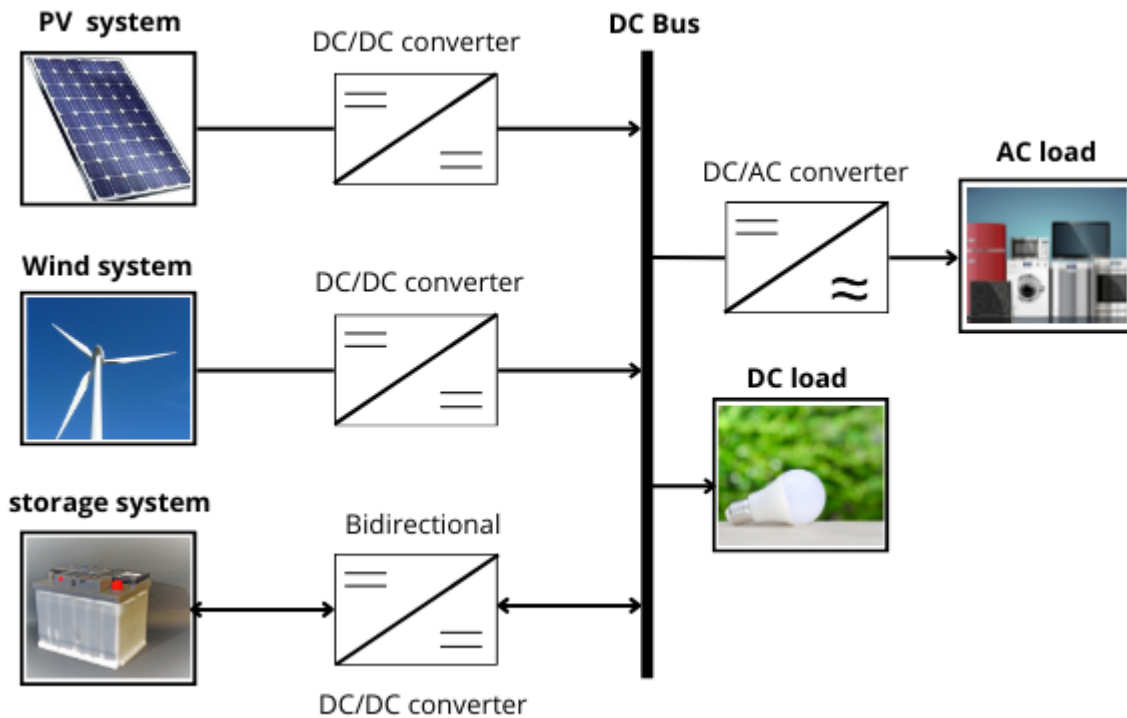
Figure 2.12: Studied Hybrid System architecture

8 Conclusion

This chapter offers an in-depth exploration of renewable energy resources, with a particular focus on photovoltaic and wind energy. We delve into the principles of electricity generation from these renewable sources and discuss various energy storage systems. Furthermore, we introduce hybrid energy systems and present the hybrid wind-photovoltaic system that will be the focus of our study.

The following chapter focuses on the modeling and control of a photovoltaic system in detail. This in-depth analysis will provide the foundation for understanding the complex dynamics of these systems and their integration within a larger hybrid energy system context.

Chapter 3

Modeling and Control of the Photovoltaic System

1 Introduction

This chapter focuses on the modeling and control of the photovoltaic generator with the aim of maximizing its power (Maximum Power Point Tracking (MPPT). We will begin by establishing the mathematical model of the PV generator, then move on to the modeling of the buck converter, and finally apply the MPPT algorithm (P&O).
Following the modeling and control of the PV generator and the power converter, the integration of a storage system is conducted utilizing a battery storage system, with a bidirectional DC/DC converter.
This system enables:

- Controlling the power generated by the PV generator.

- Maintaining a constant DC bus voltage.

2 Architecture of the PV System
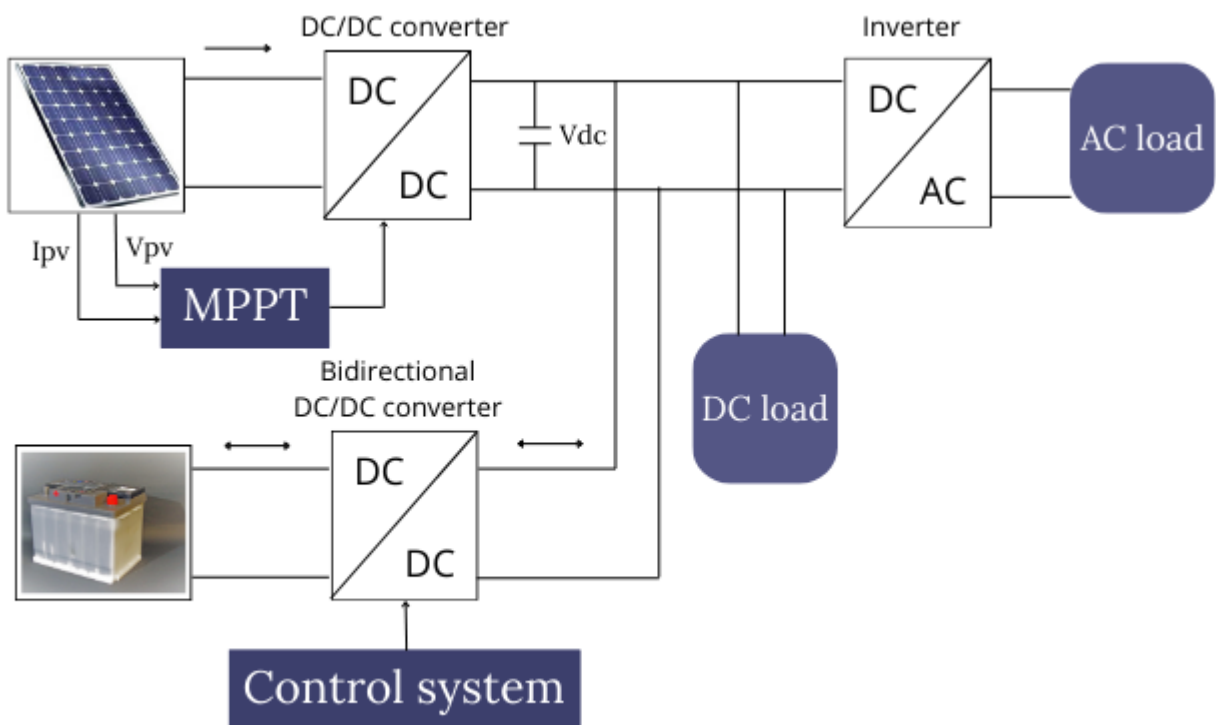
Figure 3.1: Architecture of the PV-Battery System

3 Photovoltaic Panel Model

3.1 Model of a photovoltaic cell

The most commonly used model for photovoltaic cells is the equivalent circuit model with one diode, as shown in the figure 3.2
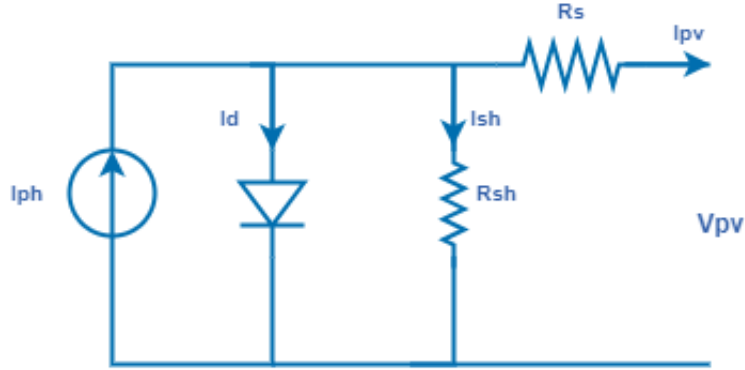
Figure 3.2: Equivalent circuit of a solar cell

In this equivalent circuit, the PV cell is considered as a current source with the photovoltaic effect. The output current is expressed as [38]

$$I_{pv_{cell}} = I_{ph} - I_d - I_{Rsh} \tag{3.1}$$

Where:

- $I_{pv_{cell}}$: current delivered by the cell (A)

- I_{ph}: photocurrent of the PV generator (A)

- I_d: diode current (A)

- I_{sh}: shunt curren R_{sh} (A)

The current through these elements is governed by the voltage across them:

$$V_{pv_{cell}} = V_d - I_{pv_{cell}}R_s \tag{3.2}$$

where

- V_d: voltage across the diode and the resistor R_{sh} (V)

- $V_{pv_{cell}}$: voltage across the output terminals (V)

- R_s: series resistor (Ω).

4 PV panel modeling

The PV panel modeling involves the configuration of Ns (number of PV cells in series) and Np (number of PV cells in parallel).

The current delivered by PV panel expressed as :

$$I = N_p I_{pv_{cell}}$$

And the voltage :

$$V = N_s V_{pv_{cell}}$$

4.1 Photo-Current I_{ph}

When the cell operates under short-circuit conditions, $V = 0$, and the current I_{pv} flowing through the terminals is referred to as the short-circuit current (I_{sc}). For a high-quality PV cell (characterized by low values of R_s and a high value of R_{sh}) [39], the photo-current is expressed as:

$$I_{ph} \approx I_{sc}$$

The current I_{ph} considering the impact of irradiance and temperature, is expressed as:

$$I_{ph} = \frac{G}{G_r}[I_{scr} + a_i(T_c - T_r)]$$

Where:

- G: irradiance (W/m²).

- T_c: cell temperature (K).

- I_{scr}: short-circuit current measured in Standard Test Conditions (A).

- G_r: Standard illumination (1000 W/m²).

- T_r: standard temperature (298.15 K).

- a_i: temperature coefficient of short-circuit current(K)

4.2 Diode current I_d

The current through the diode is expressed as:

$$I_d = I_0 \cdot \left(exp\left(\frac{V_d}{nV_t}\right) - 1\right) \tag{3.3}$$

with:

- I_0: saturation current (A).

- n: diode ideality factor (1 for an ideal diode).

- V_t: Thermal voltage (V)

$$V_t = \frac{N_s K T_c}{q}$$

where:

- K: Boltzmann's constant (1.3806×10^{-23} J/K),

- T_c: Temperature (K)

- q: Elementary charge (1.6022×10^{-19} coulomb).

4.3 Saturation Current I_0

The saturation current is defined by the equation [38]:

$$I_0 = I_{0_{\text{ref}}} \cdot \exp\left(\left(\frac{q \cdot E_g}{n \cdot K}\right) \cdot \left(\frac{1}{T_r} - \frac{1}{T_c}\right)\right] \left(\frac{Tc}{Tr}\right)^3$$

where:

- $I_{0_{\text{ref}}}$: Reference saturation current

- E_g: Band gap energy

- N_s: The number of solar cells connected in series in a photovoltaic panel

- n: Diode ideality factor

4.4 Reference saturation current $I_{0_{\text{ref}}}$

Defined at a specific reference temperature and solar radiation level. It serves as a fundamental value for characterizing the behavior of solar cells under standard conditions, It can be expressed as : [38]

$$I_{0_{\text{ref}}} = \frac{I_{sc}}{\exp\left(\frac{V_{oc}}{V_t}\right) - 1}$$

The open-circuit voltage is expressed as:

$$V_{OC} = V_{OCr} + a_v \left(T - T_r\right)$$

With:

- V_{OCr} : open-circuit voltage in STC.

- a_v : temperature coefficient of open circuit voltage.

The short-circuit current is expressed as :

$$I_{sc} = I_{scr} + a_i \left(T - T_r \right)$$

With:

- I_{scr} : Short-circuit current in STC.

- a_i : temperature coefficient of Short-circuit current.

4.5   Series resistor R_s

Its value can be provided by the manufacturer. Otherwise, we can estimate it using the following equation:[38]

$$R_s = \frac{nV_{tr}ln(1 - (I_{mp}/Iscr)) - V_{mp} + V_{ocr}}{I_{mp}}$$

In this study, we consider R_s as constant.

The final equation for the current and voltage of a PV panel becomes:

$$I = N_p \left(I_{ph} - I_0 \left(\exp \left(\frac{V_d}{nV_t} \right) - 1 \right) \right) - \frac{V + IR_s}{R_{sh}} \tag{3.4}$$

5   Simulation Results & Performances :   Temperature and irradiance effect

We used the "SOLAR-FABRIK Pro L3 poly panel" as a model and represented its parameters in the table below to proceed with this step. Its parameters under standard conditions (25°C, 1000 W/m²) are provided by the manufacturer.
The detailed model of a photovoltaic panel consisting of 60 cells in series is developed in the MATLAB environment, based on the mathematical equations discussed earlier. The inputs for this model are solar irradiance G and ambient temperature T_c. By utilizing data provided by the standardized panel data-sheet, we are able to calculate the parameters of the model (R_s, R_{sh}, I_{ph}, I_0).enables us to obtain the output current.The model parameters utilized in the simulation are detailed in Table 3.1

Table 3.1: Solar panel parameters for Pro L3 poly.

Parameter	Value
Maximum power (Pmax)	250.0332 W
Current at maximum power point (Imp)	8.34 A
Voltage at maximum power point (Vmp)	29.98 V
Short-circuit current in STC (Iscr)	8.84 A
Open circuit voltage in STC (Vocr)	37.54 V
Number of cells in series (Ns)	60
Number of cells in parallel (Np)	1
Current temperature coefficient (a_i)	$0.034 \cdot 10^{-2}$
Voltage temperature coefficient (a_v)	$-0.34 \cdot 10^{-2}$

5.1 Solar Irradiance Effect

The current-voltage characteristics of the model for different solar irradiances, and at a temperature of 25°C are illustrated in 3.3

(a) I-V characteristic

(b) P-V characteristic
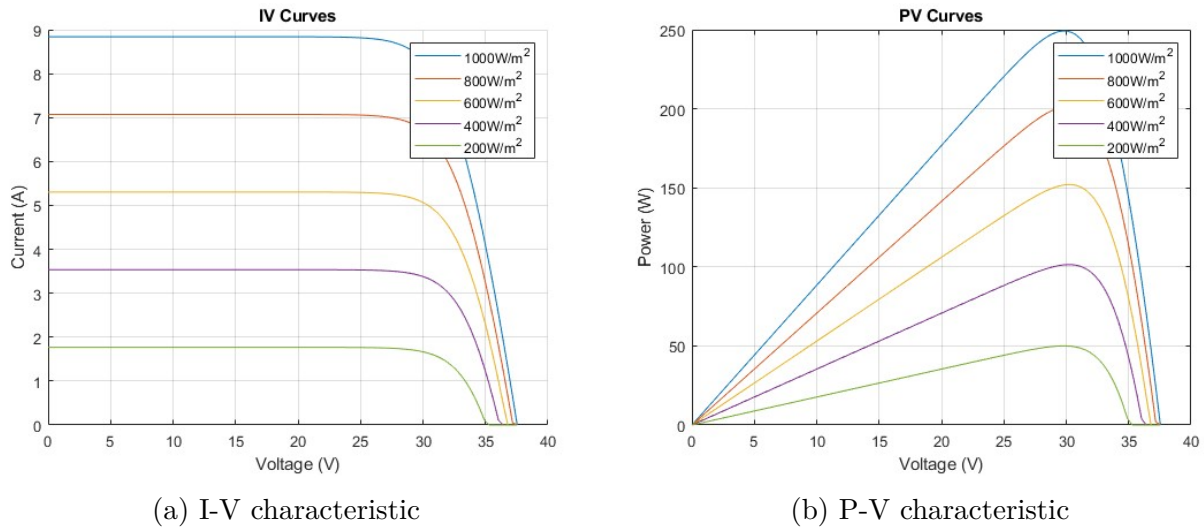
Figure 3.3: Effects of solar irradiance at constant temperature on the PV panel

The value of the short-circuit current is directly proportional to the irradiance G. In contrast, the open-circuit voltage does not vary in the same proportions but remains nearly constant even at low value of G . This implies that: The optimal power of the cell (Pmax) is practically proportional to the G. The points of maximum power are located at approximately the same voltage**PSG**.

5.2 Temperature Effect

The current-voltage characteristics of the model for different Temperatures, and at an irradiance of 1000w/m2 are illustrated in 3.4

(a) I-V characteristic

(b) P-V characteristic
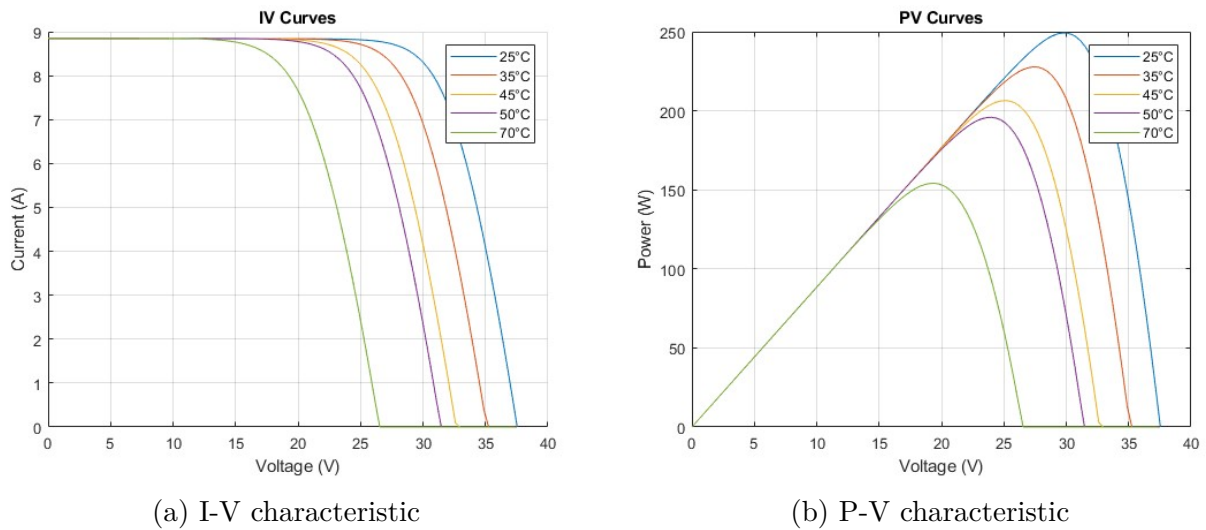
Figure 3.4: Effects of Temperature at constant solar irradiance on the PV panel

The temperature has a negligible influence on the value of the short-circuit current. However, As temperature increases, the open-circuit voltage (Voc) of the PV panel decreases, leading to a reduction in power output. This decrease in Voc due to elevated temperatures impacts the efficiency and overall performance of the panel. Additionally, the efficiency of a PV panel decreases with rising temperatures, highlighting the importance of managing heat dissipation and optimizing operating conditions to maintain optimal performance levels.

6 PV generator model

The PV generator or string is composed of 4 solar panels, each with a power rating of 250 W, and is arranged in a specific configuration with 2 panels connected in series (Nss=2) and 2 panels connected in parallel (Npp=2) , as illustrated in Figure 3.5.

Figure 3.5: Photovoltaic Generator

The current delivered by PV generator expressed as :

$$I_{pv} = 2I$$

where I represents the current delivered by a single PV panel.
Similarly, the voltage is given by:

$$V_{pv} = 2V$$

where V denotes the voltage of a single PV panel.

7 Photovoltaic control system

Control systems are crucial in PV systems to regulate the voltage and current produced by the solar panels, ensuring maximum power output and system efficiency, to harvest the maximum am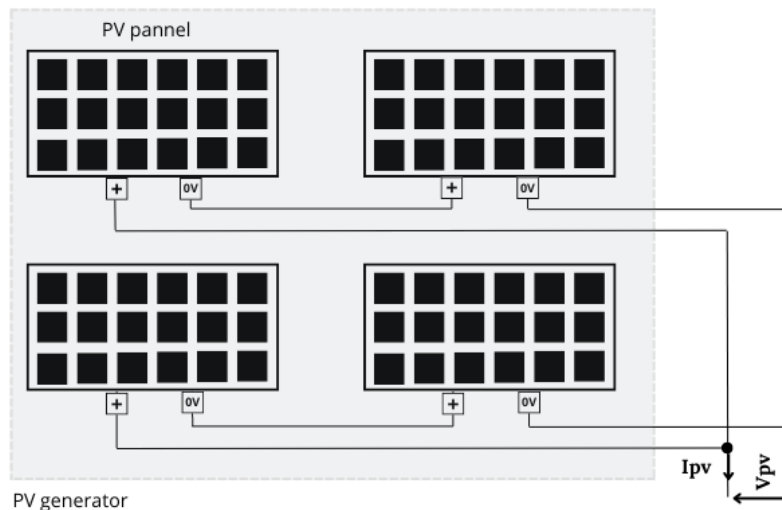ount of power and operate the PV generator at its maximum power point, the load needs to be properly adapted. Directly connecting a load is not recommended for maximum power output and efficiency. Instead, a power converter.

7.1 Power Converters

Power converters are electronic devices that can be used as impedance adapters to maximize the power output of PV generators. By adjusting the input impedance of the power converter. DC-DC converters are a type of power converter that is essential in many modern energy applications. The switching characteristics of DC-DC converters are used to convert dc voltage of one level (normally unregulated voltage) to dc voltage of another level (regulated voltage). The conversion is carried out using a circuit containing storage elements such as inductors and capacitors and power devices like transistors, MOSFETs, IGBTs and diodes**DC**.
The converters perform important work in PV power generation systems for MPPT and interfacing PV system output with varying types of loads. There are three primary types of DC-DC converters categorized by the relationship between output and input voltages:

- Buck Converter.

- Boost Converter.

- Buck-Boost Converter.

7.2 DC-DC Buck converter

This type of converter is utilized to reduce the input DC voltage to a lower DC voltage at the output. It comprises the same components as a boost converter, but the difference lies in the placement of components.The input voltage on the LC circuit is manipulated using pulse width modulation (PWM), which involves applying the supply voltage,V_i, for a fraction of the cycle time and leaving it at zero for the rest of the cycle. The duty cycle, d, is the ratio of the time that the supply voltage is applied to the total cycle time, and it serves as the control signal for the Buck converter, ranging from 0 to 1.Figure 3.6 illustrates the buck converter topology [40].
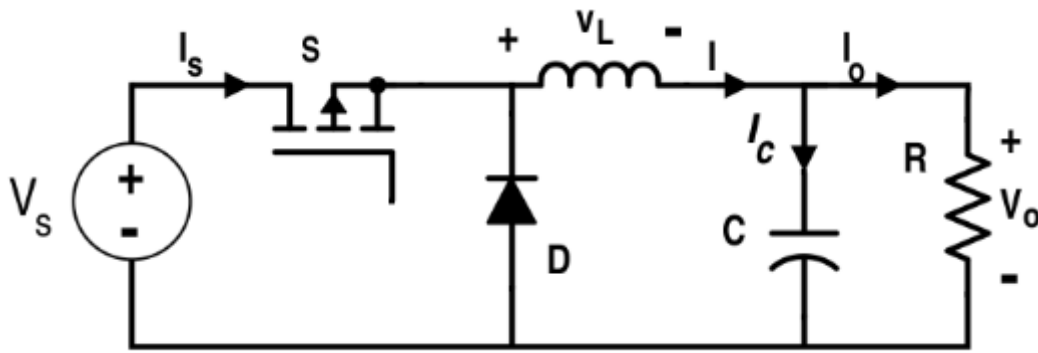
Figure 3.6: Buck converter circuit diagram

The equivalent circuit during switch on and off condition of the switch S is shown in Figure 3.7 and Figure 3.8 respectively:
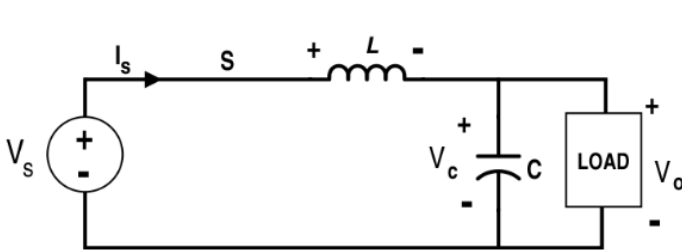
Figure 3.7: Buck converter circuit when switch S is ON
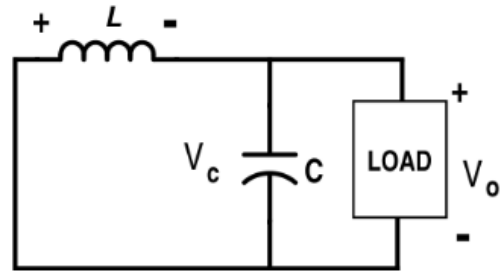
Figure 3.8: Buck converter circuit when switch S is OFF

The system must be modeled in order to establish the relationship between the input signal and the output. Two operating intervals of the converter are distinguished :

0,DT : (S :closed , D :blocking)

During this interval the switch S is ON (S=1), the switch conducts and input voltage V_i is applied to inductor directly so inductor current increases ,storing energy. Inductor voltage and current equations are given in 3.7.Output capacitor feeds the load and discharges, simultaneously while inductor stores energy. The equations of the capacitor are given in 3.8 [40]

$$V_L = L\frac{di_L}{dt} = V_i - V_o \tag{3.5}$$

$$i_c = C\frac{dV_o}{dt} = i_L - \frac{V_o}{R} \tag{3.6}$$

- $[DT, T]$: (S :opened , D :bypass)

$$V_L = L\frac{di_L}{dt} = -V_o \tag{3.7}$$

$$i_c = C\frac{dV_o}{dt} = i_L - \frac{V_o}{R} \tag{3.8}$$

Duty Cycle D The first step is to determine the duty cycle D, It allows adjusting the average output voltage for a given average input voltage. In our specific case D is determined by a control system,which is the Maximum Power Point Tracking (MPPT) algorithm.

$$D = \frac{t_{on}}{T}$$

Where:

- V_i: Voltage at the terminals of the PV generator (V)

- V_o: Output voltage of the converter (V)

- T: Switching period of the switch signal (S), with:$T = \frac{1}{f_s}$

- f_s: Switching frequency

- t_{on}: Switching period of the switch (K)

In accordance with the inductor volt-second balance principle, the average voltage across the inductor remains zero during steady-state operation.

$$\langle V_L \rangle = DT(V_i - Vo) + (1-D)T(-V_o) = 0$$

Therefore, we obtain:

$$D(V_i - Vo) = (1-D)V_o \tag{3.9}$$

This leads to:

$$V_o = DV_i \tag{3.10}$$

This expression highlights that the Buck converter acts as a current step-up device. Furthermore, it underscores that the duty cycle "D" allows for the adjustment of the average output voltage relative to a given average input voltage.

7.2.1   Inductance and capacitor selection :

The inductance L ensures energy storage and the ripple current through it.which is introduced by the following equations:[41]

$$\Delta I_L = I_{L_{max}} - I_{L_{min}}$$

from 3.7 Current increment during switch on:

$$\Delta I_{\mathrm{L}} = I_{\max} - I_{\min} = \frac{V_i - V_o}{L} DT \tag{3.11}$$

We deduce the following expression for ΔI_L:

$$\Delta I_L = \frac{(1 - D) \cdot V_o}{L \cdot f}$$

from 3.10 we obtain :

$$\Delta I_L = \frac{(1 - D) V_o}{L \cdot f}$$

The inductance for a buck converter is given by the equation:

$$L = \frac{(1 - D) V_0}{\Delta I_L f} \tag{3.12}$$

Calcuate of Capacitor C The capacitor aims to absorb current ripple and maintain a relatively constant voltage to generate sinusoidal output voltages.
The value of the output capacitor C can be calculated using the following formula:

$$C = \frac{\Delta I_o}{8 f_s \Delta V_o}$$

ΔV_o : The allowed ouptup voltage ripple.
ΔI_o : The allowed output current ripple

7.3   Maximum Power Point Tracking

MPPT employs an algorithm to continuously adjust the voltage of the photovoltaic generator to approach its maximum power point. The duty cycle of the DC-DC converter plays a crucial role in managing this tracking process, ensuring efficient control and optimization of the PV system's power output[42]. This control strategy utilizes PWM technology to adjust the duty ratio of PWM pulses, optimizing the relationship between the input and output of the DC/DC converter for effective MPPT control[43].

7.3.1   Perturb & Observe Algorithm

The Perturb and Observe algorithm tracks the Maximum Power Point in response to changes in weather conditions by perturbing the system. This perturbation involves either decreasing or increasing the output voltage through changes in the duty cycle and observing the resulting impact on the output power. As depicted in Figure 3.9, if the PV output power (Ppv) increases

(P(k)>P(k-1)), the output voltage (Vpv) is regulated in the same direction as the previous cycle. Conversely, if the output power decreases(P(k)>P(k-1)), the output voltage is perturbed in the opposite direction. Once the MPP is detected, the output voltage will stabilize around the maximum operational voltage.
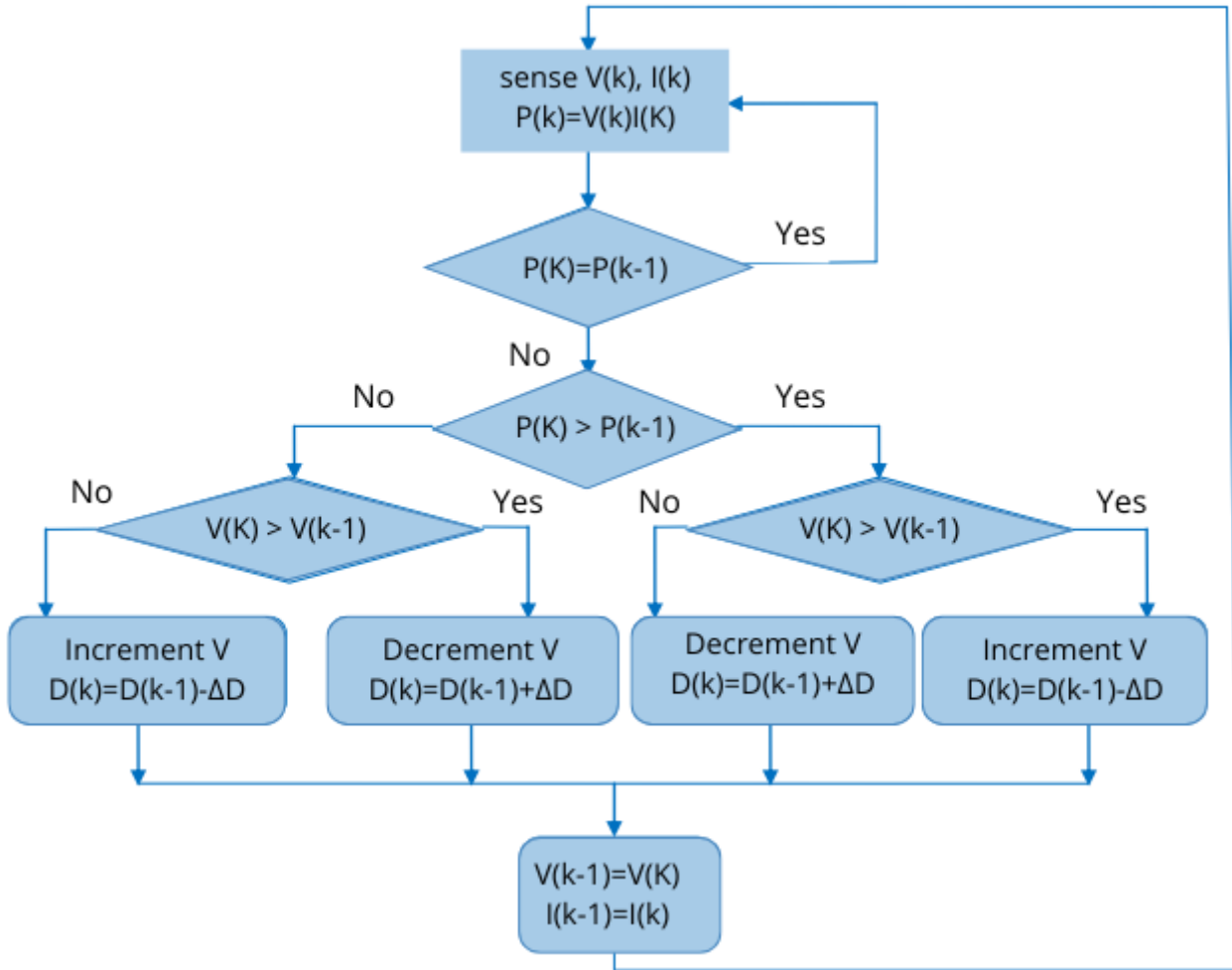
Figure 3.9: P&O method Flowchart

7.4 Simulation result and Analysis

7.4.1 Description

The MATLAB simulation involves modeling a 1 kW photovoltaic solar system, consisting of 4 solar panels, each rated at 250 Wp, A buck converter with MPPT using Perturb and Observe method (P&O) algorithm is employed to optimize solar energy conversion efficiency. The electrical parameters of the adopted PV panel "SOLAR-FABRIK Pro L3 poly" are summarized in Tables 3.1.

7.4.2 Results

The model is simulated under constant temperature of $25 \deg^C$ and different irradiation values as illustrated in figure 3.10a

(a) Solar Irradiation
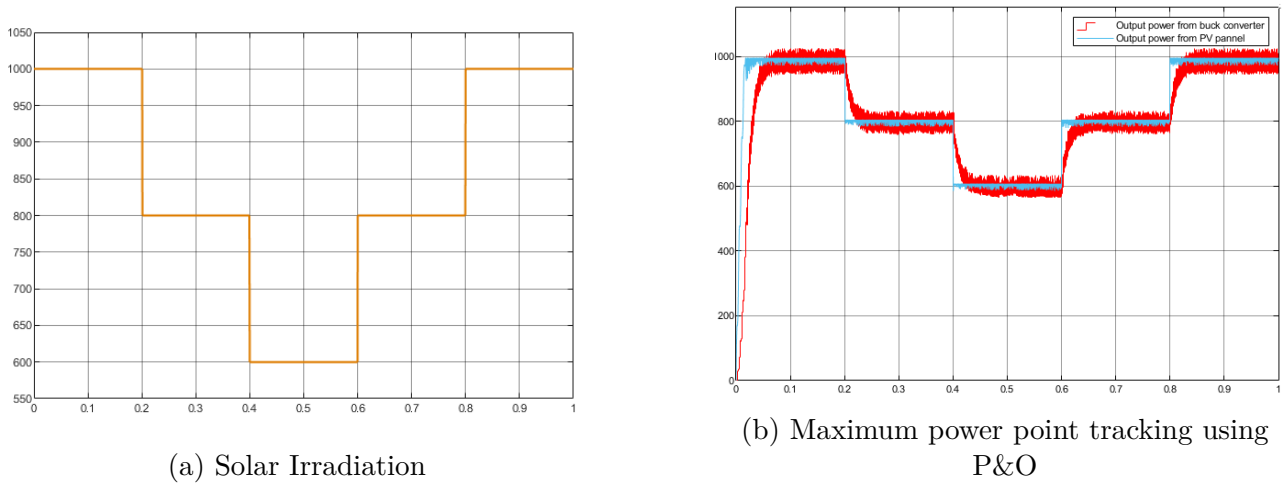

(b) Maximum power point tracking using P&O

Figure 3.10: MPPT Simulation results

7.4.3 Results Interpretation

- Figure 3.10b clearly demonstrates that the Perturb and Observe (P&O) algorithm provides good reference tracking with acceptable dynamic.However, oscillations around the Maximum Power Point (MPP) are still present.

- the Perturb and Observe (P&O) algorithm is well-suited for the studied system despite the presence of oscillations and a relatively slow response. The simplicity of the P&O methodology makes it an attractive choice for implementation in the system. The algorithm's ability to track the Maximum Power Point (MPP) even under variations in irradiance and temperature, along with its ease of implementation, justifies its selection for the system.

8 battery-Integration: PV System with Battery Storage using Bidirectional DC-DC Converter

A battery bank that contains 4 batteries rated at 260 Ah 12V connected in series to achieve a voltage of 48V in the DC bus. Battery modeling is an essential aspect of designing photovoltaic (PV) systems, as it enables the optimization of energy storage and management.

8.1 Battery modelling

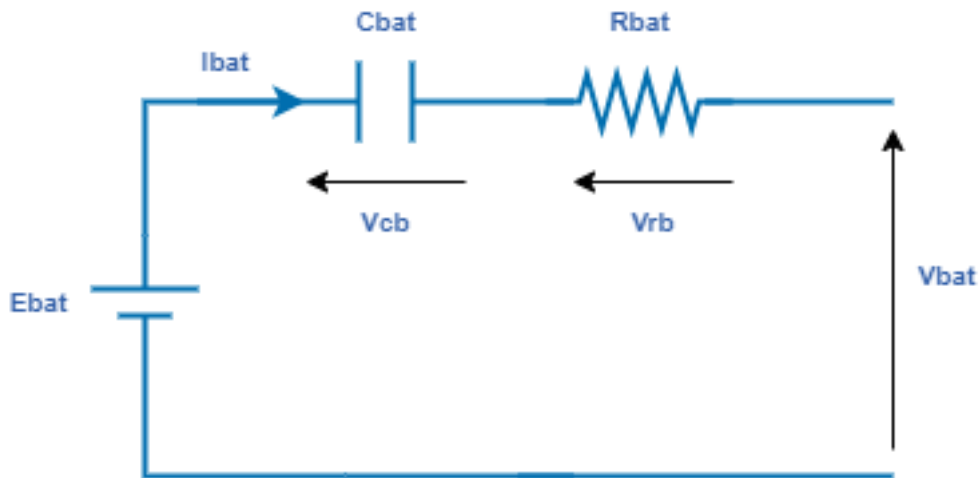The electrical model of a battery can be defined as follows:

Figure 3.11: Simplified Equivalent circuit of battery

A battery can be presented as the equivalent circuit given in Figure 3.17, it behaves like a generator, with a positive discharge current flowing in the same direction as the generator and a negative charge current flowing in the opposite direction. The capacity and the resistance of the battery are given by C_{bat} and R_{bat}, respectively and the voltage across its terminals can be found by applying Kirchhoff's voltage law, resulting in the following equations:
In case of discharge, the battery output voltage, V_{bat} , is expressed as:

$$V_{bat} = E_{bat} - V_{rb} - V_{cb}$$

During the charge process, the battery voltage is expressed as:

$$V_{bat} = E_{bat} + V_{rb} + V_{cb}$$

The voltage source E_{bat} signifies the open-circuit voltage across the battery terminals, which is a result of the energy stored in the battery through electrochemical reactions $V_{oc} = f(SOC)$. It is clear that this term is directly related to the stored energy. The resistor r_{bat} represents the losses, which encompasses the effects of the operating point (I, SOC, T) and the battery's health.[44] The state of charge is considered as an indicator of the electrical charge stored in the battery. The value range is 0<SOC<1. The equation for the State of Charge (SoC) of a battery can be expressed as[42]:

$$Soc = 1 - \frac{Q_d}{C_{\text{bat}}} \tag{3.13}$$

Where:

- Soc is the State of Charge of the battery.

- C_{bat} is the nominal capacity of the battery.

- Q_d is the amount of charge missing relative to the nominal capacity of the battery.

The output voltage is multiplied by four, the number of series cells, to model a 48V battery.

Parameters	Values
Nominal voltage V	48V
Initial Soc	45%
Battery internal resistance R_i	$10^{-3}\Omega$
Rated capacity	260 Ah

Table 3.2: Battery storage system parameters

8.2 Design of Bidirectional Converter

Bidirectional DC-DC converters facilitate bidirectional power transfer between two DC sources, allowing energy exchange in both directions. They are used in various applications one of which is PV storage systems, enabling the efficient transfer of power from and to the battery.
Figure 3.12 the structure of the bidirectional Buck-Boost DC/DC converter associated with a battery.
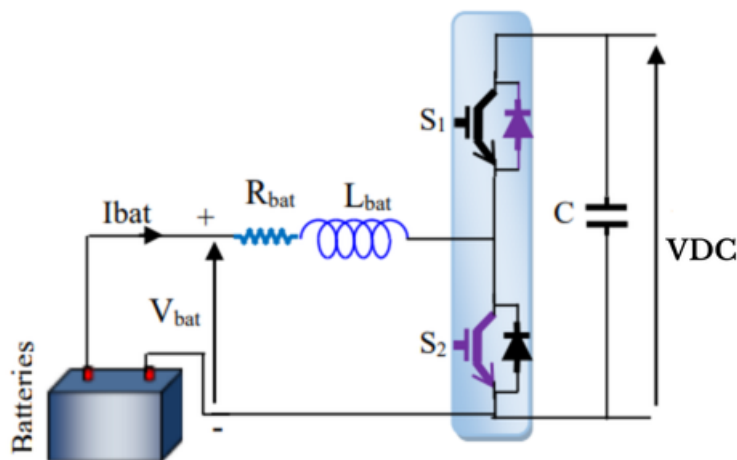
Figure 3.12: Circuit for Bidirectional DC-DC Converter [45]

Depending on the direction of power transfer, the converter can function in either a buck mode or a boost mode.The converter operation is as follows:

1. **Buck mode** : This mode is used to charge the battery, Switch S_1 is ON while switch S_2 remains off.
   When switch S_1 is ON, the input current rises and flows through S_1 and the inductor L, When S_1 is turned OFF, the inductor current falls until the next cycle. The energy stored in the inductor L is then supplied to charge the battery[46].
   This step-down operation allows the converter to efficiently charge the battery from the higher voltage DC bus.

2. **Boost mode**: Conversely, in this mode, the converter functions to discharge the battery. Switch S_2 is activated while switch S_1 remains off. When S_2 is ON, the input current

rises, flowing through S_2 and the inductor L. Upon S_2 being turned OFF, the inductor current gradually decreases until the next cycle. The energy stored in inductor L is then directed towards the load[46].

8.2.1 Mathematical modeling

The switches S_1 and S_2 are controlled simultaneously with complementary duty cycles: d and $1 - d$. It therefore appears two operating phases of the converter according to the states of S_1 and S_2, if we use the first configuration d for s1(buck) and 1-d for s2 (boost):
So the operating sequences be as follows [45]

- **Phase1 : [0 dT](S_1:Open , S_2:Closed)**

$$V_{bat} = L_{bat}\frac{di_{bat}}{dt} \tag{3.14}$$

$$C\frac{dV_{dc}}{dt} = -\frac{V_{DC}}{R_{dc}} \tag{3.15}$$

- **Phase2 : [dT T](S_1:Closed , S_2: Open)**

$$V_{bat} = L_{bat}\frac{di_{bat}}{dt} + V_{dc} \tag{3.16}$$

$$C\frac{dV_{dc}}{dt} = i_{bat} - \frac{V_{dc}}{R_{DC}} \tag{3.17}$$

The average value of a signal $x(t)$ over an interval T is expressed as:

$$\langle x(t) \rangle = \bar{x}(t) = \frac{1}{T}\int_{t-T}^{t} x(t)\, dt$$

Using the last principle, we can deduce the average model of this converter, which is described by the following system of equations:

$$\begin{cases} L_{bat}\frac{d\bar{i}_{bat}}{dt} = V_{bat} - \bar{V}_{dc}(1 - \bar{d}) \\ C\frac{d\bar{V}_{dc}}{dt} = -\frac{\bar{V}_{dc}}{R_{dc}} + \bar{i}_{bat}(1 - \bar{d}) \end{cases} \tag{3.18}$$

where V_{bat}, I_{bat} and R_{dc} are the BESS terminal voltage, BESS current and equivalent output resistance, respectively

$$\begin{cases} \bar{i}_{bat}(t) = I_{bat} + \hat{i}_{bat}(t) \\ \bar{V}_{dc}(t) = V_{dc} + \hat{v}_{dc}(t) \\ \bar{d}(t) = D + \hat{d}(t) \end{cases}$$

8.3 DC-Bus

In the PV-Battery system, two energy sources (PV panels and batteries) supply power to a load. All components are connected to the common DC bus via different power electronic converters (Figure 3.1). According to this DC-coupling, the capacitor current of the DC-link i_{dc} is expressed as:

$$i_{dc} = i_{PV} + i_{bat} - i_{Load} \tag{3.19}$$

The current coming from the storage element

where:

- i_{PV}: the current coming from the PV converter.

- i_{Bat}: the current coming from the battery converter

- i_{Load}: the current consumed by the load.

The DC-link is governed by the following equation:

$$C_{dc}\frac{dV_{dc}}{dt} = i_{dc} \tag{3.20}$$

where C_{dc} is the DC-link capacitor.

8.4 Control of DC-DC Bidirectional Converter of Battery for DC Voltage Regulation

8.4.1 System Configuration

A battery storage system is connected to the DC bus through a bidirectional buck-boost converter, while a controlled PV generator is connected on the other side of the DC bus.

8.4.2 Control Strategy

8.4.3 PI Control Implementation

Figure 3.13 illustrates the scheme implementation of the proposed technique based on proportional-integral (PI) regulators.
Two control loops are considered:

- **DC Bus Voltage Regulation**: This outer loop regulates the voltage of the DC bus and generates the reference current $Ibat-ref$.

- **Battery Current Control**: This inner loop controls the current I_bat to generate the switching signal d.

In the case where V_{dc} is higher than its reference value $V_{dc-ref} = 48V$, the charging circuit operates as a buck converter in charging mode. Conversely, when V_{dc} is lower than its reference value, the charging circuit operates as a boost converter in discharging mode.
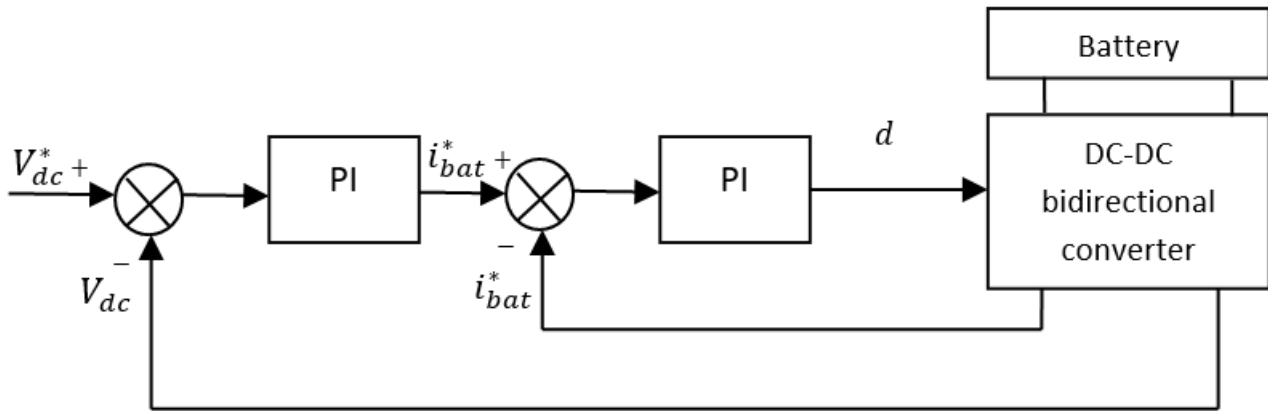

Figure 3.13: Closed loop control strategy with DC converter of BES

Regulators parameters are determined in appendix 2.

8.5 Simulation result and Analysis

8.5.1 description

The system operates on a 48V DC bus. Additionally, 4 batteries rated at 260 Ah 12V are connected in series to achieve a voltage of 48V. Finally, a 385 W load is connected to the system, which utilizes energy stored in the batteries or direct solar energy based on the requirements.

8.5.2 Results & Interpretation

In reference to the solar irradiation and temperature profiles, Figure 3.14 illustrates the changes in solar irradiation while maintaining a constant temperature of $T = 25°C$. This approach is taken to accurately reflect potential real-world atmospheric conditions.
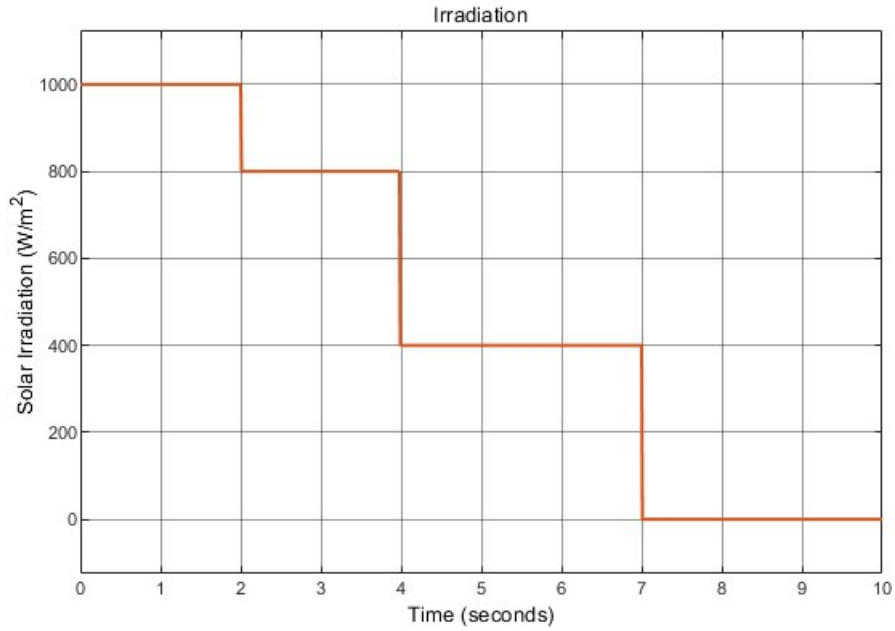
Figure 3.14: Curve of Irradiation profile

Figure 3.15 shows that the DC voltage (V_{dc}) always converges towards the reference value $V_{dc-ref} = 48$ V, despite variations in solar irradiation at a constant temperature of $T = 25°$C. The effectiveness of the control minimizes these variations, even in the case of rapidly increasing irradiation, which is the main challenge.
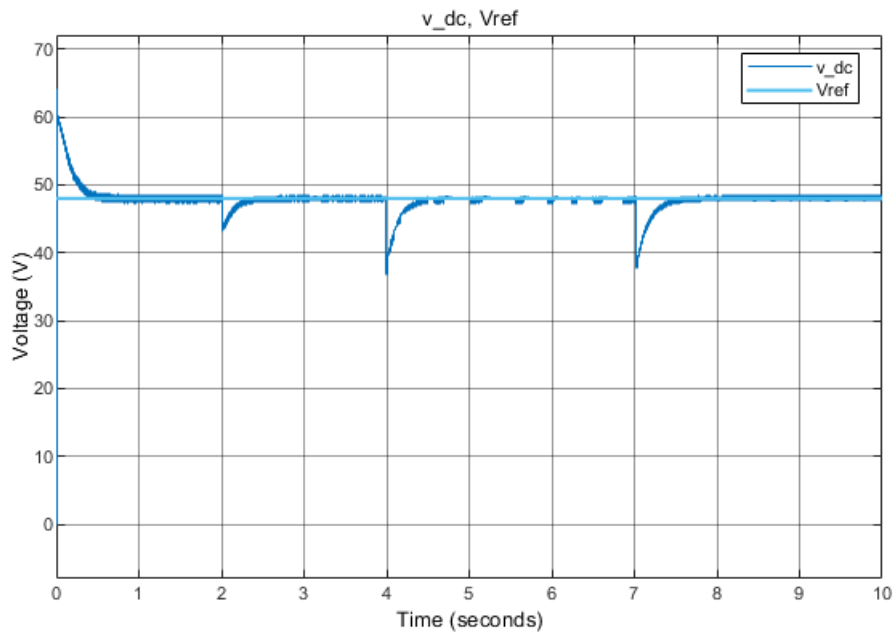

Figure 3.15: DC bus voltage

It is clear in figure 3.16 that the proposed P&O-MPPT algorithm tracks the new MPP without overshoots. For example, when the solar irradiation dicreases gradually from 800W/m^2

up to 400W/m^2, the active power instantly changes from 0.8 to 0.4 kW, which corresponds to the MPP for the values of solar irradiation G. Thus, the MPPT is still verified.
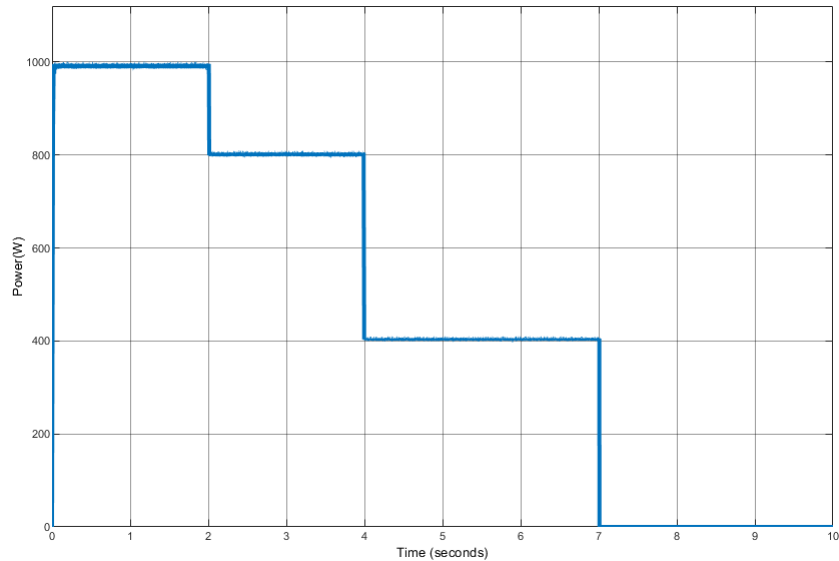
Figure 3.16: PV power response to changes in solar irradiation.

Figure 3.17 shows the State of Charge (SOC) of the battery, which proves two modes of operation. The battery discharges when the solar irradiation experiences a significant decrease so that $P_{pv} < P_{load}$ and vice versa. The battery charges when $P_{pv} > P_{load}$, corresponding to an increase in G. The figure 3.18 illustrates the current of charge and discharge of the battery: $I < 0$ indicates charging, and $I > 0$ indicates discharging.
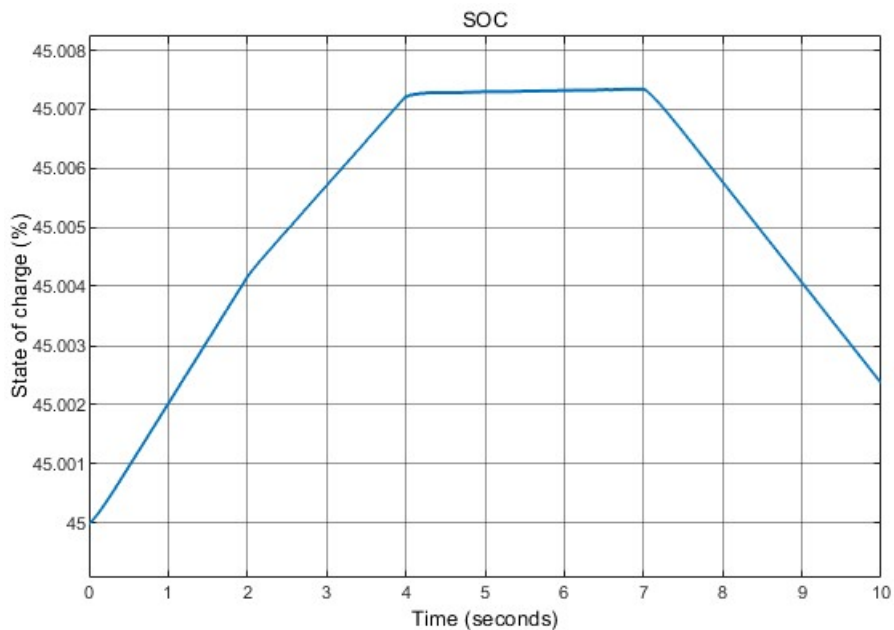
Figure 3.17: State of charge (SOC %)
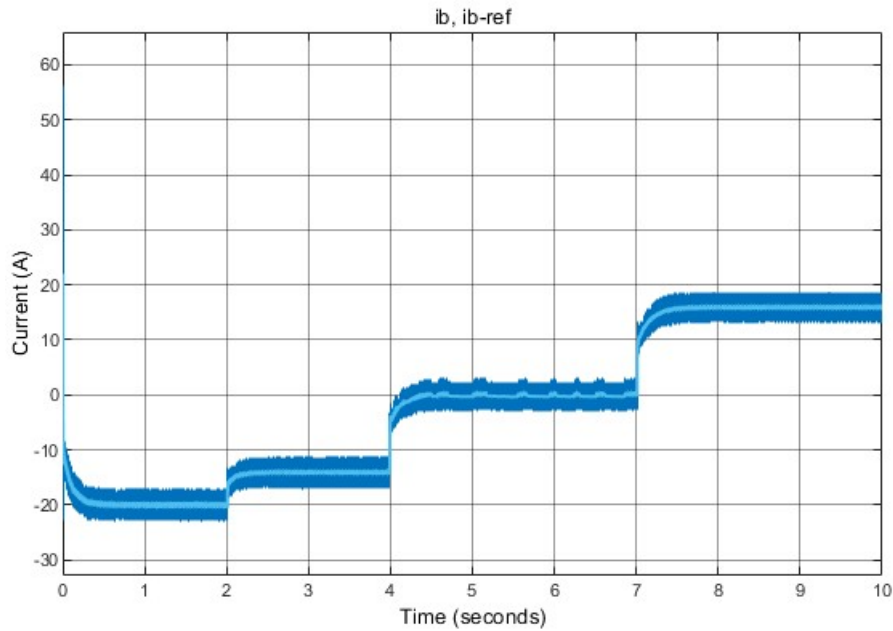
Figure 3.18: Battery current

9 Conclusion

In conclusion, this chapter has thoroughly addressed the modeling and simulation of a complete photovoltaic system. We established a detailed mathematical model of the PV generator and subsequently modeled the buck converter to maximize the power of the generator using the PO MPPT technique. The modeling of the battery and the DC load has allowed us to understand their essential role in energy storage and their impact on the overall performance of the system. These models and simulations have enabled us to analyze the interactions between the components and optimize the energy efficiency of the photovoltaic system under different conditions. In the next chapter, we will examine the second energy source in this hybrid system, the wind power system.

Chapter 4

Modeling and control of the Wind Power Generation System

1   Introduction

In this chapter, we will delve deeply into the comprehensive modeling of a wind turbine system. We will commence by constructing the model of a wind turbine coupled with its electrical generator, opting for Permanent Magnet DC Generator as a Wind Power Generator. Subsequently, our focus will shift towards implementing control strategies aimed at maximizing power output from the system. Finally, we will validate our findings through MATLAB simulations encompassing the entire system along with the control systems.

2   Modeling of Wind Energy System

The wind turbine under study comprises three blades, each with a length R_t, attached to a drive shaft connected to a gearbox with a gear ratio of G. The gearbox drives the electrical generator (DCG) through a transmission shaft, Figure 5.5 illustrates the schematic of the mechanical components of the wind generator (The turbine, The gearbox, The transmission shaft)
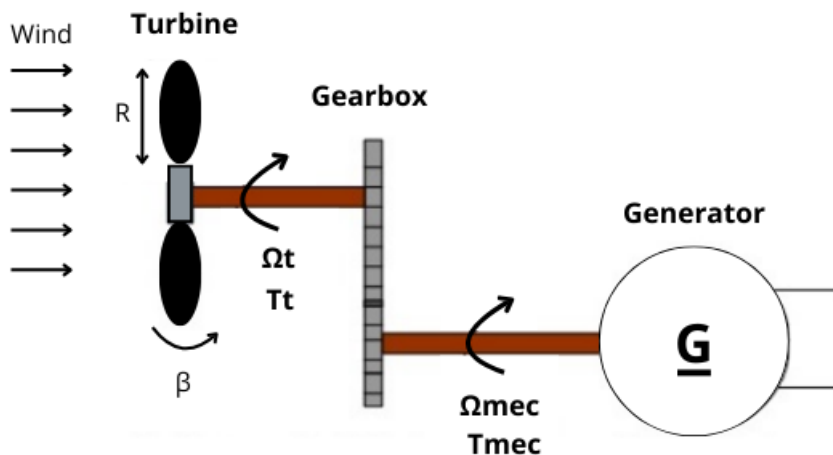

Figure 4.1: Structure of the wind system

2.1   Turbine modeling

The power available in the wind P_w is expressed as follows:

$$P_w = \frac{1}{2} \cdot \rho \cdot S \cdot v_w{}^3 = \frac{1}{2} \cdot \rho \cdot \pi R^2 \cdot v_w{}^3$$

Where:

- S: The surface swept by the turbine blades (m^2).

- ρ: Density of the air ($\rho = 1.225\,\text{kg/m}^3$).

- V_w: The wind speed (m/s).

- R: The rotor radius (m).

The kinetic energy of the wind captured by the blades across an air surface area S undergoes conversion into mechanical energy. However, due to the inability to fully exploit this energy, a performance coefficient C_p emerges, contingent upon the aerodynamic characteristics of the blades. According to Betz's theory, the relationship between the mechanical power P_{mec} and the wind power P_w is expressed through the following equation:

$$P_{\text{t}} = C_p(\lambda, \beta) \cdot P_w = \frac{1}{2} C_p(\lambda, \beta) \cdot \rho \cdot S \cdot v_w^3$$

Where:

- $C_p(\lambda, \beta)$: The wind turbine's power coefficient.

This coefficient exhibits a nonlinear behavior and can be expressed in several forms. For our study, we select the most commonly used form, the polynomial form:

$$C_p(\lambda, \beta) = c_1 \left(c_2 \frac{1}{\lambda_1} - c_3 \beta - c_4 \right) e^{-\left(\frac{c_5}{\lambda} \right)} + \lambda c_6$$

Where the parameter λ_1 is also expressed as a function of λ and β as follows:

$$\frac{1}{\lambda_1} = \frac{1}{\lambda + 0.08\beta} - \frac{0.035}{1 + \beta^3}$$

The constants c_i (for $i = 1:6$) depend on the type of turbine and the manufacturer.
For our study: $c_1 =$, $c_2 = 116$, $c_3 = 0.4$, $c_4 = 5$, $c_5 = 21$, and $c_6 = 0.0068$.
The tip-speed ratio λ is defined as the ratio between the linear speed of the blades and that of the wind:

$$\lambda = \frac{R \cdot \Omega_t}{v_w} \tag{4.1}$$

Where:

- Ω_t: The rotational speed of the turbine

  To give an idea of the magnitude of λ:

- $\lambda < 3$: The wind turbine is considered slow.

- $\lambda > 3$: The wind turbine is considered fast.

The figure below illustrates the effect of the pitch angle β on the variations of the power coefficient $C_p(\lambda)$.

Figure 4.2 illustrates the power coefficient C_p as a function of the tip speed ratio λ for various pitch angle values β, It is evident that for a fixed value of β, a maximum Cp is achieved when the tip speed ratio is at its optimal value λ_{opt}. and from 4.1 , for a given wind speed (v), to achieve the maximum Cp, then the rotor speed should be adjusted to the optimal value Ω_{opt}[47].
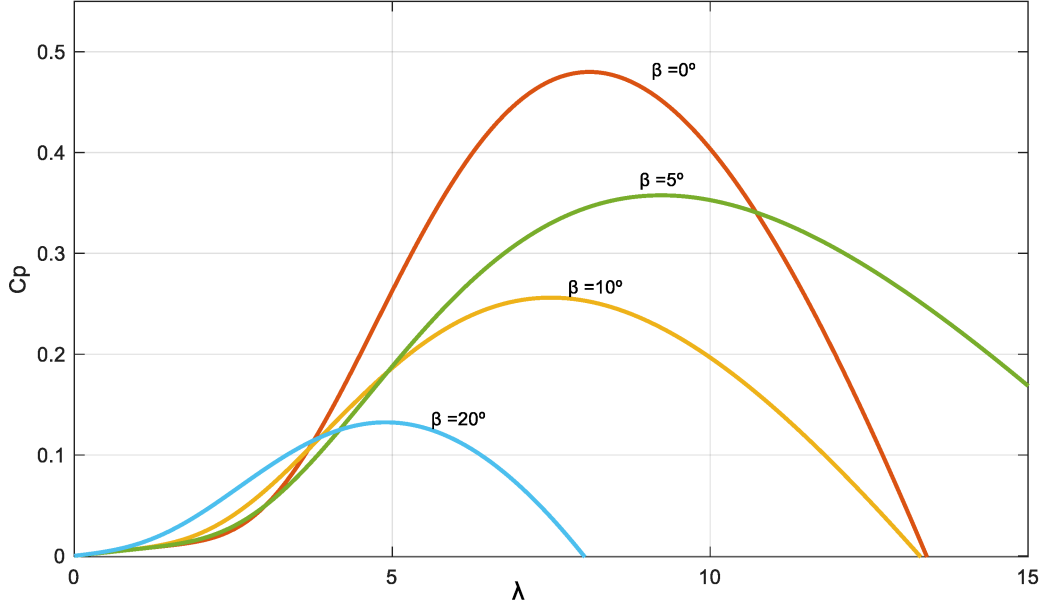

Figure 4.2: Power coefficient characteristics

To simulate the wind turbine's behavior, the aerodynamic torque (T_t) is practically calculated from the aerodynamic power (P_t) using the wind turbine's rotational speed (Ω_t), as expressed in Equation 4.2[30]:

$$T_t = P_t \Omega_t \tag{4.2}$$

2.2 Gearbox model

The GearBox is mathematically modeled by a gain G existing between the turbine and generator speeds:

$$\Omega_t = \frac{\Omega_{\text{mec}}}{G} \tag{4.3}$$

By energy conservation $P_t = P_{mec}$, the relationship between the wind-generated torque on the shaft driving the generator and the aerodynamic torque can be expressed as follows:

$$T_g = \frac{T_t}{G}$$

Where:

- Ω_{mec} represents the angular speed of the generator (rad/s or r/min).

- G is the speed multiplier gain.

58

2.3   transmission Shaft

The mechanical transmission modeling can be summarized as follows:

$$T_{\text{mec}} = J\frac{d\Omega_{\text{mec}}}{dt} = T_g - T_{\text{em}} - T_{\text{vis}} \tag{4.4}$$

Where:

- T_{mec} is the mechanical torque.

- J is the moment of inertia.

- $\frac{d\Omega_{\text{mec}}}{dt}$ is the angular acceleration.

- T_g is the torque from the gearbox.

- T_{em} is the electromagnetic torque produced by the generator.

- T_{vis} is the torque due to viscous friction, given by $T_{\text{vis}} = f\Omega_{\text{mec}}$, where f is the coefficient of viscous friction and Ω_{mec} is the mechanical angular velocity.

The expression for the equivalent inertia, J applied on the high-speed shaft (generator side) is given by:

$$J = \frac{J_t}{G^2} + J_g \tag{4.5}$$
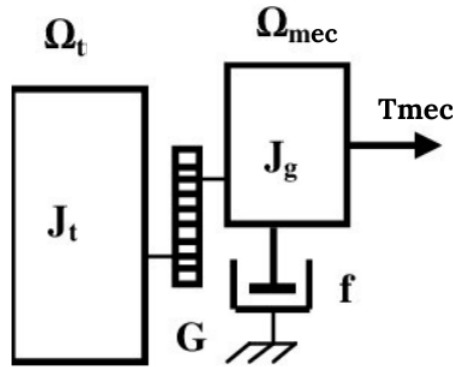

Figure 4.3: Mechanical model of the wind turbine system

2.4   Global WES model

The turbine generates an aerodynamic torque T_t transmitted to the gearbox. The aerodynamic torque (T_t) can be calculated based on the wind speed V_w and the performance coefficient C_p determined according to the blade angle orientation β and the tip speed ratio λ. The gearbox

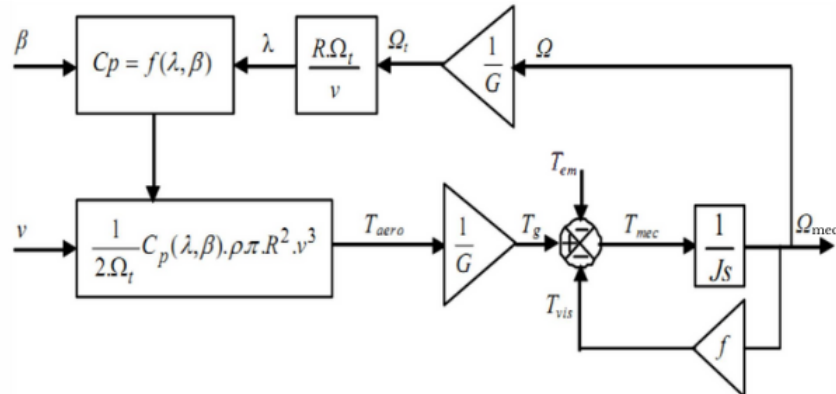converts the turbine speed and aerodynamic torque into mechanical speed and torque of the motor shaft.

Figure 4.4: Diagram block for the global model of the turbine[34]

From the diagram, it's evident that as the wind speed changes, the rotor speed and the power captured by the wind turbine will also change accordingly. For a certain wind speed, the power will vary with respect to the rotor speed Ω, and there exists a point where the power is maximized, i.e., at the optimal rotor speed ω_{opt} as shown in Figure 4.5.

Therefore, to extract the maximum power from the wind turbine, the rotor speed should be operated at the optimal speed (Ω_{opt}) corresponding to the prevailing wind speed. This technique is known as Maximum Power Point Tracking (MPPT) which will be discussed next.
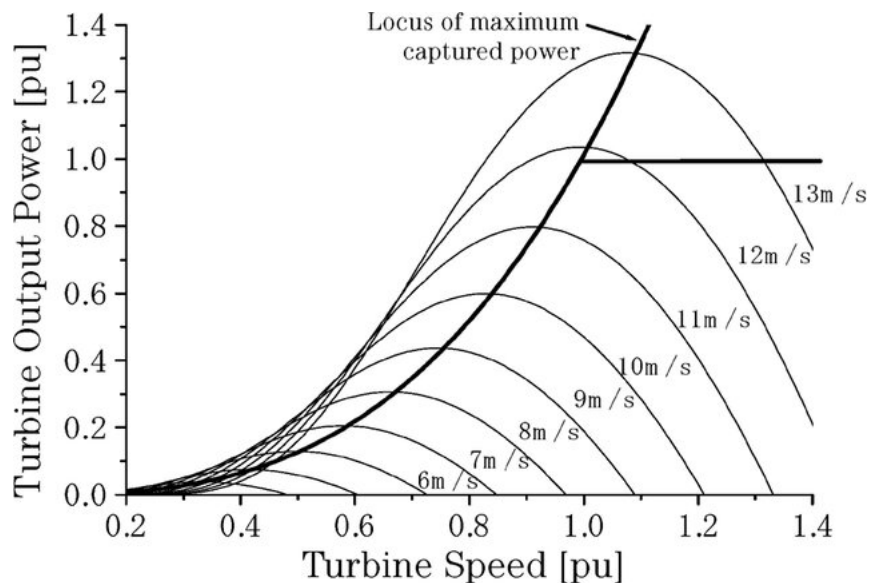

Figure 4.5: Turbine characteristics with maximum power point tracking[48]

3 Direct-Current Machines

A DC machine is an electromechanical converter that enables the bidirectional conversion of energy from an electrical installation, traversed by a direct current, into mechanical energy.

So there are two types of DC machines; **DC generator**, and **DC motor**, A DC generator converts mechanical power into DC electrical power, whereas, a DC motor operates in the reverse direction.

There is no real difference between the construction of both machines generator and motor , the only difference is in for the direction of power flow, so a DC generator can be used as a DC motor without any structural changes, and vice versa is also possible**dcmachine**.

3.1 Basic parts of DC Machines

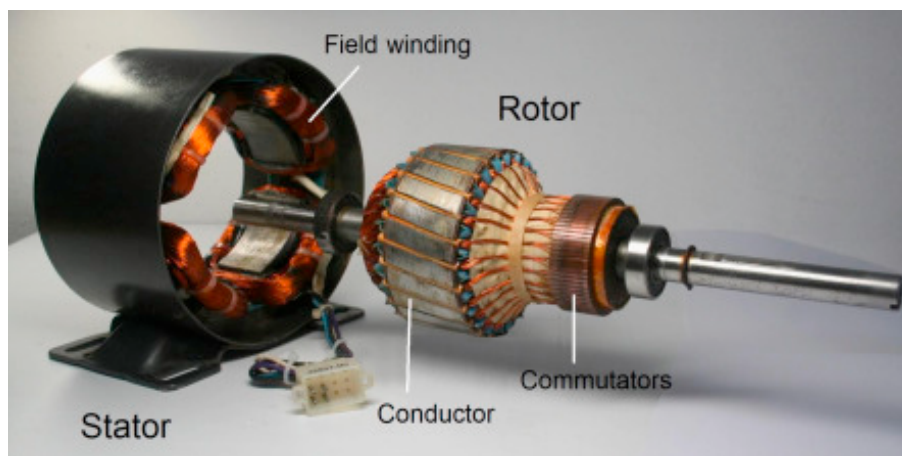As shown in figure 4.6, DC machine has mainly two main parts:

Figure 4.6: DC machine construction

3.1.1 Stationary Part (Stator)

- **Yoke or Frame** : is the outer frame of a DC machine, in practice made of cast steel. It provides mechanical protection and support for the internal components, ensuring the structural integrity of the assembly[49].

- **field winding**: made from copper These windings are pre-wound and placed on each pole, connected in series to ensure efficiency. When energized, they create alternating North and South magnetic poles, a configuration essential for generating the required magnetic flux. This flux, produced through the former-winding method, interacts with the armature winding, ultimately generating torque or voltage within the DC machine

3.1.2 Rotating Part(Rotor)

- **Conductor**: or The armature is a configuration of conductors or coils that have the ability to rotate unrestrictedly on supportive bearings. The operational torque and elec-

tromotive force (EMF) are generated within the coils of the armature.

- **commutator**: The physical connection to the armature winding in a DC machine is established through a commutator-brush arrangement. In a DC generator, the commutator's role is to collect the current generated in the armature conductors. Conversely, in a DC motor, the commutator functions to provide current to the armature conductors.

3.2 Working principle of DC generator

An electrical generator functions by converting mechanical energy, typically from rotor blades, into electrical power, It achieves this concept through the use of Faraday's laws of electromagnetic induction, where its rotating energy generates e.m.f. that is proportional to its speed of rotation and magnetic field strength.The electrical generators can be designed in different shapes and sizes; the most ideal for the wind energy systems is the permanent magnet DC generator or PMDC generator [50].

Figure 4.7: wt with DC generator [50]

3.3 Types of DC generators

A simple DC generator can be constructed using different configurations, depending on how the magnetic field coils are connected to the armature.

1. **Self-Excited DC Generators**

   In self-excited DC generators as shown in figure , the field winding is not excited by an external power source. Instead, the voltage induced in the armature winding is used to excite the field winding.

This type of DC generator is further classified into three types; Shunt type generator, Series type generator, Compound generators. the electrical model of the three types is illustrated in figure 4.8
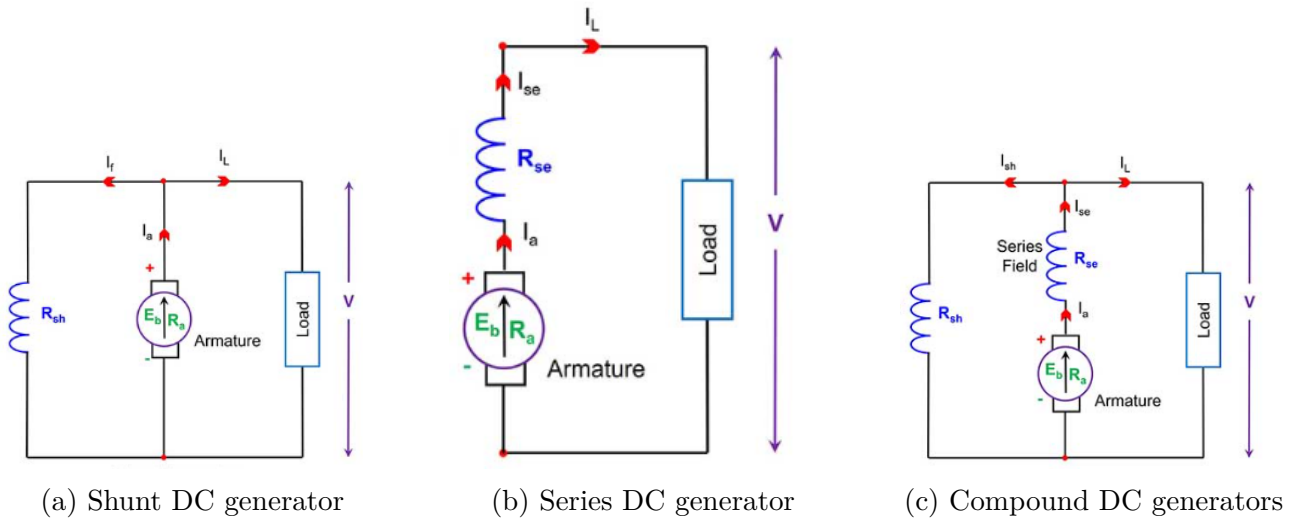

(a) Shunt DC generator   (b) Series DC generator   (c) Compound DC generators

Figure 4.8: DC generator types [51]

2. **Separately Excited DC Generator**
   In separately excited DC generator shown in figure 4.9 There is no physical connection between the armature and field windings. The field winding is connected to the external DC source. The armature is driven mechanically by a prime mover which is the rotor blades.
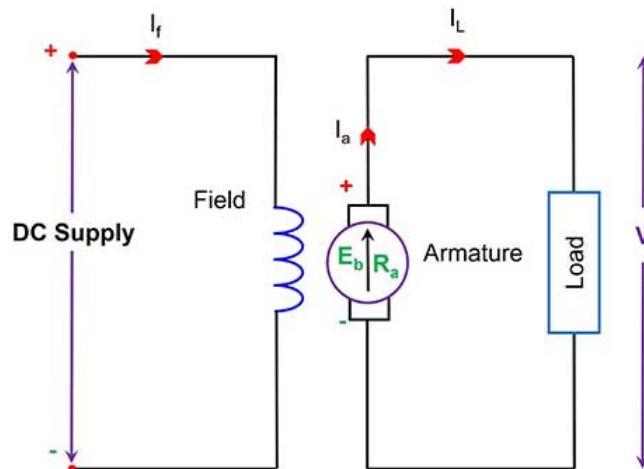

Figure 4.9: Separately Excited DC Generator [51]

3.4   DC Generator mathematical model

In the following analysis, a mathematical model is developed for a separately excited DC generator directly coupled to a wind turbine via a horizontal shaft. A resistive load is connected

at the end of the generator.

By applying Kirchhoff's Voltage Law and fundamental rotational motion equations, a comprehensive model can be derived for this system:

$$U_a = E_a - R_a I_a \tag{4.6}$$

Where:

- U_a: Terminal voltage

- E_a: The induced emf in the generator

- R_a: Armature resistance

- I_a: Armature current

According to Faraday's law of electromagnetic induction, the magnitude of the induced electromotive force (E.M.F.) in a conductor is given by:

$$E_a = K \cdot \Phi \cdot \Omega \tag{4.7}$$

Where:

- K: Proportionality constant

- Φ: Magnetic flux

- Ω: Angular velocity

Equation for torque:

$$P_{em} = \frac{T_{em}}{\Omega} = E_a I_A \tag{4.8}$$

Which yields:

$$T_{em} = K \cdot \Phi \cdot I_a \tag{4.9}$$

Mechanical equation:

$$T_{em} - T_r - f\Omega = J \cdot \frac{d\Omega}{dt} \tag{4.10}$$

Where:

- T_{em}: Electromagnetic torque

- P_{em}: Electromagnetic power

- T_r: Resistance torque imposed by the load

- J: Total moment of inertia (machine + driven load)

- f: Friction proportional to the rotational speed

64

4 Presentation of the Whisper 200 Wind Turbine

The wind turbine chosen for this project is the Whisper 200. The Whisper 200 is a small-scale HAWT (Horizontal Axis Wind Turbine) designed by the American manufacturer Southwest Windpower. It is intended for operation in sites with medium to high wind speeds (3.6 m/s and above). Its peak electrical power is 1 kW, achieved at the rated wind speed range of 11.6 m/s to 13 m/s. [52].

Figure 4.10: The Whisper 200 wind turbine[52]

The key technical specifications of the Whisper 200 are presented in the table below:

Table 4.1: WHISPER 200 Specifications

Parameter	Value
Rotor Diameter	2.7 m
Weight	30 kg
Start-Up Wind Speed	3.1 m/s
Voltage	24, 36, 48 VDC (HV available at 120V, 230V)
Rated Power	1000 watts at 11.6 m/s
Turbine Controller	Whisper controller
Blades	3-Carbon reinforced fiberglass
Kilowatt Hours Per Month	200 kWh/mo at 5.4 m/s)
Survival Wind Speed	25 m/s

5 Maximum power point tracking control

Wind energy systems are designed to capture the kinetic energy of the wind and convert it into electrical energy. However, as demonstrated in the previous section, the output power of a wind energy system is highly dependent on wind speed V_w. Due to the nonlinear characteristics of wind turbines, it is crucial to maintain the maximum power output of the wind turbine across all wind speed conditions.

The concept of Maximum Power Point Tracking (MPPT) has been widely adopted in the solar photovoltaic (PV) industry since the 1970s. The energy-speed relationship of wind turbines is analogous to the volt-ampere characteristics of solar panels. Therefore, the MPPT techniques developed for PV systems can be effectively applied to wind energy systems to ensure the maximum utilization of the available wind energy ($C_p = C_{pmax}$)[53].

5.1 Principle of MPPT Control

Figure 4.11 shows the overall scheme of the wind power control system using MPPT. The Perturb and Observe (P&O) technique is one of the most widely used Maximum Power Point Tracking methods for wind energy conversion systems. This technique is based on perturbing the rotor speed in small steps and observing the changes in power output. In a WECS with a DC generator (DCG), the output current and voltage are proportional to the torque and rotor speed, respectively. Therefore, perturbing or varying the output voltage of the generator will cause a corresponding variation in the rotor speed [47]. Perturbing the voltage could be performed by adjusting the duty cycle (PWM signal) of the DC/DC converter.
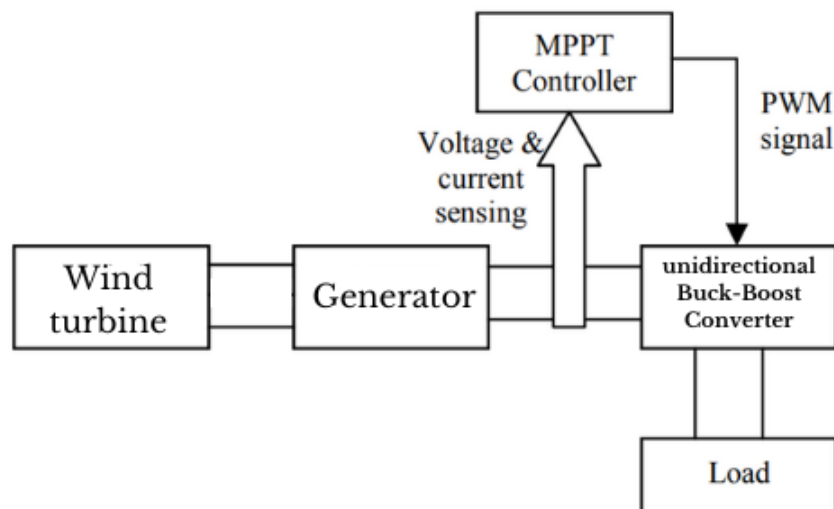
Figure 4.11: Overall scheme of the wind power control system using MPPT

The Whisper 200 wind turbine is designed to operate with voltages of 24, 36, 48 V DC, with higher voltage options available at 120V and 230V, as indicated in the characteristic table 4.1. In our case, the DC bus voltage is fixed at 48V. Hence, we employ a unidirectional buck-boost converter capable of stepping up or down the voltage to match the varying output voltage of the Whisper 200 to the fixed 48V DC bus.

The converter only allows power to flow from the wind turbine to the DC bus, not in the reverse direction. The output voltage of the unidirectional Buck-Boost Converter can be adjusted based on the duty cycle of the switching transistor to optimize power extraction from the wind turbine.

6   Simulation and Results

The model of wind energy system with MPPT control is simulated using MATLAB Simulink. A buck-boost converter with MPPT using Perturb and Observe method (P&O) algorithm is employed to optimize wind energy conversion efficiency. The electrical parameters of the adopted WT "Whisper 200" are given in Table4.2.

Parameters	Symbol	Value
Wind Turbine		
Base Power	P_t	1000 W
Maximum power at base wind speed p.u	P_w	0.85
Base rotational speed p.u	Ω	1.2
Base wind speed	V_w	12 m/s
Buck-Boost converter		
Inductance	L	3.65 mH
Capacitance	C	3 mF

Table 4.2: System Parameters

The simulation is conducted under variable wind speed values indicated in figure 4.12 used to compare the wind energy system with and without MPPT control.
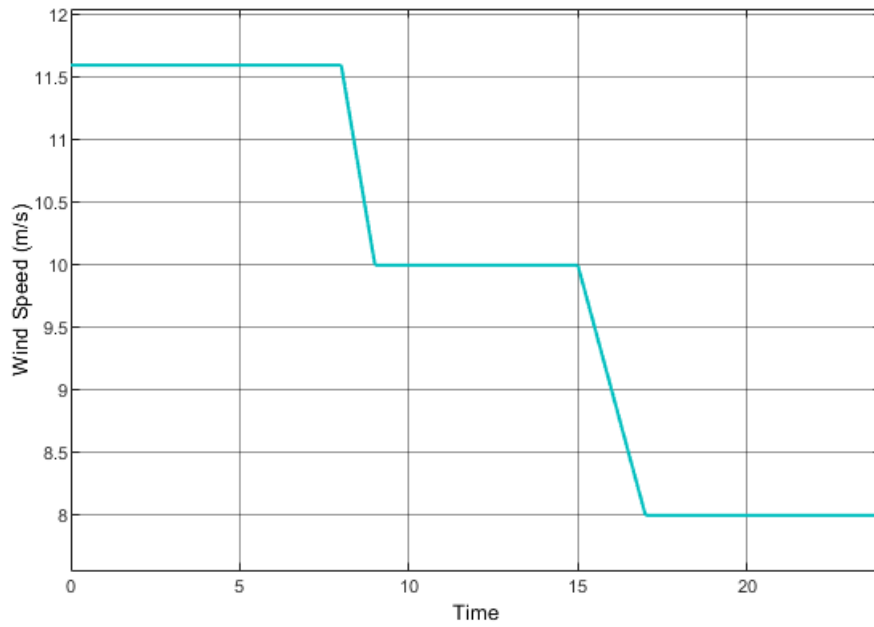
Figure 4.12: Wind speed Profile

In the system without MPPT control, the output voltage of the wind generator remained fixed. Conversely, in the system with MPPT control, the voltage was dynamically adjusted by the MPPT controller. The simulation results for both systems are presented in figure 4.13 (without MPPT control) and figure 4.14 (with MPPT control). These figures provide a comparative analysis of the system's behavior under different wind conditions
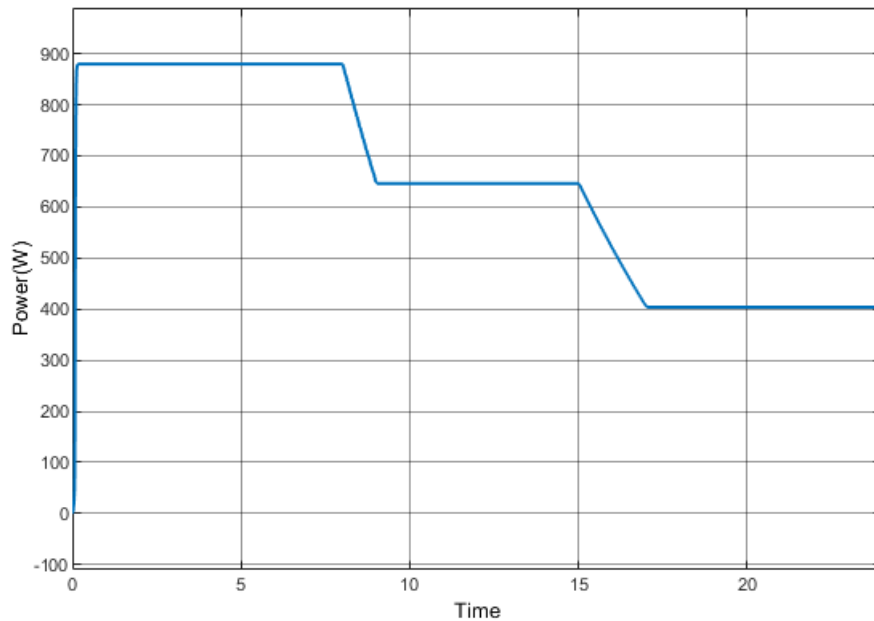

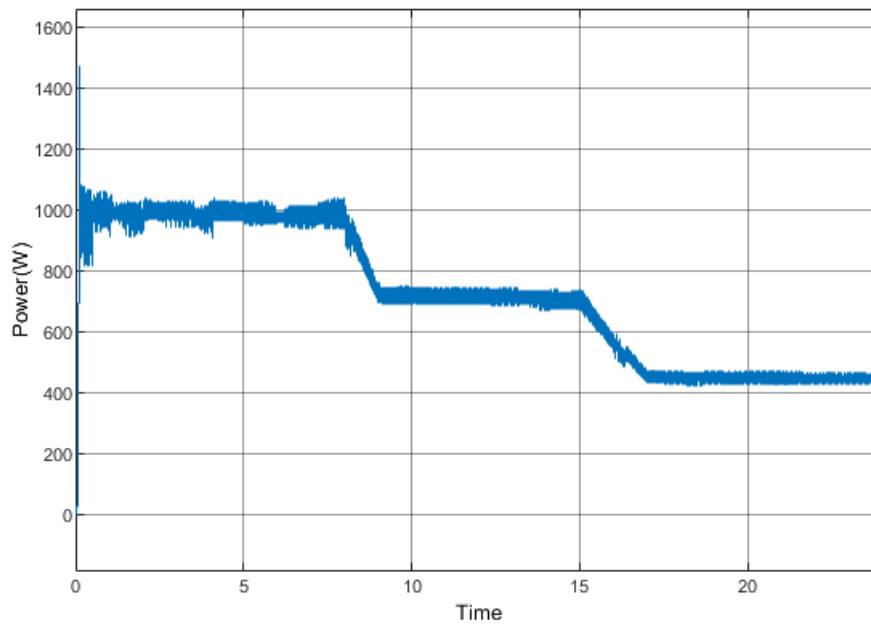Figure 4.13: Generator output power of wind turbine system without MPPT

Figure 4.14: Generator output power of wind turbine system with MPPT

The simulation results (Figures 4.13 and 4.14) clearly demonstrate that the wind energy system operating with MPPT control consistently generates higher power output compared to the system with a fixed output voltage. This highlights the effectiveness of the MPPT technique in maximizing power extraction from the wind generator, particularly under fluctuating wind conditions.

7 Conclusion

In this chapter, we delved deeply into the modeling and control of a wind turbine system, highlighting the significance of maximizing power output. Through detailed simulations and analysis, we showcased the effectiveness of MPPT control in optimizing power extraction from the system. These insights pave the way for our upcoming chapter, where we will delve into the integration of wind turbines with photovoltaic (PV) systems and battery storage. This investigation into hybrid energy systems will aim to enhance efficiency and sustainability by harnessing the collective strengths of diverse renewable sources.

Chapter 5

Hybrid system: Sizing and energy management

1 Introduction

In the preceding chapters, we have thoroughly examined the two primary types of RES: solar and wind. Specifically, we delved into the PV system with Maximum Power Point Tracking in Chapter 2 and the wind energy system in chapter 3. Additionally, We tested the integration of battery storage with the PV system by developing and implementing algorithms for efficient charging and discharging.

Now, we embark on a crucial step: combining all these elements into a unified standalone hybrid system (PV-Wind-Battery). This chapter focuses on a detailed description and the architectural design of our hybrid system, currently being implemented in the "Process Control Laboratory" of "Ecole Nationale Polytechnique".

To begin, we will analyze the estimated load profile which our hybrid system is designed to support. This analysis will be based on the techno-economic study of this hybrid energy production system, composed of photovoltaic solar panels, wind turbines, and the battery energy storage system, using the HOMER Pro software. Next, we will delve into the elaboration of an energy management system, essential for ensuring optimal performance of the HES. We will use MATLAB/Simulink to implement the EMS. These systems will regulate and the energy flow, ensuring reliable and sustainable power supply.

2 Architecture and Description

Our case study focuses on a Hybrid Energy System (HES) designed to power the Process Control Laboratory at "Ecole Nationale Polytechnique" that is designed with the following components:

- Two chains of PV systems.

- Two Wind Energy systems.

- Storage system(Batteries).

- AC Load.

The schematic diagram illustrating the configuration of the HES is depicted in Figure 5.1. Additionally, the detailed electrical wiring diagram is provided in Appendix 1. For this study, the renewable resources, including the wind turbines (WTs) and photovoltaic (PV) systems, have been doubled to enhance the overall capacity of the system.
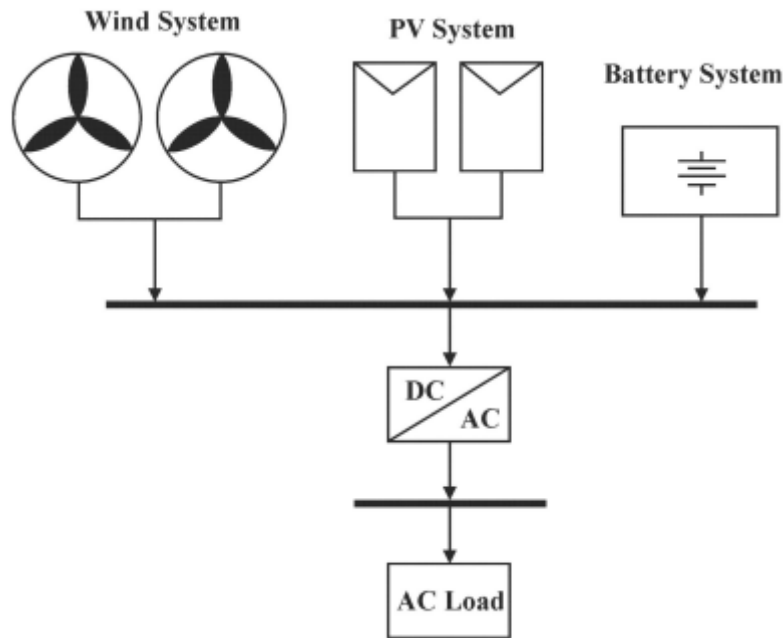
Figure 5.1: Structure of the hybrid PV/wind/battery system considered[54]

3 System sizing and load profiling

The study is structured into two primary phases: Load Estimation and Techno-Economic Analysis. The HOMER Pro software was selected for conducting techno-economic analysis simulations, testing various load demand scenarios for the predetermined and pre-sized HES considered in our study. Our goal is to estimate the load where the optimized configuration given by HOMER Pro is the same as the one of the "Process Control Laboratory".

3.1 Homer Pro software presentation

HOMER Pro is a specialized software developed by the US National Renewable Energy Laboratory (NREL) for the technical and financial evaluation of both on-grid and off-grid power systems[55]. This powerful tool excels in simulating micro-grid operations, assessing all potential equipment combinations to identify the most practical and economically efficient system configurations [56].
HOMER Pro models system configurations by simulating their operation for an entire year using hourly time steps. This detailed approach allows the software to accurately capture the variability in load and renewable energy resources throughout the year [55]. By doing so, it ensures that the system design is robust and capable of meeting demand under varying conditions.
HOMER Pro's advanced optimization capabilities make it superior to traditional mathematical models for this project. Its ability to incorporate complex inputs, like outage and load data, allows us to identify the optimal load profile for our pre-defined hybrid energy system. This ensures our system design, as determined by HOMER Pro, is not only technically feasible but also economically viable.

3.2   Homer Pro's Workflow

1. **Site Selection**
   The hybrid system is installed in the "Process Control Laboratory" at Ecole Nationale Polytechnique in Algiers, located in northern Algeria.
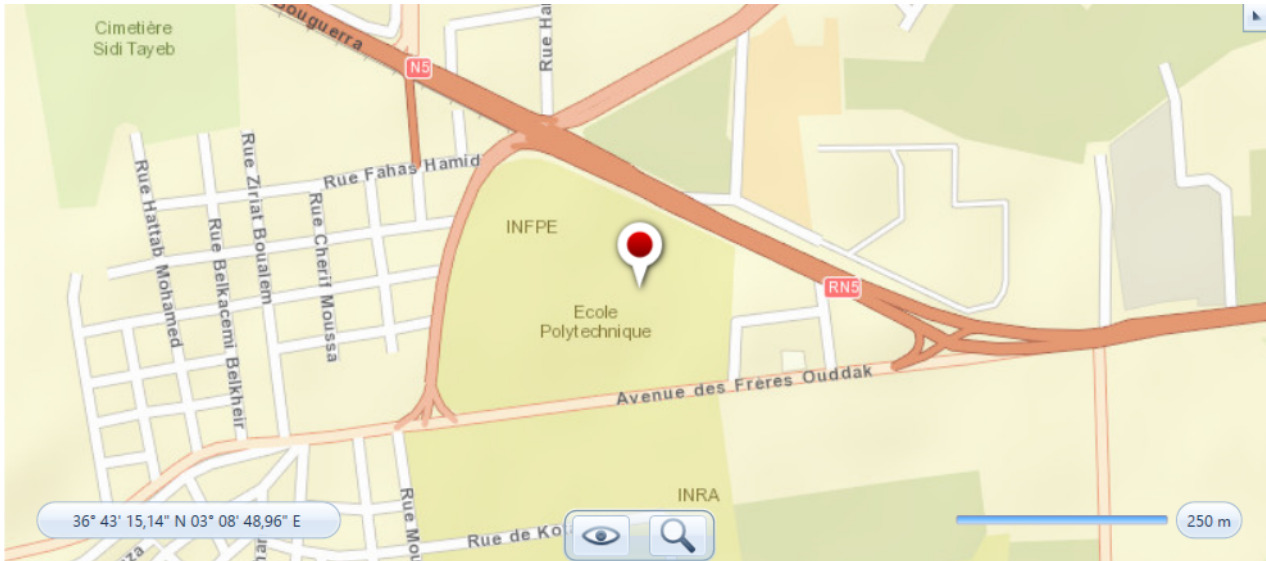

Figure 5.2: Selected location for proposed standalone HES

2. **Components considered**
   The proposed standalone hybrid system comprises photovoltaic panels, wind turbines, power converters, and a battery energy storage system.
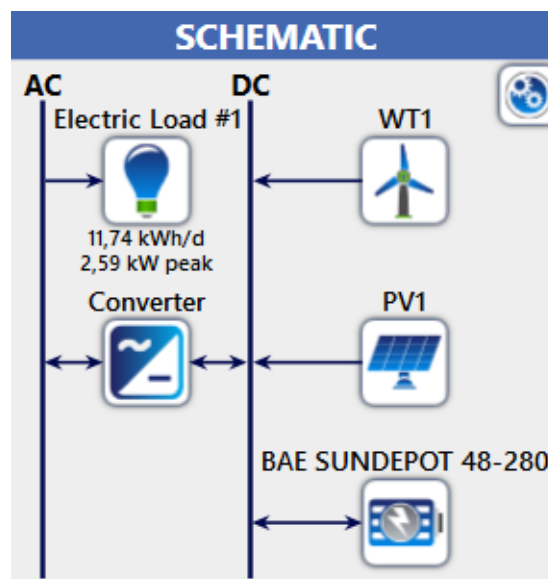

Figure 5.3: Schematic configuration of a hybrid system using HOMER Pro

The specifications provided are for 4 photovoltaic panels of "Solar Fabrik pro L3 poly"

type, with a power of 250Wc each. The price of one panel is 100.07$, which is equivalent to 92.43€[42].

As shown in Figure 5.4, the photovoltaic panels utilized for this simulation are generic flat plate PV 1 kW. The typical cost of this PV panel is approximately 369,72€, and the replacement cost is 369,46€. Additionally, the yearly cost of operation and maintenance is estimated to be 10€.
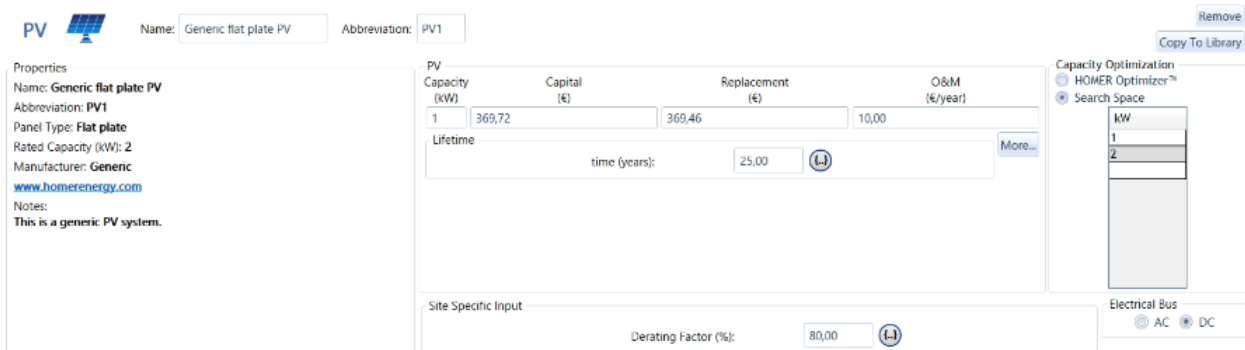

Figure 5.4: PV panel selection parameters

The wind turbine system utilized for this simulation is a generic 1 kW system, as depicted in Figure 5.5. The cost of this turbine system is approximately 1000€. The estimated costs for replacement are 1000€. Additionally, the yearly cost of O&M is estimated to be 20€.
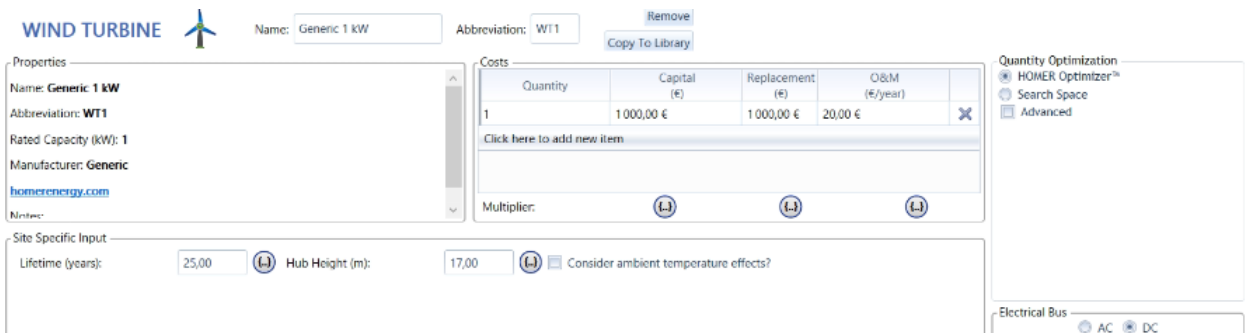

Figure 5.5: Wind turbine selection parameters

We also have four lead-acid batteries, with a voltage of 12V, a capacity of 260Ah, a cost of 1363,32 (340,83€*4), and an estimated lifespan of 10 years[42].
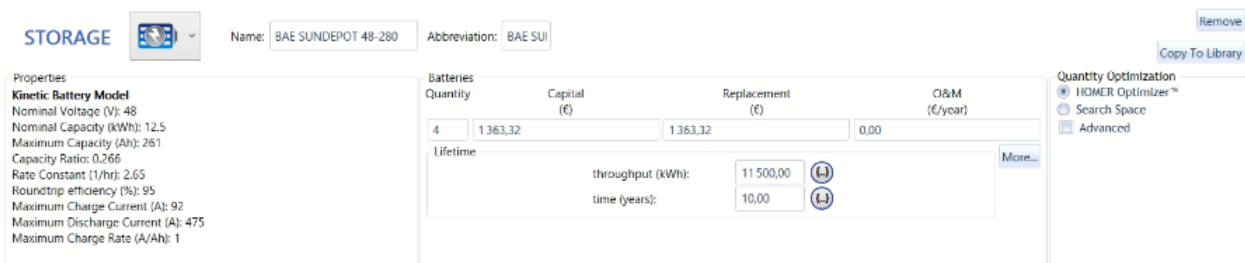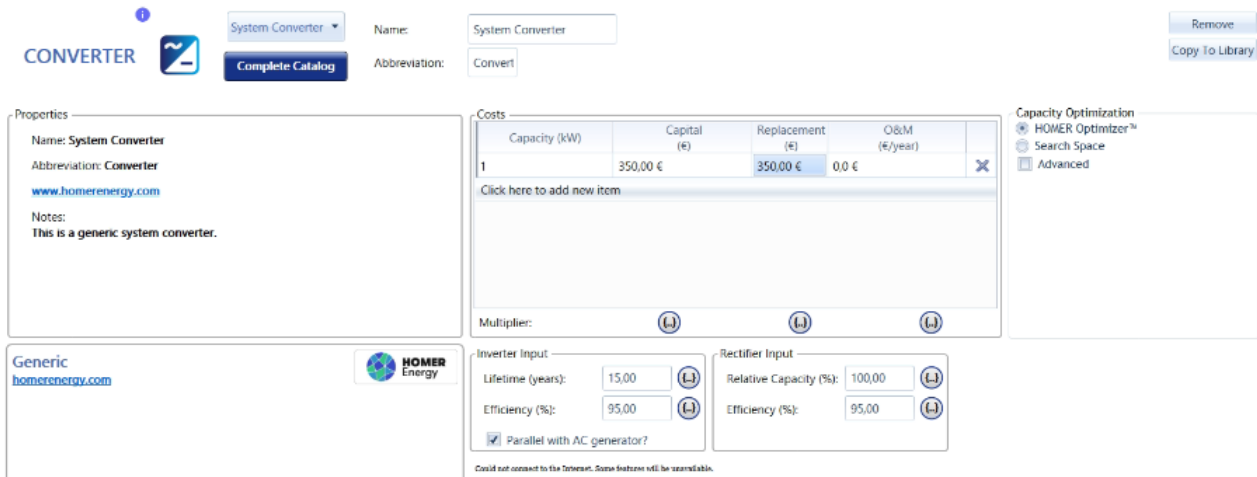

Figure 5.6: Battery energy storage system

We also add a converter (DC/AC) for the entire system profile, with a lifespan of 15 years and an efficiency of 95%. The estimated price of an inverter is 350€.

Figure 5.7: Power converter settings

3. **Meteorological Data Assessment**

In this simulation, meteorological data from HOMER Pro for each geographic location were utilized, focusing on wind speed, solar radiation, and temperature. These data were sourced from the solar energy database and NASA surface meteorology. Monthly solar irradiance, temperature, and wind speed statistics were specifically gathered for the coordinates (36°43.4 N, 3°9.00 E). Figures 5.8a, 5.8b, and 5.8c visually represent the monthly solar radiation in kWh/m2/day, the monthly temperature profile, and the monthly wind speed, respectively, for the year 2022.
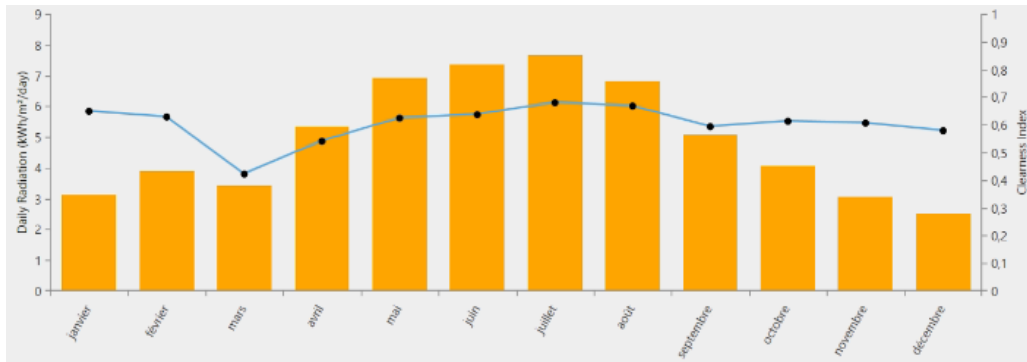
(a) Monthly solar irradiation
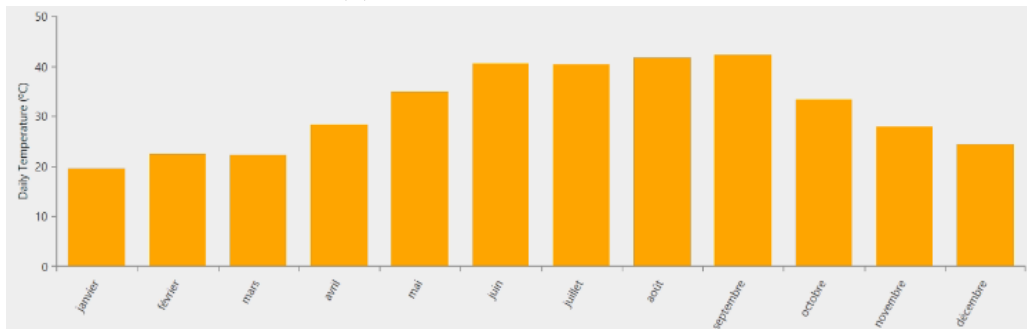
(b) Monthly temperature profile

(c) Average monthly wind speed

Figure 5.8: Meteorological data

4. **Load demand**

The considered Process Control Laboratory contains laboratories, leading to distinct load profiles for different periods: the study period (September to June) and the holiday season (July to August).

The proposed load, shown in Figure 5.9, was chosen from various proposed scenarios because it provides the optimized technical and economic configuration of the hybrid system in HOMER, which exactly matches our pre-sized real system.
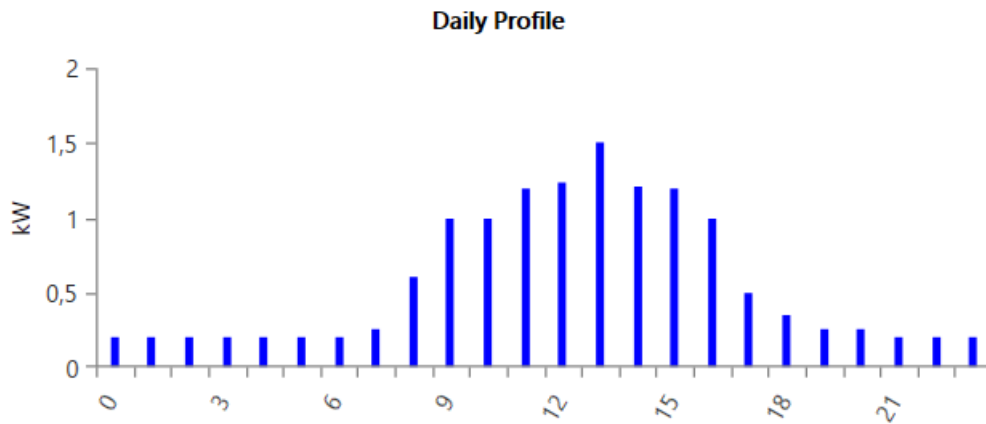
Figure 5.9: Daily load profile

To create a realistic load profile, a 20% safety factor has been added to the calculated load on a daily and hourly basis, accounting for random variations in the load. Figure 5.10 illustrates the monthly load profile
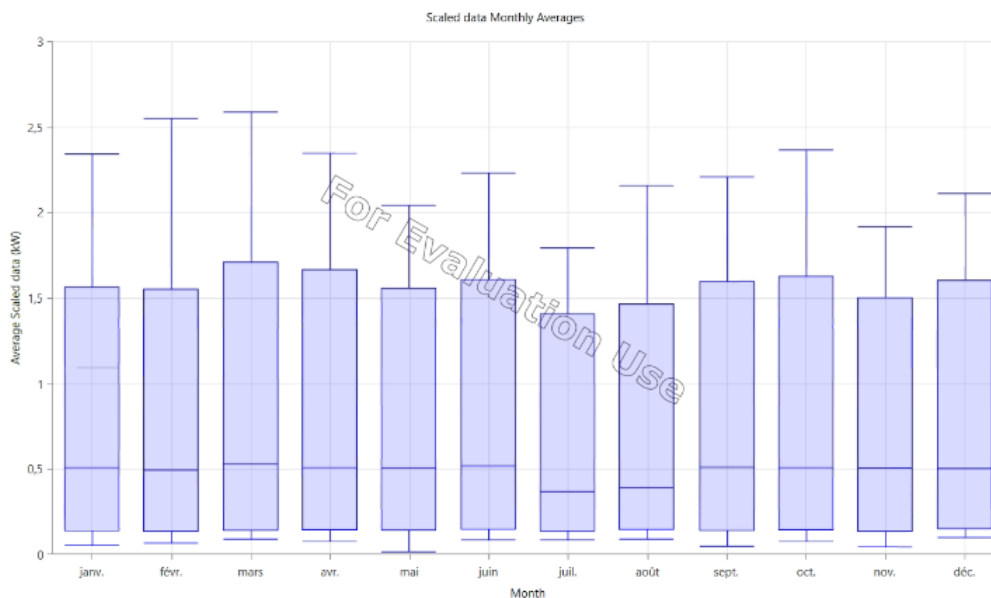
Figure 5.10: Load demand over the year

5. **Optimization Results and Discussion**

   The optimal configuration achieved the minimum values of renewable resources, as depicted in Figure 5.11, compared to other configurations. This optimal configuration involves a hybrid system comprising photovoltaic (PV) panels, wind turbines, batteries, and a converter. Specifically, the optimal configuration consists of:

   - 2 kW photovoltaic panels (arranged in two parallel strings).

   - 2 wind turbines (each with a 1kW).

   - 4 batteries.

Interestingly, this optimal configuration closely aligns with the existing system configuration. This outcome suggests that the current system design is already well-suited to the energy demands and resource availability in the location.

Figure 5.11: Screenshot of HOMER Pro Optimization Result

6. **Economic Analysis**

Figure 5.12 illustrates the Net Present Cost (NPC) by component for the optimum configuration in euro, including the PV, system converter, wind turbine, and battery bank. The findings indicate that the most economically feasible configuration was achieved with a minimum total NPC of 6981,62€.

The Levelized Cost of Energy(LCOE) per unit of energy generation is 0,1249€ per KWh.
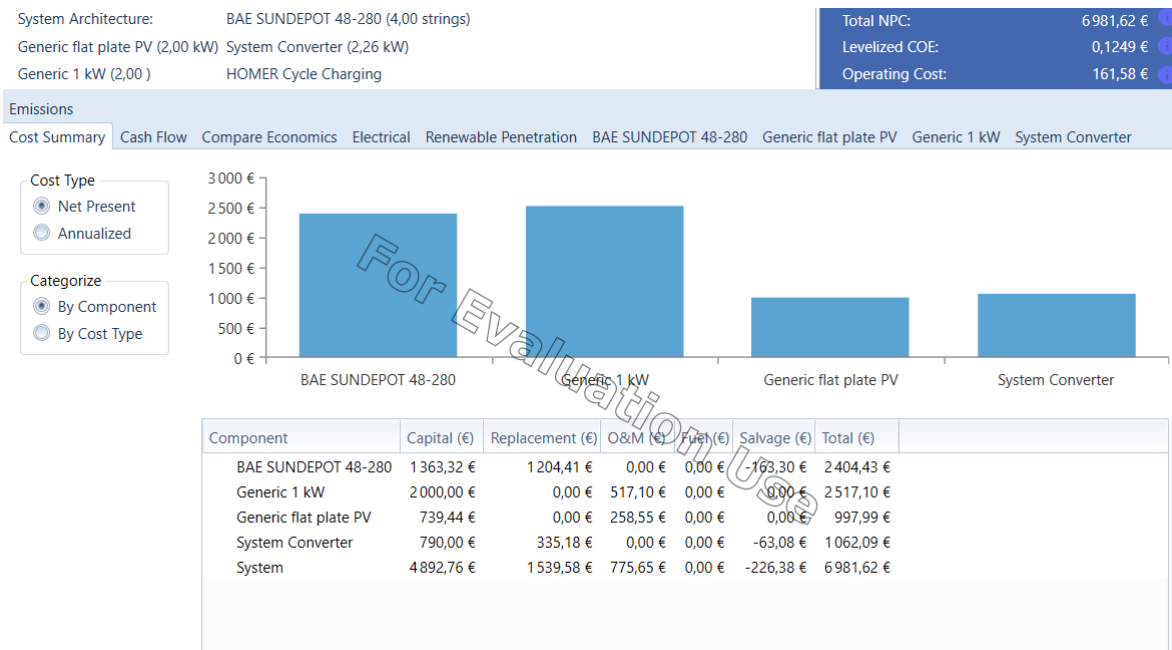
Figure 5.12: Net present cost of different component for optimum configuration

The table presents the cost breakdown for the system over its lifespan periods:

System	Cost (€)
Initial Investment	4892,76 €
Replacement Costs	1539,58 €
Annual O&M Costs	775.65€
Cost of Salvage	-226,38 €
Net Present Cost (NPC)	**6981,62 €**

Table 5.1: Cost Breakdown for the System

The cost of each component is shown in the following figure:
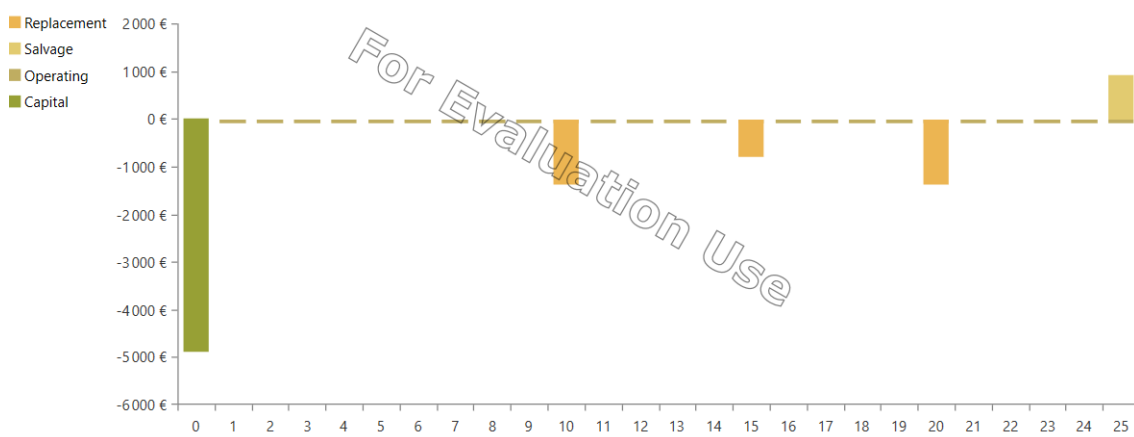
Figure 5.13: The distribution of costs for each component over a period of 25 years.

Figure 5.13 illustrates the total expenses for each year of the project. The first bar represents the initial year, which includes the system's investment costs. The bars are all negative, indicating expenses, as the system is autonomous and not connected to the grid. There are no positive values, as there will be no sale of electricity, and the electricity produced will only be used to power the building. The expenses include the cost of component replacement and operations and maintenance (O&M)[42].

7. **Electricity Production**

Figure 5.14 illustrates the distribution of monthly average electricity produced in KW by the solar PV systems and wind turbines.
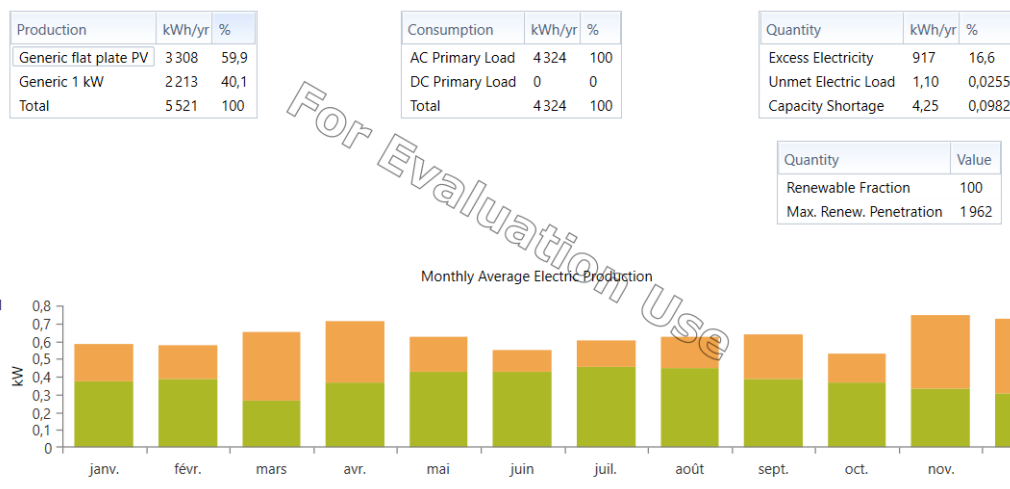
Figure 5.14: monthly average electricity production

According to the results obtained, the utilization of photovoltaic energy accounts for 50.9%, while the use of wind turbines represents 40.1%. Notably, the contribution of wind turbines is more significant during the winter months, whereas PV energy plays a

more prominent role during the summer months.

The load supplied by the system is of the AC type and consumes 5521 kWh/year. The system's batteries are used to store the excess energy produced by the two sources, as indicated in results of figure 5.14.

8. **Environmental impact**

These studies emphasize the significance of achieving 100% renewable penetration in standalone hybrid systems to enhance efficiency and sustainability.
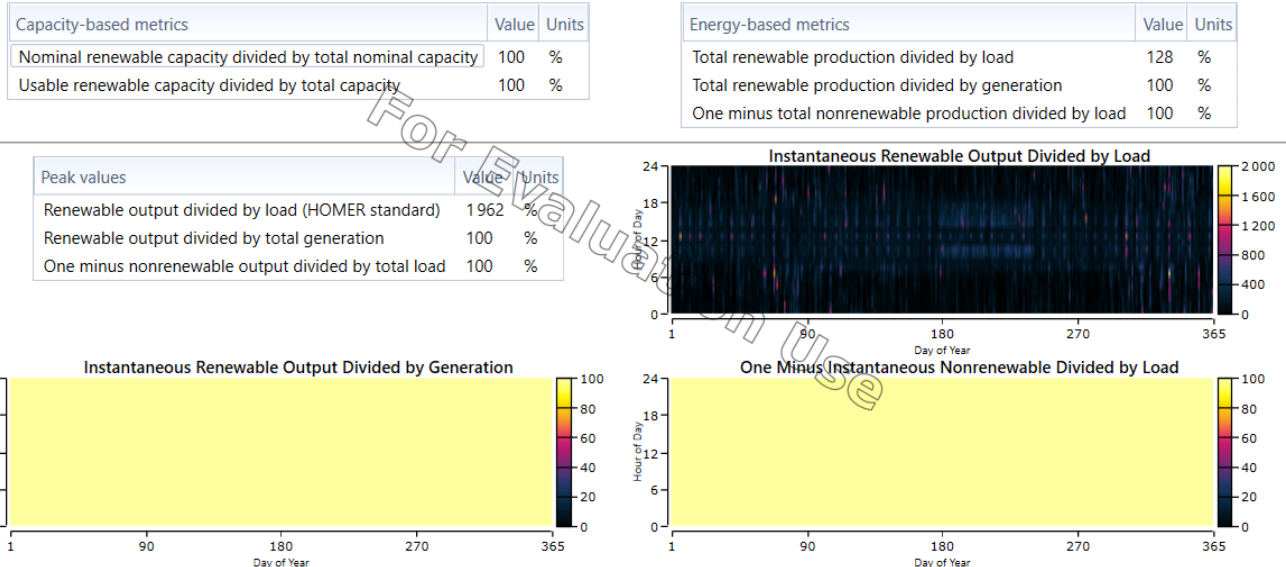
Figure 5.15: Renewable energy penetration details (from HOMER PRO)

The optimized hybrid systems designed with HOMER Pro aim to significantly decrease greenhouse gas emissions. Specifically, our system has achieved zero CO2 emissions. As a result, we evaluate the environmental impact of our hybrid system by calculating the equivalent barrels of oil replaced and the reduction in CO_2 emissions.

Equivalent Barrels of Oil:

$$\text{Equivalent Barrels of Oil} = \frac{\text{Total Energy Output (kWh)}}{1700\,\text{kWh/barrel}} \tag{5.1}$$

For our system producing 5521 kWh per year:

$$\text{Equivalent Barrels of Oil} = \frac{5521\,\text{kWh}}{1700\,\text{kWh/barrel}} \approx 3.25\,\text{barrels} \tag{5.2}$$

CO_2 Emissions Reduction:

$$CO_2 \text{ Reduction (kg)} = \text{Equivalent Barrels of Oil} \times 430\,\text{kg/barrel} \tag{5.3}$$

$$CO_2 \text{ Reduction} = 3.25\,\text{barrels} \times 430\,\text{kg/barrel} = 1397.5\,\text{kg of } CO_2 \tag{5.4}$$

By implementing our hybrid system, we replace the energy equivalent of approximately 3.25 barrels of oil annually, reducing CO_2 emissions by about 1397.5 kg each year.

4 Energy Management of proposed Hybrid System

The integration of a supervisory controller in hybrid energy systems plays a crucial role in overseeing operational modes and managing power flow to match renewable power generation with overall load demand[34]. By setting local controllers for different components, the supervisory controller optimizes their operation in various modes, enhancing system efficiency and reliability.

The power balance equation, as described in the equation, is utilized to maintain equilibrium between power generation and load demand:

$$P_W + P_{pv} = P_L + P_{bat} \tag{5.5}$$

where $P_{pv} = P_{pv1} + P_{pv2}$ is the power from the two PV chains, $P_W = P_{W1} + P_{W2}$ is the power from the two wind turbines, P_L is the power demanded by the load, and P_{bat} is the power of the battery.

4.1 Overview of Load Integration

The single-phase resistive load is connected to the hybrid energy system through a single-phase DC-AC inverter (Single-Phase H-Bridge PWM Inverter) and a transformer that steps up the voltage from 48V AC to 230V AC. A resistive-inductive (RL) filter is used to remove the higher order harmonics from the output AC voltage.

The DC-AC inverter converts the DC voltage from the hybrid energy system to an AC voltage suitable for the load. The inverter operates in PWM (Pulse Width Modulation) mode to control the output voltage and frequency. The H-Bridge configuration of the inverter allows for efficient switching and control of the AC output.
The transformer steps up the inverter output voltage from 48V AC to 230V AC, which is the standard voltage for residential and commercial applications. This ensures that the power delivered to the load meets the required voltage levels.

The RL filter, consisting of resistors and inductors, is implemented to filter out high-frequency harmonics generated by the inverter's switching operation. This ensures a clean sinusoidal AC voltage is delivered to the load.

4.2 Operating modes

First, the constraint conditions are defined as:

$$SOC_{min} < SOC(t) < SOC_{max} \tag{5.6}$$

with: $SOC_{min} = 20\%$ and $SOC_{max} = 80\%$,

$$V_{DC} = 48V \tag{5.7}$$

The different operating modes of the off-Grid hybrid system can be summarized as follows:

81

1. **Mode 1**: If the power generated by the renewable sources (PV1, PV2, W1, W2) is insufficient for the demand power at the load side ($P_L > P_{PV1} + P_{PV2} + P_{W1} + P_{W2}$), and the battery can provide backup power ($SOC > SOC_{min}$):

   - RES: MPPT mode
   - Battery's converter operates in boost mode (discharge) to supplement the RES power.

2. **Mode 2**: If the power generated by the renewable sources (PV1, PV2, W1, W2) is insufficient for the demand power at the load side ($P_L > P_{PV1} + P_{PV2} + P_{W1} + P_{W2}$) and the battery is deeply discharged ($SOC = SOC_{min}$):

   - The system operates on a load prioritization principle, as detailed in [34]. Power is allocated based on load priority levels (Highest, Second, and Lowest), ensuring critical functions are maintained during limited power availability.

3. **Mode 3**: When RES power exceeds load power ($P_{PV1} + P_{PV2} + P_{W1} + P_{W2} > P_L$) and the battery is not fully charged ($SOC < SOC_{max}$):

   - RES: MPPT
   - The excess RES power is used to charge the battery in buck mode.

4. **Mode 4**: When RES power exceeds load power ($P_{PV1} + P_{PV2} + P_{W1} + P_{W2} > P_L$) and the battery is fully charged ($SOC = SOC_{max}$): Several scenarios is required in this mode trying to manage the available power from PVs and WTs sources while ensuring the DC bus voltage stays stable.
   So considering the weather conditions, we elaborate possible scenarios in this mode: **Objective:** Manage excess RES power while maintaining stable DC bus voltage.

Table 5.2: Scenario 1: High Solar Irradiance

Scenario	PV1	PV2	WT1	WT2
1a: One PV is sufficient	Off-MPPT	Off	Off	Off
1b: Two PVs needed	MPPT	Off-MPPT	Off	Off

Table 5.3: Scenario 2: High Wind Speed

Scenario	PV1	PV2	WT1	WT2
2a: One WT is sufficient	Off	Off	Off-MPPT	Off
2b: Two WTs needed	Off	Off	MPPT	Off-MPPT

Table 5.4: Scenario 3: Moderate Solar Irradiance and Moderate Wind Speed

Scenario	PV1	PV2	WT1	WT2
3a	MPPT	MPPT	Off-MPPT	Off
3b	MPPT	MPPT	MPPT	Off-MPPT
3c	MPPT	Off-MPPT	MPPT	MPPT
3d	Off-MPPT	Off	Off-MPPT	MPPT

The various modes of operation of the energy management system are presented in the flowchart in figure 5.16
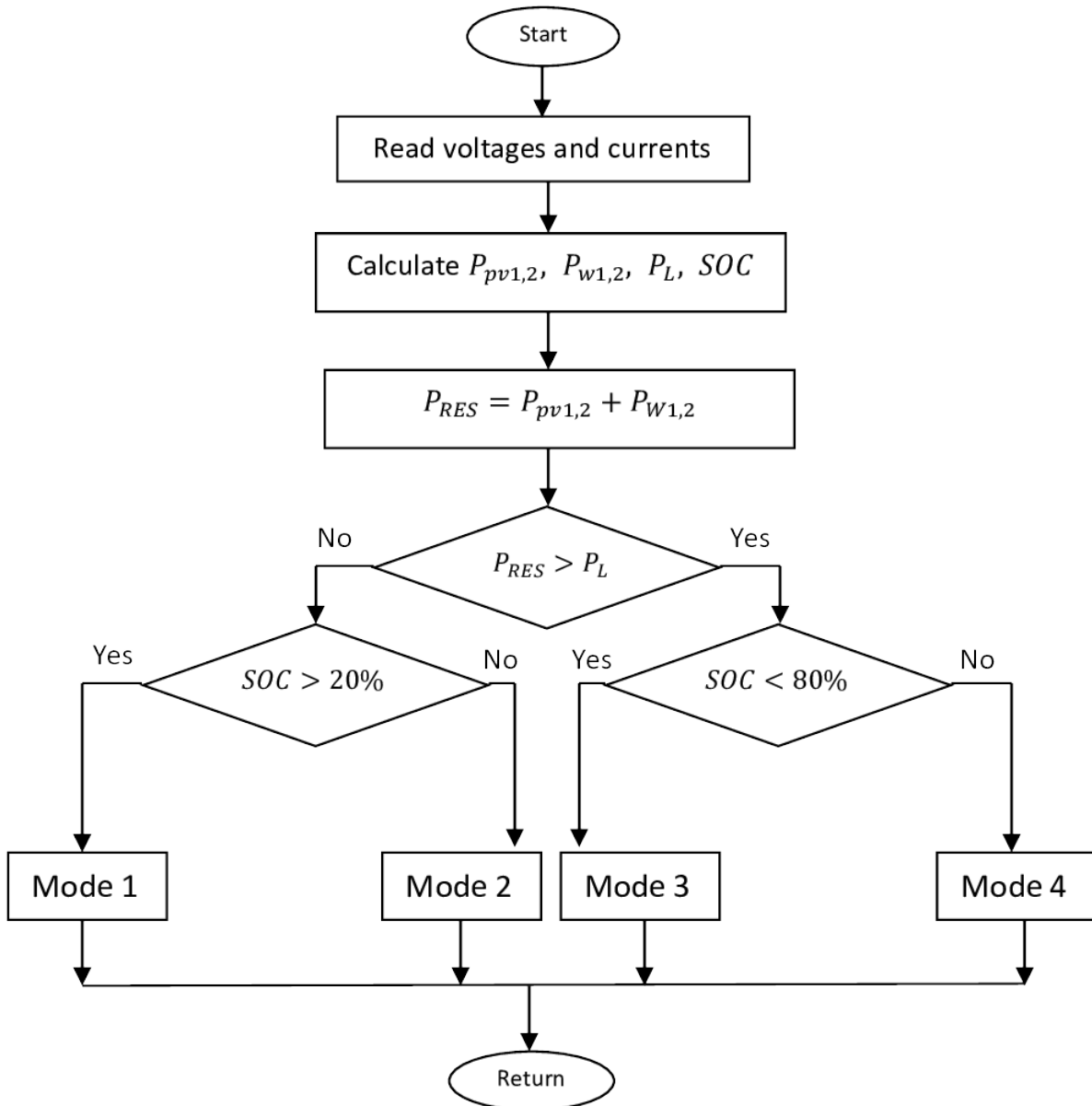

Figure 5.16: Energy management system

The scenarios pertaining to mode 4 are illustrated below:
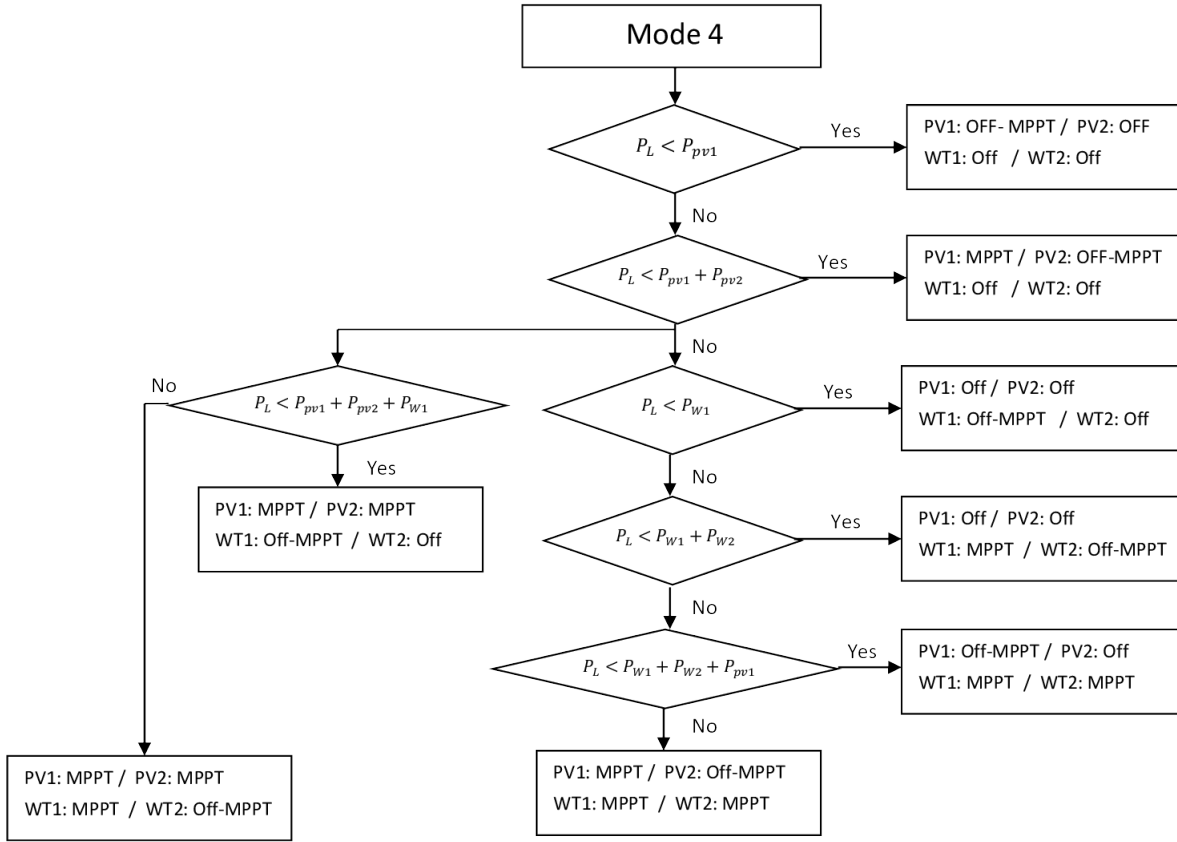
Figure 5.17: Mode 4 scenarios

4.3 Control of System Components

The system is controlled with the help of control signals provided by the controller to the switches connecting the solar PV, WTs, Batteries. The system switches between different operating conditions as per the energy demand and generation The proposed energy management system achieves energy balance by monitoring the currents of each converter. reference currents to control each converter according to the modes of operation.
The reference current to maintain the DC voltage is decided by the voltage control loop. This is the current drawn or injected by the PVs,WTs or BESS in order to stabilize bus voltage at the desired value.

4.3.1 Bi-Directional DC/DC Converter Control

In Chapter 2, we proposed a control strategy for the bi-directional DC/DC converter used for charging and discharging the battery. In this section, we incorporate state of charge (SOC) constraints to ensure the battery operates within its safe operating limits, as illustrated in Figure 5.18.
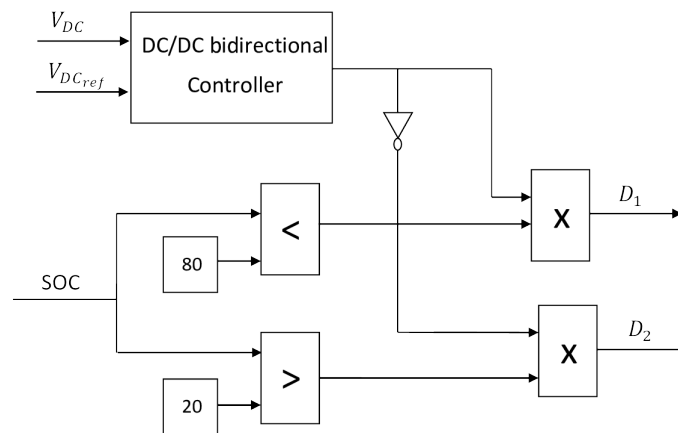
Figure 5.18: BESS converter control

The duty cycles for the switches in the converter are defined as follows:

- D_1: Duty cycle of S_1 (buck mode)

- D_2: Duty cycle of S_2 (boost mode)

4.3.2 DC/DC Converters Control

The PV and WT converters control involves two modes: MPPT (Maximum Power Point Tracking) discussed in detail in chapter 2 and OFF MPPT. The off MPPT control strategy ensures that the power flow from the PVs is regulated to maintain a stable DC bus voltage.
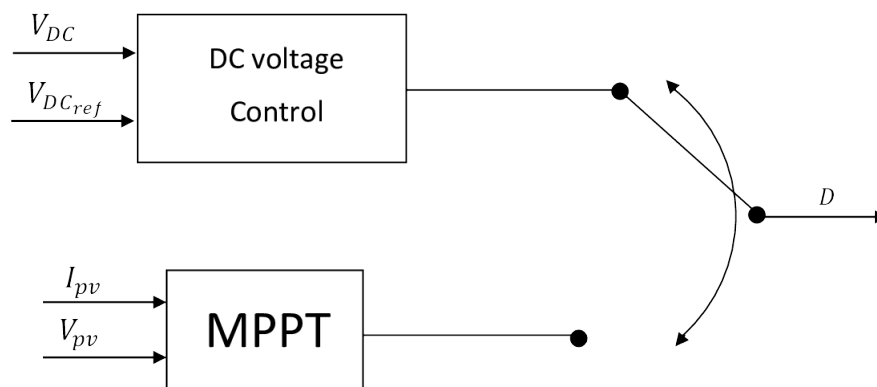
Figure 5.19: DC-DC Converters Controller

1. **MPPT mode** : discussed in details in chapter 2.

2. **Off-MPPT: Voltage Control mode** In Off-MPPT mode, the control strategy focuses on Voltage Control to regulate power flow from the PVs, ensuring a stable DC bus voltage. In this case, the PV generator does not work in MPPT mode and only generates the power requested by the load.

5 Simulation

This section presents the simulation results of a hybrid PV-wind-battery system using MAT-LAB/Simulink. The simulation evaluates the effectiveness of the proposed energy management strategy under varying environmental conditions, specifically focusing on modes 1 and 3 where the battery's state of charge (SOC) remains within its operating range (minimum to maximum). The simulation was conducted for a duration of 2 seconds, chosen to demonstrate the system's responsiveness to rapid changes in weather conditions and load demand. To mimic real-world fluctuations, solar irradiance and wind speed were varied at specific intervals.

Figures 5.20b and 5.20a illustrate the simulated solar irradiance and wind speed profiles, respectively.
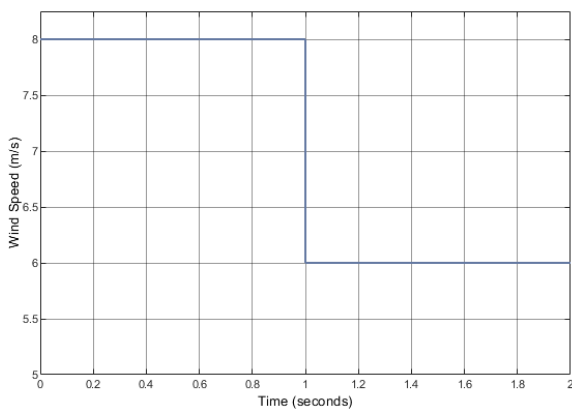
(a) Wind speed levels.
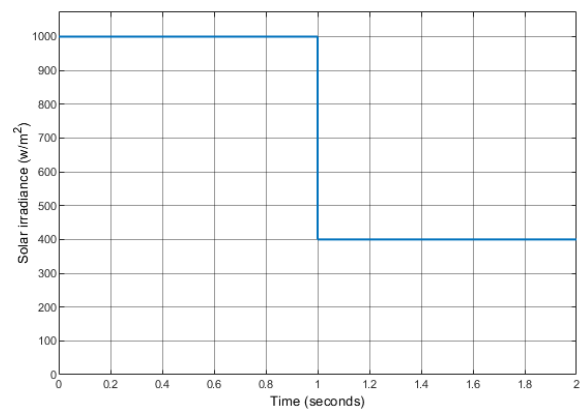
(b) Solar irradiance levels.

Figure 5.20: Environmental conditions: (a) Wind speed levels, (b) Solar irradiance levels.

Figures 5.21a and 5.21b show the power produced by the WECs and PVs, respectively.
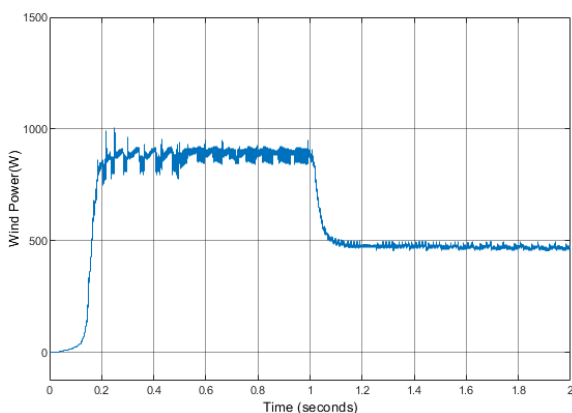
(a) Wind power
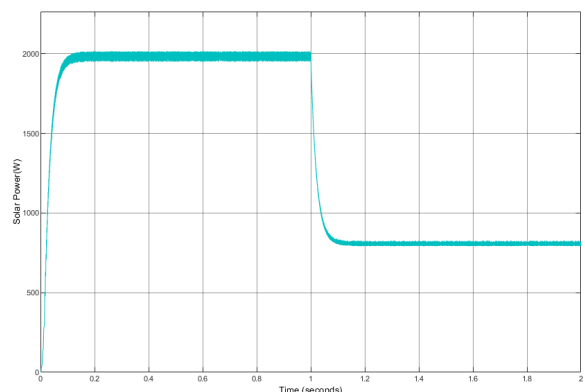
(b) Solar power

Figure 5.21: Power (a) Wind speed, (b) Solar

Figure 5.22 shows the load demand and the total produced power from renewable energy

sources (RES).
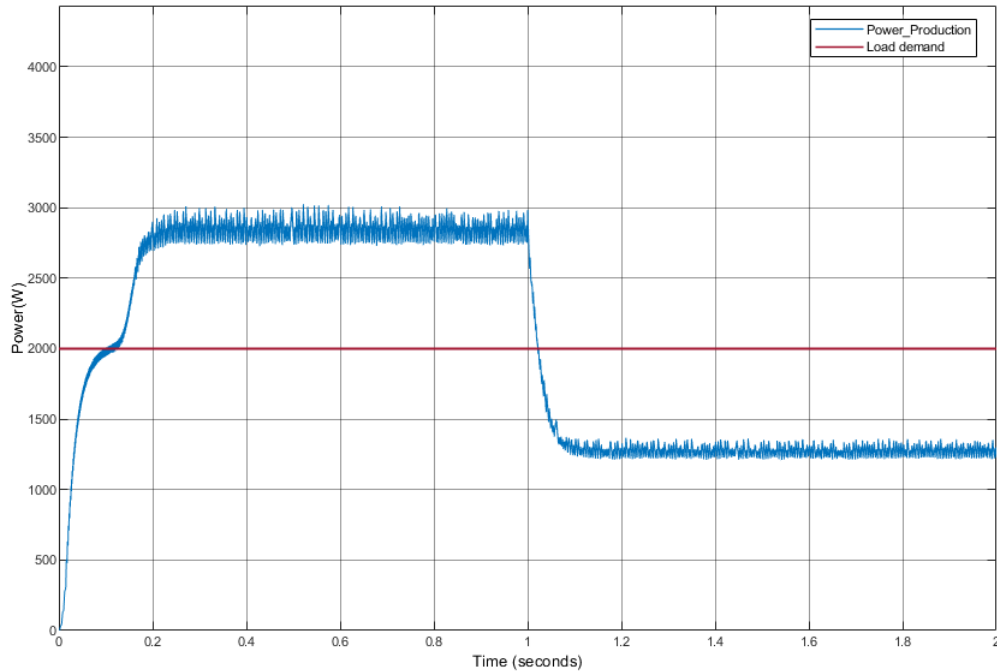
Figure 5.22: Load demand and total produced power from RES

Figure 5.23 shows the state of charge (SOC) of the battery, including the discharging and charging modes according to the power generated and power consumed. The break even point between charging (mode 3) and discharging (mode 1) of the battery is highlighted at the point where the power generated and power consumed are equal, resulting in zero error.
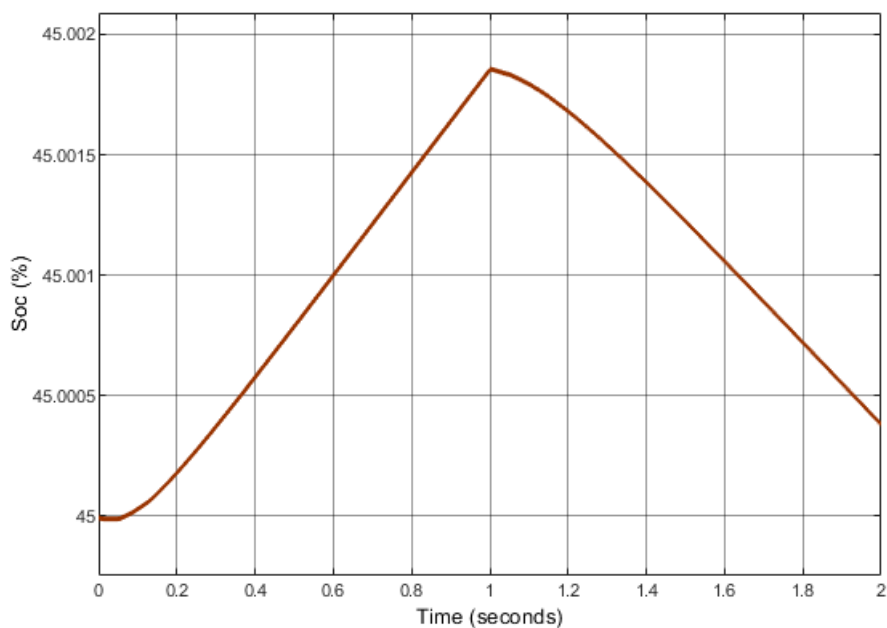
Figure 5.23: State of charge (SOC) of the battery

These simulation results clearly demonstrate the possible scenarios for modes 1 and 3, as described previously in the supervision algorithm. Therefore, the objective of the proposed HES's energy management strategy is achieved for these two modes.

6 Conclusion

In this chapter, we successfully integrated the photovoltaic (PV) system, wind energy system, and battery storage into a cohesive standalone hybrid energy system (HES) designed for the "Process Control Laboratory" at Ecole Nationale Polytechnique. Our approach involved a comprehensive techno-economic analysis using HOMER Pro software, which helped us determine the optimal configuration of the system components. This optimal configuration, consisting of PV panels, wind turbines, and battery storage, aligns closely with our pre-sized real system, demonstrating its technical feasibility and economic viability.

Furthermore, we implemented an energy management system (EMS) using MATLAB/Simulink to ensure efficient power flow and reliable operation of the HES. The EMS manages various operating modes, adapting to different conditions and maintaining a balance between power generation and load demand. The integration of this EMS enhances the system's overall efficiency and sustainability.

Our analysis also highlighted the significant environmental benefits of our HES, achieving zero $CO2$ emissions and reducing reliance on fossil fuels. The system's design and operation contribute to a more sustainable and resilient energy supply for the Process Control Laboratory at Ecole Nationale Polytechnique.

Chapter 6

Conclusion and future work

1   General conclusion

This study successfully demonstrated the feasibility and effectiveness of standalone hybrid energy systems integrating PV, wind, and battery storage. Through mathematical modeling and control strategies, the research highlighted the efficacy of the P&O MPPT algorithm for maximizing power output from both PV and wind sources. The integration of battery storage facilitated efficient charge/discharge management and ensured stable DC bus voltage control, initially validated with the PV system.

The techno-economic analysis substantiated the technical and economic viability of the proposed hybrid system. By leveraging real weather data, the study provided a realistic estimate of the load profile that this system can reliably power. The energy management system effectively optimized the utilization of available renewable resources, enhancing overall system efficiency. These findings provide valuable insights for the development of the standalone hybrid installation.

This study allowed us to draw several conclusions:

- The importance of selecting the site for the hybrid installation based on solar (solar radiation) and wind (wind speed) resources.

- The necessity of proper sizing to meet the electricity demand of the load.

- For effective management, it is essential to know the power supplied by the different sources (wind and photovoltaic), the power demanded by the load, and the state of charge of the storage elements (batteries).

2   Future work

For future research, it would be beneficial to:

- Integrate hybrid storage systems.

- Implement management strategies using artificial intelligence methods.

- Maximize power output by utilizing alternative MPPT techniques.

- Simulate the proposed scenarios for mode 4 operation.

- Develop a load prioritization method.

- Stabilize the DC bus using PV and wind turbines (off-MPPT).

- Implement all proposed algorithms and methods in a real-world system (experimental phase).

- Model the inverter and use it to control the DC bus voltage.

Appendices

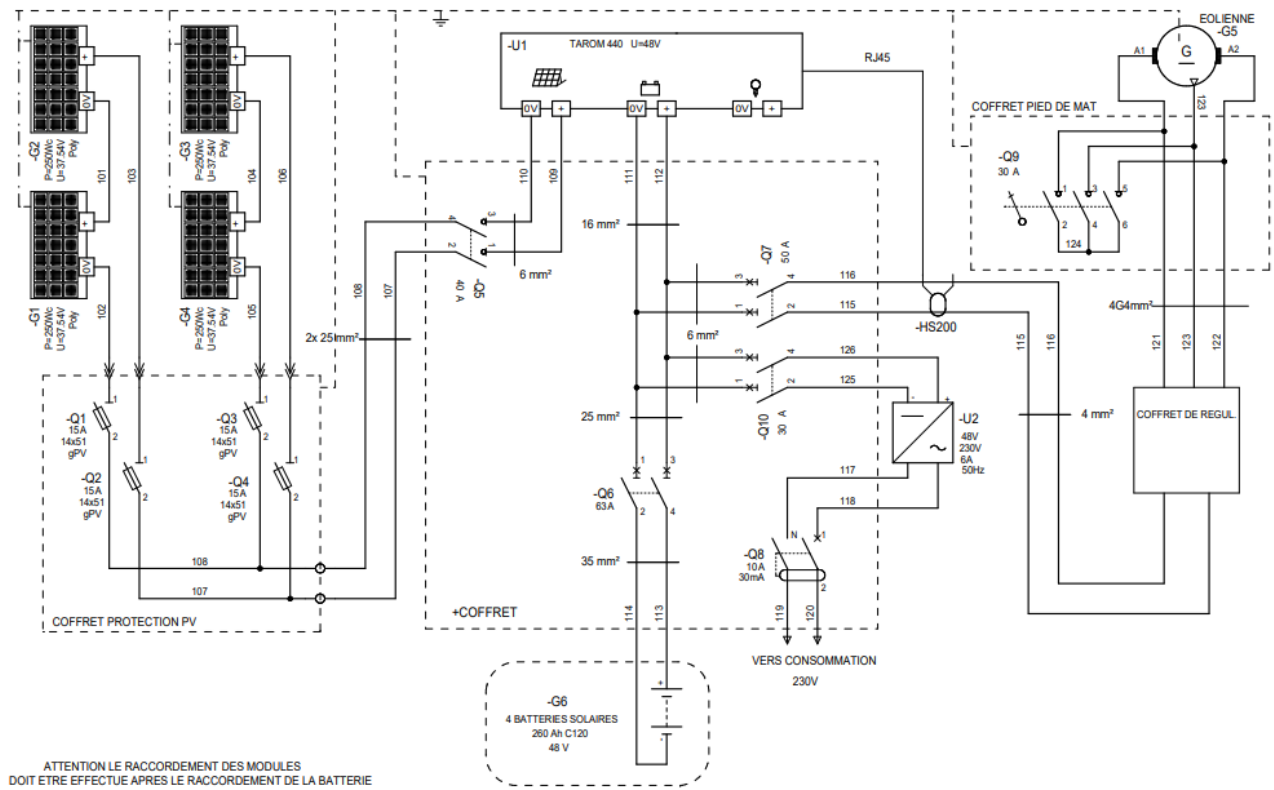# Appendix A: Electrical Diagram of the studied installation

Figure 1: Electrical Wiring Diagram of studied hybrid system

Appendix B: Calculation of PI Regulator Parameters

To design the PI regulators for the DC-DC bidirectional converter of the Battery Energy Storage System (BESS), we first need to determine the linearized model of the converter.

Linearized Model of the DC-DC Bidirectional Converter

For the control loop presented in Figure 3.13, we need to determine the transfer functions G_1 and G_2. The work presented in [57] provides the following linearized transfer functions:
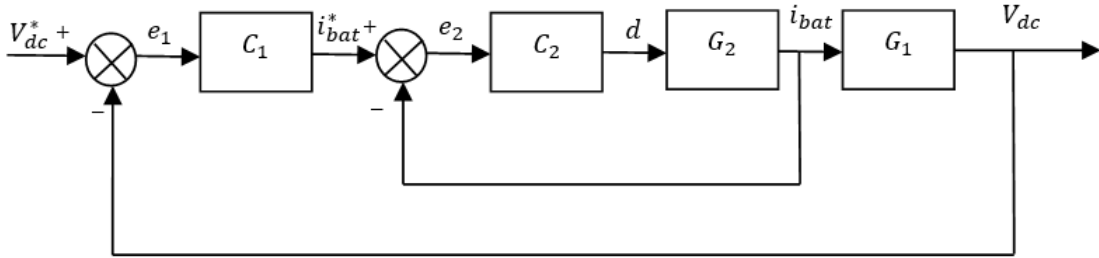
Figure 2: Bidirectional DC-DC Converter Control Scheme

The transfer function of battery current to the duty cycle is derived as:

$$G_1(s) = \frac{\hat{I}_{\text{bat}}(s)}{\hat{d}(s)} = \frac{2 + sR_{\text{dc}}C_{\text{dc}}}{s^2 L_{\text{bat}}C_{\text{dc}} + s\frac{L_{\text{bat}}}{R_{\text{dc}}} + (1-d)^2} \left(\frac{V_{\text{bat}}}{R_{\text{dc}} + (1-d)} \right) \tag{1}$$

The transfer function of DC-bus voltage V_{dc} to the battery current I_{bat} is derived as:

$$G_2(s) = \frac{\hat{v}_{\text{dc}}(s)}{\hat{I}_{\text{bat}}(s)} = \frac{(R_{\text{dc}} - sL_{\text{bat}})(1-d)}{sC_{\text{dc}}R_{\text{dc}} + (1-d^2) + 1} \tag{2}$$

Design of PI Controllers

The DC-bus voltage V_{dc} is compared with a reference voltage $V_{\text{dc,ref}}$, and the error signal is passed through the PI controller to generate the reference battery current I_{bat}^*. This is represented as:

$$C_v(s) = K_{pv} + \frac{K_{iv}}{s} \tag{3}$$

Then, I_{bat}^* is compared with the sensed battery current I_{bat}, and the error signal is passed through another PI controller to obtain the control signal d_{bat} for pulse width modulation (PWM):

$$C_i(s) = K_{pi} + \frac{K_{ii}}{s} \tag{4}$$

To design the PI controllers, we can use pole placement to determine the appropriate values for the proportional and integral gains K_{pv}, K_{iv}, K_{pi}, and K_{ii}. This method involves placing the

poles of the closed-loop transfer function at desired locations in the s-plane to achieve specific performance criteria, such as stability, fast response, and minimal overshoot.

The closed-loop transfer function of the system can be derived by combining the plant transfer functions $G_1(s)$ and $G_2(s)$ with the PI controllers $C_v(s)$ and $C_i(s)$. Let's denote the combined transfer function of the inner current loop as $G_{\text{inner}}(s)$ and the outer voltage loop as $G_{\text{outer}}(s)$.

The inner current loop transfer function is:

$$G_{\text{inner}}(s) = \frac{G_1(s)C_i(s)}{1 + G_1(s)C_i(s)} \tag{5}$$

The outer voltage loop transfer function is:

$$G_{\text{outer}}(s) = \frac{G_2(s)G_{\text{inner}}(s)C_v(s)}{1 + G_2(s)G_{\text{inner}}(s)C_v(s)} \tag{6}$$

By placing the poles of the closed-loop transfer functions at desired locations, we can achieve the required dynamic performance. The desired pole locations are often chosen based on the desired natural frequency ω_n and damping ratio ζ, which determine the transient response characteristics of the system.

For the inner current loop, the characteristic equation of the closed-loop transfer function is:

$$1 + G_1(s)C_i(s) = 0 \tag{7}$$

Substituting $G_1(s)$ and $C_i(s)$, we get:

$$1 + \left(\frac{2 + sR_{\text{dc}}C_{\text{dc}}}{s^2 L_{\text{bat}}C_{\text{dc}} + s\frac{L_{\text{bat}}}{R_{\text{dc}}} + (1-D)^2} \left(\frac{V_{\text{bat}}}{R_{\text{dc}} + (1-D)} \right) \right) \left(K_{pi} + \frac{K_{ii}}{s} \right) = 0 \tag{8}$$

For the outer voltage loop, the characteristic equation is:

$$1 + G_2(s)G_{\text{inner}}(s)C_v(s) = 0 \tag{9}$$

Substituting $G_2(s)$, $G_{\text{inner}}(s)$, and $C_v(s)$, we get:

$$1 + \left(\frac{(R_{\text{dc}} - sL_{\text{bat}})(1-d)}{sC_{\text{dc}}R_{\text{dc}} + (1-d^2) + 1} \right) \left(\frac{G_1(s)C_i(s)}{1 + G_1(s)C_i(s)} \right) \left(K_{pv} + \frac{K_{iv}}{s} \right) = 0 \tag{10}$$

By equating the characteristic equations to the desired polynomial with the desired poles, we can solve for the PI parameters.

Matching the coefficients of the characteristic polynomial with the expanded form of the closed-loop transfer function equations, we can determine the values of K_{pv}, K_{iv}, K_{pi}, and K_{ii}.

By placing the poles of the closed-loop transfer functions at the desired locations, we can achieve the required dynamic performance, such as stability, fast response, and minimal overshoot.

Bibliography

[1] E. ALAGOZ and Y. ALGHAWI, "The energy transition: Navigating the shift towards renewables in the oil and gas industry," *Journal of energy and natural resources*, 2023.

[2] I. P. M. Tsangas and A. Zorpas, "Sustainable energy planning in a new situation," *Energies*, 2023. DOI: `10.3390/en16041626`.

[3] S. Kumar and K. Rathore, "Renewable energy for sustainable development goal of clean and affordable energy," 2023. DOI: `10.56896/ijmmst.2023.2.1.001`.

[4] M. B. M.S. Chikhi and M. Zerouti, "Factors of investment in renewable energy and energy efficiency in algeria," *Economics (Bijeljina)*, 2022. DOI: `10.2478/eoik-2022-0020`.

[5] N. I. A. W. N. Sulaiman and H. Hizam, "Implementation of hybrid optimized battery controller and advanced power management control strategy in a renewable energy integrated dc microgrid," *PLOS ONE*, 2023. DOI: `10.1371/journal.pone.0287136`.

[6] Y. S. G. Meng and C. W. T. Yu, "A multi-objective control strategy of the energy storage system in distribution networks with a high proportion of renewable energy," *Journal of physics*, 2023. DOI: `10.1088/1742-6596/2520/1/012005`.

[7] A.CHOUMANE and O. BOUKHARI, "L'énergie éolienne en algérie: Potentiel et réalisations,"

[8] S. Kumar and K. Rathore, "Renewable energy for sustainable development goal of clean and affordable energy," 2023. DOI: `10.56896/ijmmst.2023.2.1.001`.

[9] E. Q. Allahverdiyev, *Use of renewable energy resources in agriculture*, 2023.

[10] I. G. F. Ayadi I. Colak and H. Bulbul, "Targets of countries in renewable energy," 2020.

[11] A. Q. et al, "Towards sustainable energy: A systematic review of renewable energy sources, technologies, and public opinions," *IEEE Access*, 2019.

[12] *Comparative Study of Power System Security Assessment using Deterministic and Probabilistic Methods*, 2023.

[13] J. Zhu, *Application of renewable energy*, 2015.

[14] Z. Mazyar, "Technology and energy management with renewable energy aspects," in *Conference Paper*, Mar. 2024.

[15] E. Gbenga and O. Samuel, "Review of sustainable energy and electricity generation from non-renewable energy sources," *Journal of Energy Technologies and Policy*, 2015.

[16] IEA, *Electricity 2024*, Paris, 2024. [Online]. Available: `https://www.iea.org/reports/electricity-2024`.

[17] R. Costa, *The importance of renewable energy in developing countries*, 2022.

[18] International Energy Agency, *Global energy investment in clean energy and in fossil fuels, 2015-2023*, Paris, 2023.

[19] M. Allali and S. Mouhadjer, "The impact of economic growth and energy consumption on co2 emissions in algeria," *Research Article*, 2023.

[20] Y. Zahraoui, M. R. B. Khan, I. AlHamrouni, S. Mekhilef, and M. Ahmed, "Current status, scenario, and prospective of renewable energy in algeria: A review," 2021. DOI: `10.3390/en14092354`.

[21] K. E. Sarah, "A review of solar photovoltaic technologies," *International Journal of Engineering Research & Technology*, 2020. DOI: `10.17577/IJERTV9IS070244`.

[22] A. A. T. Alkhalidi and N. H. Al Dulaimi, "Design of an off-grid solar pv system for a rural shelter," *ResearchGate*, 2018. DOI: `10.13140/RG.2.2.24352.07689`.

[23] R. S. Jadhav and S. B. Patil, "Design and implementation of pv-wind battery hybrid system for off-grid and on-grid," 2020.

[24] L. B. G. Cook and R. Adcock, *Photovoltaic FUNDAMENTALS*.

[25] S. M. Sulthan and D. Devaraj, *Simulation and analysis of stand-alone photovoltaic system with boost converter using matlab/simulink*, 2015.

[26] *Prediction of power generation in wind turbines*, 2023.

[27] H. Ibrahim, A. G. Ibrahim, J. O. Eichie, and B. Ige, *Wind energy resource utilization: A review of its necessity, interception technology and implementation challenges*, 2022.

[28] D. R. Masurkar, O. P. Tawde, P. P. Chavan, S. S. Bavkar, and P. P. Tajane, "Overview of traffic wind turbines," *Unpublished Manuscript*, 2024.

[29] R. N. Clark, "Chapter three - wind turbine components and descriptions: Essential components to have a productive, reliable, and safe wind machine," in *Small Wind*, R. N. Clark, Ed., Boston: Academic Press, 2014, pp. 39–67.

[30] F. MECHIKAR and N. LOUKKAS, "Étude et commande d'un système hybride éolien-photovoltaïque connecté au réseau," Mémoire de projet de fin d'études, École Nationale Polytechnique, Algiers, Algeria, 2013.

[31] WindmillsTech, *Wind turbine components*, Accessed: 2024-05-29.

[32] S. Ould Amrouche, D. Rekioua, T. Rekioua, and S. Bacha, "Overview of energy storage in renewable energy systems,"

[33] B. Kanagasakthivel and D. Devaraj, "Simulation and performance analysis of solar pv-wind hybrid energy system using matlab/simulink," 2015.

[34] E. M. B. A. Bouharchouche and T. Ghennaml, "Control and energy management of a grid connected hybrid energy system pv - wind with battery energy storage for residential applications," 2013.

[35] H. T. S. Faquir A. Yahyaouy and J. Sabor, "A type-1 fuzzy logic algorithm to manage the flow of energy in a stand-alone pv/wind/battery hybrid system," 2015.

[36] L. Chrifi-Alaoui, S. Drid, M. Ouriagli, and D. Mehdi, "Overview of photovoltaic and wind electrical power hybrid systems," *Energies*, 2023. DOI: `10.3390/en16124778`.

[37] O. Suwi and J. J. Justo, *Optimal energy management for off-grid hybrid renewable energy systems*, 2023.

[38] S. Aissou, D. Rekioua, N. Mezzai, T. Rekioua, and S. Bacha, "Modeling and control of hybrid photovoltaic wind power system with battery storage," *Laboratoire LTII, Universite de Bejaia, 06000, Algeria and G2elab Laboratory, INPG Grenoble, France*,

[39] D. Lu, "Conception et contrôle d'un générateur pv actif à stockage intégré: Application à l'agrégation de producteurs-consommateurs dans le cadre d'un micro réseau intelligent urbain," Ph.D. dissertation, ECL Lille, 2010.

[40] I. EVREN, "Modeling and simulation of dc-dc converters," 2021.

[41] M. KHELF and A. MAHIOUZ, "Supervision d'un système photovoltaïque-stockage alimentant une charge monophasée," Mémoire de projet de fin d'études, Ecole Nationale Polytechnique, 2020.

[42] A. GUERROUDJ, "Étude, dimensionnement et mise en marche d'un système hybride pv-éolienne-batteries au niveau du bloc de laboratoires de recherche," Mémoire de PGS, 2023.

[43] C. Xing, X. He, X. Xi, and M. Liu, "Research on the mppt control simulation of wind and photovoltaic complementary power generation system," 2023.

[44] A. CHOUDAR, "A local energy management and coordinated control of an active pv generator connected to an electric smart microgrid," Ph.D. dissertation, 2017.

[45] F. Akel, "Etude et commande d'un système hybride photovoltaïque-éolien en mode connecté au réseau et îloté," Ph.D. dissertation, 2017.

[46] S. N. S. Jadhav N. Devdas and V. Bajpai, "Bidirectional dc-dc converter in solar pv system for battery charging application," *Department of Electrical Engineering, Fr. C. Rodrigues Institute of Technology, Vashi, Navi Mumbai*,

[47] A. Soetedjo, A. Lomi, and W. P. Mulayanto, "Modeling of wind energy system with mppt control," 2011.

[48] H. M. Hasanien and S. M. Muyeen, "Design optimization of controller parameters used in variable speed wind energy conversion system by genetic algorithms," *IEEE Transactions on Sustainable Energy*, DOI: `10.1109/TSTE.2012.2182784`.

[49] TutorialsPoint. "Construction of dc machines." (2024).

[50] Windcycle Energy. "Permanent magnet dc generator." (2022).

[51] E. R. Tajne. "Types of dc generators | series, shunt, compound dc generator," OMG Free Study. (2021).

[52] S. CHARIF, "Caractérisation de la pale de l'éolienne whisper 100 et prédiction de performances aérodynamiques," Mémoire de projet de fin d'études, École Nationale Supérieure d'Ingénieurs, Génie Mécanique, Algérie, 2015.

[53] X. Zhang, J. Jia, L. Zheng, W. Yi, and Z. Zhang, "Maximum power point tracking algorithms for wind power generation system: Review, comparison and analysis," *Journal of Energy Storage and Conversion*, 2022. DOI: `10.1002/ese3.1313`.

[54] P. Vergara, J. Rey, L. da Silva, and G. Ordonez, "Comparative analysis of design criteria for hybrid pv/wind/battery systems," *IET Renewable Power Generation*, 2016. DOI: `10.1049/iet-rpg.2016.0250`.

[55] H. Moria, "Techno-economic optimization of solar/wind turbine system for remote mosque in saudi arabia highway: Case study," *International Journal of Engineering Research and*, 2019. DOI: `10.17577/IJERTV8IS090037`.

[56] A. Alzahrani, "Energy management and optimization of a standalone renewable energy system in rural areas of the najran province," 2023. DOI: `10.3390/en16114293`.

[57] S. J. P. K. Sahu and B. C. Babu, "Power management and bus voltage control of a battery backup-based stand-alone pv system," *Springer-Verlag GmbH Germany, part of Springer Nature*, 2021.